UNIVERSITÀ DEGLI STUDI DI NAPOLI
"FEDERICO II"

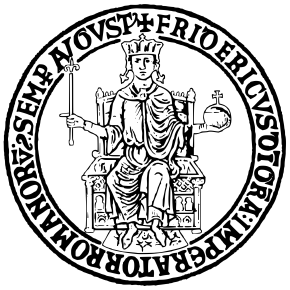

Scuola Politecnica e delle Scienze di Base

Area Didattica di Scienze Matematiche Fisiche e Naturali

Dipartimento di Fisica "Ettore Pancini"

Dottorato in Fisica

Semiclassical Methods in Conformal Field Theory

Advisor:
Prof. Francesco Sannino

Candidate:
Matías Torres Sandoval

External Referee:
Prof. Oleg Antipin
Prof. Kimmo Tuominen

Anno Accademico 2021/2024

Acknowledgements

The fact that I am writing these words indicates that this long journey is finally coming to an end. It is difficult to imagine how it would have been without the support of my family and the nice people I have met along the way.

First of all, I want to thank my advisor, Francesco Sannino, for allowing me to pursue my PhD in his group, and for his support and guidance.

Second, I want to thank my two principal collaborators, Jahmall Bersini and Alessandra D'Alise, without whose help much of this thesis would not have been possible. I am especially grateful to Jahmall, who often felt like a second advisor.

I would also like to thank my former professor, Fabrizio Canfora, with whom I have worked since my master's. Besides teaching me how to deal with differential equations, he taught me that solving them requires more than just a set of techniques or ansatzes; it is a matter of resilience. This lesson, of course, applies to many aspects of life as well.

A warm greeting and thanks to the people I met at the university: Paolo, Goran, Chems, Grazia, Mara, Daniela, Pia, Marco, Martina, and Sebastien. I especially want to thank Guido, who, with immense patience, was always willing to help me in dealing with Italian bureaucracy.

This thesis is dedicated to my mother, grandmother, and sister for their care, support, and for pushing me to follow my dreams.

Foreword

The material of this thesis is based on the three following papers:

[1] Oleg Antipin, Jahmall Bersini, Francesco Sannino, and Matías Torres. The analytic structure of the fixed charge expansion. *JHEP*, 06:041, 2022.

[2] Jahmall Bersini, Alessandra D'Alise, Francesco Sannino, and Matías Torres. The θ-angle and axion physics of two-color QCD at fixed baryon charge. *JHEP*, 11:080, 2022.

[3] Jahmall Bersini, Alessandra D'Alise, Francesco Sannino, and Matías Torres. Charging the conformal window at nonzero θ-angle. *Phys. Rev. D*, 107(12):125024, 2023.

Additionally, during my PhD, I publish the following articles:

[4] Gonzalo Barriga, Fabrizio Canfora, Marcela Lagos, Matías Torres, and Aldo Vera. On the robustness of solitons crystals in the Skyrme model. *Nucl. Phys. B*, 983:115913, 2022.

[5] Jahmall Bersini, Alessandra D'Alise, Matias Torres, and Francesco Sannino. The Dilatonic Dynamics of Baryonic Crystals, Branes and Spheres. 10 2023.

[6] Gonzalo Barriga, Matías Torres, and Aldo Vera. Exact modulated hadronic tubes and layers at finite volume in a cloud of π and ω mesons. *Nucl. Phys. B*, 1001:116501, 2024.

The chapters are organized as follows:

- Chapter I is dedicated to reviewing the large charge expansion for Conformal Field theories.
- Chapter II is based on [1].
- Chapter III is based on [2] and [3].
- The Conclusions summarize the results and give possible extensions of this work.

Abstract

This thesis aims to study large charged sectors of strongly coupled Conformal Field Theories with global symmetries.

In Chapter I, we focus on the basic concepts of conformal field theories and the large charge expansion. We illustrate this method using a $U(1)$-invariant CFT in $d = 4 - \epsilon$.

In Chapter II, we investigate the analytic properties of the fixed charge expansion for several conformal field theories in different space-time dimensions. The models investigated are $O(N)$ and QED_3. In $d = 3 - \epsilon$ the contribution to the $O(N)$ fixed charge Q conformal dimensions obtained in the double scaling limit of large charge and vanishing ϵ is non-Borel summable, doubly factorial divergent, and with order $\sqrt{Q}$ optimal truncation order. For $d = 4 - \epsilon$, the situation is different since the same large Q and small ϵ regime the next order corrections to the scaling dimensions lead to a convergent series. The resummed series displays a new branch cut singularity which is relevant for the stability of the $O(N)$ large charge sector for negative ϵ.

In Chapter III we analyze the impact of the θ-angle and axion dynamics for two-color QCD at nonzero baryon charge and as a function of the number of matter fields on the vacuum properties, the pattern of chiral symmetry breaking as well as the spectrum of the theory. We show that the vacuum acquires a rich structure when the underlying CP-violating topological operator is added to the theory. We discover novel phases and analyze the order of their transitions characterizing the dynamics of the odd and even number of flavours. We further determine the critical chemical potential as function of the θ-angle separating the normal from the superfluid phase of the theory. Then, we determine the impact of the θ-angle and axion physics in the conformal phase of the large-charge baryon sector of two-color QCD. We employ an effective approach featuring Goldstone and dilaton degrees of freedom augmented by the topological terms in the theory. We investigate how different dilaton potentials, including the ones for which a systematic counting scheme can be established, affect the results. Via state-operator correspondence, we compute the corrections to the would-be conformal dimensions of the lowest large-charge operators as a function of the θ-term and dilaton potential.

Contents

Introduction

Quantum Field Theory (QFT) is nowadays one of the most successful frameworks for studying the dynamics of interacting systems. Combining the principles of Quantum Mechanics and Special Relativity, it provides a natural language for the description of fundamental interactions. The Standard Model of particle physics stands as a remarkable accomplishment of scientific thought, resulting in the unification of three of the four fundamental forces of our universe.

The path integral formulation of QFT offers a natural procedure to quantize classical fields and introduces a diagrammatic approach to perturbation theory through Feynman diagrams. Perturbation theory relies on the fact that observables can be systematically expanded as exact solutions plus deviations modulated by a "small" parameter. Despite its apparent simplicity, its importance in physics is undeniable. One of the most renowned predictions is the anomalous magnetic moment of the electron in Quantum Electrodynamics (QED), which is in agreement with the experiment in one part in ten billion, an astonishing result [7].

Nonetheless, perturbation theory falls short of giving a complete solution. In QFT as well as QM, the coefficients of the perturbative series grow factorially, leading to divergent results. Even for weakly-coupled systems, there are sectors where perturbation breaks down. An important example of this is the scattering of processes involving a large number of particles. This phenomenon is relevant for multi-legged amplitudes for the next generation of high-energy physics experiments, since perturbative unitarity may be violated in multi-Higgs or bosons W, Z production [8].

On the other hand, many open problems in theoretical physics are non-perturbative in nature. In particular, the Quantum Chromodynamics (QCD) phase diagram at low energy and its finite density effects are quite challenging to analyze at non-perturbative level [9, 10], being lattice simulations or effective field theories the most common frameworks to investigate the strong sector. These circumstances makes mandatory to expand our knowledge of methods in field theory that go beyond perturbation theory.

In this thesis, we employ different techniques to address strongly coupled QFTs. Specifically, we focus on a special class of QFTs that are invariant under conformal transformations. These types of theories are called Conformal Field Theories (CFTs), and they typically appear as fixed points of the renormalization group (RG) flow. CFTs are ubiquitous in theoretical physics, they describe second-order phase transitions in statistical mechanics, the dynamics of the worldsheet of a two-dimensional string, and provide a holographic description of gravity through the AdS/CFT correspondence. Due to their larger symmetry group, their dynamics is significantly constrained to a set of two dynamical variables $\{\Delta_i, \lambda_{ijk}\}$ collectively known as *conformal data*. Since CFTs lack an intrinsic scale, they are usually addressed by introducing extra control parameters such as the ϵ-expansion or large-N expansion, or through non-perturbative frameworks like Monte-Carlo or Conformal Bootstrap.

In this thesis, we investigate the conformal data of operators carrying a large value of conserved global charges in strongly coupled CFTs. Our starting point is the *large charge expansion*. This method relies on the fact that at large quantum numbers, the dynamics of a CFT simplifies, allowing a weakly-coupled effective field theory (EFT) description in terms of the lightest degrees of freedom. The EFT's dynamics is characterized by the symmetry-breaking pattern coming from the charge fixing, in companion with the non-relativistic Goldstone boson theorem. Quantizing the $d+1$-dimensional EFT on a compact manifold of characteristic scale R_0 at fixed charge Q, induces the following hierarchy in which the EFT expansion is valid

$$\Lambda_{\text{low}} = \frac{1}{R_0} \ll \Lambda \ll \Lambda_{\text{high}} = \frac{Q^{\frac{1}{d-1}}}{R_0},$$

Therefore, in analogy to chiral perturbation theory, we can compute the CFT data using as control parameter $\frac{\Lambda_{\text{low}}}{\Lambda_{\text{high}}} = \frac{1}{Q^{1/d}}$. This method was applied for the first time in [11], to study the critical $O(2)$ model in $d=3$. It was shown that the scaling dimension for large-charge operators behaves as

$$\Delta(Q) = c_{3/2}Q^{3/2} + c_{1/2}Q^{1/2} - 0.0937 + ...$$

where c_i denote the Wilsonian parameters that depend on the underlying theory. The first terms originate from the ground-state energy at large charge, while the Q^0-term, coming from the zero-point energy of the fluctuations around the charged vacuum, is a universal prediction in even dimensions.

Remarkably, it is possible to avoid the EFT construction if the theory posses an extra small parameter. In [12] the authors focused on a $U(1)$-invariant theory in $d = 4-\epsilon$. It was shown that it is possible to apply a semiclassical expansion at large charge, around a non-trivial saddle point in the double scaling limit

$$Q \to \infty, \quad \epsilon \to 0, \quad Q\epsilon = \text{fixed}.$$

As a result, the scaling dimension of large charge Q operators can be written as follows

$$\Delta(Q) = \sum_{k=-1} \frac{1}{Q^k}\Delta_k(x), \quad x = \epsilon Q.$$

where x is the 't Hooft coupling. Notice that this expression resums an infinite series of Feynman diagrams of the standard perturbative expansion. The terms Δ_{-1} and Δ_0 correspond to the classical and quantum contribution coming from the semiclassical expansion at all order in x. After these seminal works, several theories have been investigated using the large charge expansion such as (non-)abelian scalars models [13, 14, 15, 16], effective field theories [17, 18, 19], Chern-Simons theories [20, 21], non-relativistic conformal theories [22, 23], fermionic models [24, 25], as well as theories with Yukawa and gauge interactions [26, 27] and the Standard Model [28].

This work attempts to combine the large charge expansion with other non-perturbative frameworks such as resurgence and effective field theories near the conformal window [18]. Resurgence provides us with a concrete framework to make sense of the unpleasant feature of the perturbative approach in field theory. Most of the perturbative expansions appearing in physics are divergent. Nevertheless, the agreement with experiments of many results is quite remarkable if the perturbative expansion is truncated suitably (this is known as *optimal truncation*). Resurgence [29, 30] makes use of the non-perturbative

information hidden in perturbative expansion to turn formal divergent power series into proper functions. A systematic way to do this is using Borel resummation. By performing a Borel transform, the initial power series becomes a finite expression. Nonetheless, this expression contains ambiguities, which are expressed as lines in the complex plane. It is possible to cancel these ambiguities by including non-perturbative corrections into the original power series. In this way, by including all the non-perturbative sectors, one gets a well-defined answer.

On the other hand, the structure QCD phase diagram and its phase transitions as a function of the number of flavors, temperature, and chemical potential is one of the most challenging problems in theoretical and experimental physics [9, 10]. Since at low energies, the coupling constant increases, only refined lattice simulations, and effective models have proven useful. However, when the chemical potential is non-zero for $N_c = 3$, importance sampling is not applicable because the fermionic determinant becomes complex. This issue is known as the sign problem. For $N_c = 2$, the situation is very different since quarks transform in the pseudo-real representation of the gauge group, leading to a real action. Another interesting problem is the experimental absence of CP-violating terms stemming from the topological sector of the theory, encoded in the theta-angle term. The main motivation for considering this term is to understand the interplay between θ-physics, the structure of the vacuum at finite density, and the impact on the conformal data of charged operators near the conformal phase.

The present thesis is organized as follows. In Ch.1, we review the fundamental aspects of a CFT. We then introduce the large charge expansion applied to a $U(1)$-invariant CFT to compute the scaling dimension of charged operators ϕ^Q. We conclude this chapter by defining the notion of dilaton dressing for near-conformal theories. Ch.2 is devoted to employing resurgence techniques to study CFT data at a fixed charge for different models. First, we review the main aspects of resurgence theory, optimal truncation, Borel transform, and trans-series. Then, we study the $O(N)$ model in $d = 3 - \epsilon$ and $d = 4 - \epsilon$, as well monopoles in QED_3, finding non-perturbative corrections to the conformal dimension of charged operators. In Ch. 3, we start by reviewing the effective Lagrangian for $N_c = 2$ describing the Goldstone boson, in companion with the θ-angle and axion. We compute the ground state energy as a function of the different number of matter fields, θ-angle, and chemical potential. We discuss the chiral symmetry breaking and determine the spectrum and associated. Then, using a dilaton dressing, we compute the leading near conformal corrections on a cylinder to the scaling dimension of the lowest-lying baryon charge Q operator. The last chapter is dedicated to the conclusions and final comments.

Chapter 1

Conformal Field Theories

Our modern understanding of QFT is inherently connected with the renormalization group flow. In general terms, RG studies the evolution of a physical system at different energy scales, from the ultraviolet (UV) to the infrared (IR). At the IR fixed point, a theory can exhibit different phases like a mass(less) gap or scale invariance with a continuous spectrum. This last class is called Conformal Field Theory (CFT) and corresponds to the central object of study in this thesis.

Several physical systems at the IR scale are described by a CFT. For example, the $d = 3$ Ising model, water, and ferromagnets at the critical point are all described by the same critical ϕ^4 theory at the Wilson-Fisher (WF) fixed point. This fact illustrates the concept of universality, indicating that microscopic details become irrelevant at large distances, and different theories look the same.

In this chapter, we introduce the building blocks of CFT. Our discussion will follow mostly [31, 32]. We then explain the large charge expansion using the $U(1)$ model [13]. We conclude by discussing how to study near-conformal field theories using a dilaton field.

1.1 Conformal Algebra

Let us begin with a d-dimensional Euclidean space-time $g_{\mu\nu} = \eta_{\mu\nu}$. We say that a coordinate transformation is conformal if it leaves the infinitesimal line element invariant up to a local positive term. For a conformal transformation $x^\mu \to x'^\mu(x)$, the line element transforms in the following way

$$\mathrm{d}x'^2 = \Omega(x)^2 \, \mathrm{d}x^2, \tag{1.1.1}$$

where $\mathrm{d}x^2 = \eta_{\mu\nu}\mathrm{d}x^\mu \mathrm{d}x^\nu$. The set of transformations $x' = x'(x)$ that satisfy equation (1.1.1) constitute a Lie group known as the *conformal group*. These transformations possess the property of preserving the relative angles between vectors. When $\Omega(x) = 1$, we recover the familiar Poincaré group, given by translations, rotations, and Lorentz transformations. To understand the structure of a general conformal transformation, let us examine its infinitesimal action around the identity

$$x'^\mu = x^\mu + \epsilon^\mu(x), \quad \Omega^2(x) = 1 + f(x), \tag{1.1.2}$$

where $\epsilon(x)$ and $f(x)$ are of the same order. Plugging these expressions in (1.1.1) we get the conformal Killing equation

$$\partial_\mu \epsilon_\nu + \partial_\nu \epsilon_\mu = \frac{2}{d} \partial_\rho \epsilon^\rho \eta_{\mu\nu}. \tag{1.1.3}$$

The set of independent solutions of (1.1.3) constitutes the infinitesimal action of the conformal group. By consistence, the value of the function $f(x)$ has to be fixed to $f(x) = \frac{2}{d}\partial_\mu \epsilon^\mu$. The Table 1.1.1 displays the set of independent solutions. As long as

	Infinitesimal Transformation	Generator
Translation	$\epsilon_\mu = a_\mu$	$P_\mu = -i\partial_\mu$
Rotation	$\epsilon_\mu = \omega_{[\mu\nu]}x^\nu$	$L_{\mu\nu} = i\left(x_\mu\partial_\nu - x_\nu\partial_\mu\right)$
Dilatations	$\epsilon_\mu = \lambda x^\mu$	$D = -ix^\mu\partial_\mu$
SCT	$\epsilon_\mu = b^v\left(2x_\mu x_v - x^2\delta_{\mu v}\right)$	$K_\mu = -i\left(2x_\mu x^\nu\partial_\nu - x^2\partial_\mu\right)$

Table 1.1.1: Infinitesimal conformal transformations and their respective generators. SCT denotes Special Conformal Transformation.

$d \neq 2$, the dimension of the conformal group is given by $\frac{1}{2}(d+1)(d+2)$. The non-trivial communtation rules are written above

$$\begin{aligned}
[L_{\mu\nu}, P_\rho] &= i\left(\eta_{\nu\rho}P_\mu - \eta_{\mu\rho}P_\nu\right), \\
[L_{\mu\nu}, L_{\rho\sigma}] &= i\left(\eta_{\mu\sigma}L_{\nu\rho} + \eta_{\nu\rho}L_{\mu\sigma} - \eta_{\mu\rho}L_{\nu\sigma} - \eta_{\nu\sigma}L_{\mu\rho}\right), \\
[D, P_\mu] &= iP_\mu, \\
[K_\mu, P_\nu] &= 2i\left(\eta_{\mu\nu}D - L_{\mu\nu}\right), \\
[L_{\mu\nu}, K_\rho] &= i\left(\eta_{\nu\rho}K_\mu - \eta_{\mu\rho}K_\nu\right), \\
[D, K_\mu] &= -iK_\mu.
\end{aligned} \tag{1.1.4}$$

The previous Lie-algebra describes the conformal algebra. The next step to build a conformal invariant field theory is to comprehend how matter fields transform as irreducible representations of the symmetry group. In general, a multivector $\Phi(x)$ transforms under an infinitesimal transformation parametrized by ω_g as follows:

$$\Phi'(x') = (1 - \omega_g T_g)\Phi(x), \tag{1.1.5}$$

where T_g denotes a generator belonging to some representation of the conformal group. To characterize the form of T_g, we focus on the point $x = 0$, since it remains invariant under conformal transformations. Denoting by $S_{\mu\nu}$, $\tilde{\Delta}$ and κ_μ the respective values of the generators $L_{\mu\nu}$, D and K_μ at the point $x = 0$. These quantities must form a matrix representation of the conformal algebra group (1.1.4). If we impose that the field $\Phi(x)$ belongs to an irreducible representation of the Lorentz, by the Schur Lemma, any matrix that commutes with $S_{\mu\nu}$ must be a multiply of the identity. Therefore $\tilde{\Delta}$ is a number equal to $i\Delta$ and κ_μ has to be zero[1]. In consequence, all the fields that belong to an irreducible representation of the conformal group satisfy

$$[K_\mu, \Phi(0)] = 0. \tag{1.1.6}$$

These fields are called primary and are the building blocks of the conformal algebra. Under a finite conformal transformation, a spinless field transforms as follows

$$\Phi(x) \to \Phi'\left(x'\right) = \left|\frac{\partial x'}{\partial x}\right|^{-\Delta/d}\Phi(x), \tag{1.1.7}$$

here Δ is called scaling dimension and is a dynamical variable that depends on the model.

[1]It comes from the fact that $[\tilde{\Delta}, \kappa_\mu] = -i\kappa_\mu$

1.2 Conformal Correlators

At the quantum level, conformal symmetry plays an important role in constraining the functional form of correlation functions. Let us consider a theory involving a set of fields ϕ with action $S[\phi]$. The expectation value of any local operator $\mathcal{O}(x)$ is given by

$$\langle \mathcal{O}(x) \rangle = \frac{1}{Z} \int \mathcal{D}\phi \mathcal{O}(x) e^{-S[\phi]}, \quad Z = \int \mathcal{D}\phi e^{-S[\phi]} \tag{1.2.1}$$

where Z is the partition function of the theory and $\mathcal{D}\phi$ is the path integral measure. Given two primary fields Φ_a, Φ_b one can prove that conformal symmetry constrains the form of the two-point to

$$\langle \Phi_a(x_1) \Phi_b(x_2) \rangle = c \frac{\delta_{ab}}{x_{12}^{2\Delta}}, \quad x_{12} = x_1 - x_2 \tag{1.2.2}$$

where Δ is the scaling dimension of the field Φ_a and c is a normalization constant. For the three-point function, conformal invariance fixes the form to be as follows

$$\langle \Phi_a(x_1) \Phi_b(x_2) \Phi_c(x_3) \rangle = \frac{\lambda_{abc}}{x_{12}^{\Delta_a+\Delta_b-\Delta_c} x_{23}^{\Delta_b+\Delta_c-\Delta_a} x_{13}^{\Delta_c+\Delta_a-\Delta_b}} \tag{1.2.3}$$

where the constants λ_{abc} are called OPE coefficients. In the case of four-point functions, two independent conformal invariants can be constructed using four points, these are called anharmonic ratios

$$u = \frac{x_{12}^2 x_{34}^2}{x_{13}^2 x_{24}^2}, \quad v = \frac{x_{14}^2 x_{32}^2}{x_{13}^2 x_{24}^2} \tag{1.2.4}$$

In consequence, the form of four-point function is determined up to a conformal invariant function $f(u, v)$

$$\langle \Phi_1(x_1) \dots \Phi_4(x_4) \rangle = f(u, v) \prod_{i<j}^{4} x_{ij}^{\Delta/3-\Delta_i-\Delta_i} \tag{1.2.5}$$

where $\Delta = \sum_{i=1}^{4} \Delta_i$. For higher point functions even more conformal invariant ratios can be defined.

1.3 Operator Product Expansion

The operator product expansion (OPE) is a property of any QFT that allows expanding the product of two local operators $\Phi(x)\Phi(0)$ for $x \to 0$ as follows

$$\Phi_i(x)\Phi_j(0) = \sum_k c_{ijk}(x)\Phi_k(0). \tag{1.3.1}$$

where the sum over k runs over all fields in the theory, both primary and descendants. In a general QFT, this series is asymptotic, but for a CFT, it is convergent [33]. Indeed, scale invariance fixes the coefficients c_{ijk} to be of the form

$$c_{ijk}(x, \partial) = \lambda_{ijk} |x|^{\Delta_k-\Delta_j-\Delta_i} \left(1 + \alpha x^\mu \partial_\mu + \beta x^2 \partial^2 + \cdots\right). \tag{1.3.2}$$

where λ_{ijk} corresponds to the OPE coefficients and the coefficients α and β are determined by imposing invariance under SCT. Using the OPE, we can construct higher point functions in terms of the scaling dimension and the OPE coefficients of the primary fields. Therefore, we unequivocally solve the CFT given the set of primary operators, their scaling dimensions, along their set of OPE coefficients. This set of information is known as *conformal data* $\{\Delta, \lambda_{ijk}\}$. Now we will move to the study of the Hilbert space associated with a CFT and its quantum evolution.

1.4 State-Operator correspondence and Radial Quantization

For any QFT, the quantization scheme is linked to the space-time symmetries. Each slide of space-time is associated with a unique Hilbert space. Likewise, the space-time foliation is dictated by the space-time symmetries. This ensures that Hilbert spaces living in hypersurfaces related by symmetry transformations are connected via unitary operators. For example for a Poincare invariant theory, the most common foliation corresponds to hyper-surfaces at $t = cte$. It follows, that the operator that connects different Hilbert spaces is $U = e^{iH\Delta t}$.

In theories with conformal symmetry, it is convenient to foliate the space with spheres of different radii centered at the origin. This scheme is called, for obvious reasons, *radial quantization*. The vacuum $|0\rangle$ is defined as the state annihilated by all the conformal generators. In consequence, we can create eigenstates of the dilatation operator D by acting with primary fields inserted at the origin on the vacuum state

$$D|\Delta\rangle = D\Phi_\Delta(0)|0\rangle = [D, \Phi_\Delta(0)]\,|0\rangle + \Phi_\Delta(0)D|0\rangle = i\Delta\Phi_\Delta(0)|0\rangle = i\Delta|\Delta\rangle. \tag{1.4.1}$$

From the commutators (1.1.4) we observe that the action of the momentum operator P_μ increase the scaling dimension of these states by 1

$$P_\mu|\Delta\rangle \propto |\Delta + 1\rangle. \tag{1.4.2}$$

Therefore, we can generate all the Hilbert space by acting with mometum operators on primary fields $\mathcal{H} = \text{span}\,\{|0\rangle, \Phi_\Delta(0)|0\rangle, P_\mu\Phi_\Delta(0)|0\rangle, \ldots\}$. We can exploit conformal invariance by performing Weyl transformation[2] from Euclidean space-time $\mathbb{R}^d$ to a cylinder $\mathbb{R} \times S^{d-1}$ of radius R_0. Parametrizing $\mathbb{R}^d$ with spherical coordinates (r, Ω_{d-1}) and the cylinder $\mathbb{R} \times S^{d-1}$ by (τ, Ω_{d-1}) the maps read as

$$ds^2_{\text{flat}} = e^{2\tau/R_0}\left(d\tau^2 + R_0^2 d\Omega_{d-1}\right) \tag{1.4.3}$$

$$= e^{2\tau/R_0} ds^2_{\text{cyl}}\,, \tag{1.4.4}$$

where $\tau = R_0 \log(r/R_0)$. In this case, the unitary operator that connects Hilbert spaces living in different sections of the cylinder is $U = e^{iD\Delta\tau}$

$$U|\Delta\rangle = e^{-\Delta\tau}|\Delta\rangle = r^{-\Delta}|\Delta\rangle. \tag{1.4.5}$$

With this map, we can relate asymptotic states on the cylinder $|\Phi\rangle$ at $\tau = \pm\infty$ with local primary fields $\Phi(x)$ inserted at the points $r = 0, \infty$. Thus, the dilation operator D on the cylinder is now interpreted as the Hamiltonian

$$D \longleftrightarrow \text{Hamiltonian on the cylinder } H_{\text{cyl}},$$
$$\Phi_\Delta \longleftrightarrow \text{Asymptotic state on the cylinder } |\Delta\rangle\ .$$

This relation is known as *state-operator correspondance*, and is based on the fact that the points $x = 0, \infty$ are invariant under conformal transformations, allowing to define unequivocally states. We can exploit this relation by studying the asymptotic behavior of correlation functions both in flat space and the cylinder. Let us remember that under a Weyl transformation $g \to \Omega^2 g$ correlation functions transform as

$$\frac{1}{\langle 1\rangle_g}\left\langle \Phi_1^{(g)}(x_1)\cdots\Phi_N^{(g)}(x_N)\right\rangle_g = \frac{1}{\langle 1\rangle_{\Omega^2 g}}\left(\prod_i \Omega^{\Delta_i}(x_i)\right)\left\langle \Phi_1^{(\Omega^2 g)}(x_1)\cdots\Phi_N^{(\Omega^2 g)}(x_N)\right\rangle_{\Omega^2 g} \tag{1.4.6}$$

[2]It is important to mention that not all local Weyl transformations are generated by conformal transformations.

Concretely, let us consider the two-point function under (1.4.4)

$$\left\langle \Phi^{\dagger}\left(\tau_f\right)\Phi\left(\tau_i\right)\right\rangle_{\text{cyl}} = |x_f|^{\Delta_\Phi}\,|x_i|^{\Delta_\Phi}\left\langle \Phi^{\dagger}\left(x_f\right)\Phi\left(x_i\right)\right\rangle_{\text{flat}}\,, \tag{1.4.7}$$

taking the limit $T=\tau_f-\tau_i\to+\infty$ the left-hand side becomes

$$\lim_{T\to\infty}\langle\Phi,\tau_f\mid\Phi,\tau_i\rangle=\lim_{T\to+\infty}\langle\Phi|e^{-H_{\text{cyl}}\,T}|\Phi\rangle=e^{-E_{\text{cyl}}\,[\Phi]T}, \tag{1.4.8}$$

where $E_{\text{cyl}}\,[\Phi]$ stands as the lowest energy associated with a state with the quantum numbers Φ on the cylinder, while the left-hand side read as

$$\lim_{T\to\infty}\left(\frac{|x_f|}{R_0}\right)^{\Delta_\Phi}\left(\frac{|x_i|}{R_0}\right)^{\Delta_\Phi}\frac{1}{|x_f-x_i|^{2\Delta_\Phi}}=e^{-\frac{\Delta_\Phi}{R_0}T}. \tag{1.4.9}$$

Therefore, we deduce the following expression

$$\Delta_\Phi=R_0E_{\text{cyl}}[\Phi]. \tag{1.4.10}$$

Due to the above relation, the goal of computing scaling dimensions will often turn to the computation of the energy spectrum on the cylinder.

1.5 CFT at Large Charge

In the previous sections, we have introduced the main aspects of CFTs. We saw, in detail, how conformal symmetry constrains the CFT dynamics, being completely determined by its *conformal data* $\{\Delta,\lambda_{ijk}\}$. The task of computing this data is generally non-trivial. The technology involved is extensive, and its applications vary across sectors. Given that many Conformal Field Theories (CFTs) exhibit strong coupling, traditional perturbative methodologies often fail to provide accurate results. Numerical approaches, such as Monte Carlo simulations and the Conformal Bootstrap, are commonly used to handle strongly coupled CFTs. Conversely, perturbative approaches, like the ϵ-expansion or large-N techniques, introduce additional control parameters that help expand the *conformal data*.

The idea of the *large charge expansion* is to study sectors of CFTs that have large quantum numbers under global symmetries. The control parameter in this case is the conserved charge associated with the global symmetry. Using the *state-operator correspondace*, the scaling dimension of charged operators is related to the vacuum energy with charge on the cylinder. In this section, we will provide an overview of the strategy to study CFTs at large charge. Let us consider a d-dimensional CFT with a global symmetry group G. A primary field can carry up to rank(G) conserved charges. The symmetry group implies the existence of a conserved current j^μ

$$Q=\int d^{d-1}xj^0(x),\quad \frac{dQ}{dt}=0. \tag{1.5.1}$$

We say that an operator Φ carries charge Q if $[Q,\Phi]=Q\Phi$. Using the state-operator correspondence [34] we can relate the scaling dimension Δ_Q of the operator Φ_Q with the energy E_Q of the state $\Phi_Q(0)|0\rangle$ on the cylinder. The charged ground state energy can be extracted considering the expectation value of a charge state $|Q\rangle$ with the evolution operator $U=e^{-H_{\text{cyl}}T}$

$$\lim_{T\to+\infty}\langle Q|e^{-H_{\text{cyl}}T}|Q\rangle=e^{-E_QT}, \tag{1.5.2}$$

where we have assumed that there is an overlap between $|Q\rangle$ and the lower energy state with charge Q. This object can be computed using the path integral representation

$$\lim_{T\to+\infty}\left\langle Q\left|e^{-H_{\text{cyl}}T}\right|Q\right\rangle=\mathcal{Z}^{-1}\int\mathcal{D}\Phi e^{-S_{\text{fixed}}\,[\Phi]} \tag{1.5.3}$$

where $\mathcal{Z}$ is the partion function, S_{fixed} is the classical action at fixed charge Q and Φ represent the collective set of fields. If the theory has an extra intrinsic perturbative parameter g, we can compute the ground state energy via a semiclassical expansion using the following double-scaling limit

$$Q\to\infty,\quad g\to 0,\quad Qg=(\text{ fixed }), \tag{1.5.4}$$

according to which the scaling dimension takes the following form

$$\Delta(Q)=\sum_{k=-1}\frac{1}{Q^k}\Delta_k\left(Qg\right) \tag{1.5.5}$$

Here the leading term Δ_{-1} corresponds to the action evaluated on the classical trajectory with charge Q, while the subleading contribution Δ_0 is given by the zero point energy on the cylinder given by Gaussian path integral around the quantum fluctuations. Remarkably, this expression resummation an infinite number of Feynman diagrams in a closed form.

The classical trajectory is not invariant under translation and the internal symmetry group, but it is under an effective combination of them [35]. For a CFT with symmetry group $G=U(1)$, the symmetry breaking pattern read as

$$SO(d+1,1)\times U(1)\to SO(d)\times D', \tag{1.5.6}$$

where $D'=D+\mu Q$ and μ is the chemical potential. This corresponds to the simplest symmetry-breaking pattern and characterizes the superfluid phase [36, 37], indicating the existence of one Goldstone boson, while the rest of the degrees of freedom have a finite gap. If we are interested only in the low energy dynamics, we can integrate out the massive degrees of freedom having left with an EFT for the Goldstone boson χ. The effective action consistent $S[\chi]$ with $U(1)$ symmetry and Weyl invariance is [38]

$$S[\chi]=-c_1\int d^dx\sqrt{g}\left|\nabla\chi\right|^d+c_2\int d^dx\sqrt{g}|\nabla\chi|^d\left[\frac{\mathcal{R}}{|\nabla\chi|^2}+(d-1)(d-2)\frac{\left[\nabla_\mu|\nabla\chi|\right]^2}{|\nabla\chi|^4}\right]+\dots \tag{1.5.7}$$

where $|\nabla\chi|=\left(-g^{\mu\nu}\nabla_\mu\chi\nabla_\nu\chi\right)^{1/2}$, $\mathcal{R}$ is the Ricci scalar and c_i are the Wilsonian coefficients determined by the underlying CFT. Since we want to apply the state-operator correspondence, we have embedded our system in a cylinder $\mathbb{R}\times S^{d-1}$ of radius R_0 at fixed charge Q. This induces the following hierarchy in which our EFT is valid

$$\frac{1}{R_0}\ll\Lambda\ll\frac{Q^{\frac{1}{d-1}}}{R_0} \tag{1.5.8}$$

As we already mentioned, the scaling dimension Δ_Q has two contributions, a classical one and a quantum one. The classical corresponds to the ground state energy of configuration with charge Q, in this case, is described by $\chi=\mu t$, where μ the chemical potential related to the charge Q via the Noether theorem as

$$\frac{Q}{R_0^{d-1}\Omega_{d-1}}=i\frac{\partial\mathcal{L}}{\partial\dot{\chi}}=c_1d\mu^{d-1}-c_2(d-2)\mu^{d-3}\mathcal{R}+\dots \tag{1.5.9}$$

where $\Omega_{d-1} = \frac{2\pi^{d/2}}{\Gamma(d/2)}$ is the volume of the $d-1$-dimensional sphere. The quantum contribution corresponds to the zero-point energy of the fluctuations around the charged configuration $\chi = \mu t + \pi(x)$, which have the following spectrum

$$\omega_\ell = c_s J_\ell + \mathcal{O}\left(\frac{1}{Q^{\frac{2}{d-1}}}\right), \tag{1.5.10}$$

where $J_\ell^2 = \frac{\ell(\ell+d-2)}{R^2}$ is the quantized momentum on the sphere and $c_s = 1/\sqrt{d-1}$ is the speed sound, which comes from the tracelesness of the energy-momentum tensor. The final results read as

$$\Delta_Q = \underbrace{Q^{\frac{d}{d-1}}\left[\alpha_1 + \alpha_2 Q^{\frac{d-2}{d-1}} + \dots\right]}_{\text{classical}} + \underbrace{Q^0\left[\beta_0 + \beta_1 Q^{\frac{-2}{d-1}} + \dots\right]}_{\text{quantum}} + \dots \tag{1.5.11}$$

where the α_i coefficients depend on c_i as

$$\alpha_1 = \frac{c_1(d-1)\Omega_{d-1}}{(c_1 d\Omega_{d-1})^{\frac{d}{d-1}}}, \quad \alpha_2 = \frac{c_2(d-1)(d-2)\Omega_{d-1}}{(c_1 d\Omega_{d-1})^{\frac{d-2}{d-1}}}, \tag{1.5.12}$$

while the β_i coefficients comes from the zero-point energy at large charge

$$\frac{R}{2}\sum_\ell n_\ell \omega_\ell = \beta_0 + \beta_1 Q^{-\frac{2}{d-1}} + \dots, \tag{1.5.13}$$

where n_ℓ is multiplicity on the sphere given by

$$n_\ell = \frac{(2\ell+d-2)\Gamma(\ell+d-2)}{\Gamma(\ell+1)\Gamma(d-1)}. \tag{1.5.14}$$

Since the leading-order dispersion relation in Eq. (1.5.10) depends only on the dimension d, this implies that the β_i coefficients are functions only of the dimension [38]. For odd dimensions β_0 is universal, it does not depend on the CFT, while for even dimensions the expansion predicts instead a term $Q^0\log(Q)$, coming from the renormalization of β_0 which manifests a pole in $d=4$.

1.6 $U(1)$ at Large Charge

In this section, we will illustrate how fixing the charge affects the loop expansion in a QFT. For our purposes, we focus on a $U(1)$-invariant CFT with a quartic interaction. Following [13], we will introduce a semiclassical expansion to compute the CFT-data at large charge. The Lagrangian in Euclidean space-time is given by

$$\mathcal{L} = \partial_\mu\bar{\phi}\partial^\mu\phi + \frac{\lambda_0}{4}(\bar{\phi}\phi)^2. \tag{1.6.1}$$

In $d=4$, this theory has trivial infrared physics, whereas $d = 4-\epsilon$ exhibits a weakly coupled infrared Wilson-Fisher (WF) for $\epsilon \ll 1$. We renormalize the field and the coupling according to

$$\phi = Z_\phi[\phi], \quad \lambda_0 = M^\epsilon \lambda Z_\lambda, \tag{1.6.2}$$

where M is the energy scale. Working on minimal subtraction (MS) scheme, the beta function $\beta(\lambda) = M\frac{\partial}{\partial M}\lambda$ up to two-loops read as

$$\beta(\lambda) = -\epsilon\lambda + 5\frac{\lambda^2}{(4\pi)^2} - 15\frac{\lambda^3}{(4\pi)^4} + \mathcal{O}\left(\frac{\lambda^4}{(4\pi)^6}\right) \tag{1.6.3}$$

The WF fixed point $\lambda = \lambda^*$, defined by $\beta(\lambda^*) = 0$ read as follows

$$\frac{\lambda^*}{(4\pi)^2} = \frac{1}{5}\epsilon + \frac{3}{25}\epsilon^2 + \mathcal{O}\left(\epsilon^3\right). \tag{1.6.4}$$

By virtue of the Noether theorem, one can prove that the operator ϕ carries charge $+1$ and thus ϕ^Q carries charge Q. Our goal is to compute the scaling dimension Δ_{ϕ^Q} of the operator ϕ^Q as a function of the charge Q. The common procedure to compute scaling dimensions of operators is via their renormalization [39]. Denoting by $\left[\phi^Q\right]$ the renormalized field related to the bare ϕ^Q according to $\phi^Q = Z_{\phi^Q}\left[\phi^Q\right]$. At the fixed point, the scaling dimension becomes a physical observable. The scaling dimension of the operator ϕ^Q at the fixed point is given by

$$\Delta_Q = Q\left(\frac{d}{2} - 1\right) + \gamma_Q\left(\lambda^*\right) \tag{1.6.5}$$

where γ_Q is the anomalous dimension related to the renormalization factor Z_{ϕ^Q} via

$$\gamma_Q(\lambda) = \frac{\partial \ln Z_{\phi^Q}}{\partial \lambda}\beta(\lambda). \tag{1.6.6}$$

Is it possible to extract the renormalization factor Z_{ϕ^Q} by studying the correlator

$$\left\langle \phi^q \bar{\phi}(p)\bar{\phi}(p)\ldots\bar{\phi}(p)\right\rangle = Z_{\phi^q} Z_\phi^q \underbrace{\left\langle [\phi^n]\,[\bar{\phi}](p)[\bar{\phi}](p)\ldots[\bar{\phi}](p)\right\rangle}_{\text{finite}} \tag{1.6.7}$$

and finding the renormalization constant Z_{ϕ^Q} such that $\left\langle \left[\phi^Q\right][\bar{\phi}](p)[\bar{\phi}](p)\ldots[\bar{\phi}](p)\right\rangle$ is finite. Instead of computing Z_{ϕ^Q} via a diagrammatic approach, we will first demonstrate that even in a weakly coupled theory, the diagrammatic loop expansion breaks down for sectors with large values of Q. However, it is possible to make sense of the perturbative expansion at large charge by employing a double-scaling limit with 't Hooft coupling $\lambda_0 Q$. Let us begin by using the path integral representation. The two-point function read as follows

$$\left\langle \bar{\phi}^Q\left(x_f\right)\phi^Q\left(x_i\right)\right\rangle = \frac{\int \mathcal{D}\bar{\phi}\mathcal{D}\phi\bar{\phi}^Q\left(x_f\right)\phi^Q\left(x_i\right)\exp\left[-\int\mathcal{L}\right]}{\int\mathcal{D}\phi\mathcal{D}\phi\exp\left[-\int\mathcal{L}\right]} = Z_{\phi^Q}^2\left\langle\left[\bar{\phi}^Q\right]\left(x_f\right)\left[\phi^Q\right]\left(x_i\right)\right\rangle. \tag{1.6.8}$$

Pertubation theory

Expanding the path integral around the trivial saddle point $\phi = 0$, we found that at first order in λ correlator takes the form

$$\begin{aligned}\left\langle \bar{\phi}^Q\left(x_f\right)\phi^Q\left(x_i\right)\right\rangle = Q!D(x_{fi})^Q\Bigg(1 - \frac{\lambda}{4}\Bigg[2QD(x_{fi})^{-1}\int d^dx D(x_f - x)D(x - x_i)D(0) \\ +4Q(Q-1)D(x_{fi})^{-2}\int d^dx D(x_f - x)^2 D(x - x_i)^2 + \mathcal{O}\left(\lambda^2\right)\Bigg]\Bigg)\end{aligned} \tag{1.6.9}$$

where $D(x)$ corresponds to the free propagator which value in d dimensions is

$$D(x) = \frac{1}{\Omega_{d-1}(d-2)\left(x^2\right)^{d/2-1}}, \quad \Omega_{d-1} = \frac{2\pi^{d/2}}{\Gamma(d/2)}. \tag{1.6.10}$$

In $d = 4 - \epsilon$, the perturbative expansion leads to

$$\left\langle \bar{\phi}^Q (x_f) \phi^Q (x_i) \right\rangle = \frac{Q! \left[1 - \frac{\lambda_0 Q(Q-1)}{2(4\pi)^2} \left(\frac{2}{\epsilon} + \log x_{fi}^2 + 1 + \gamma + \log \pi \right) + \mathcal{O}\left(\lambda_0^2\right)\right]}{\left[\Omega_{d-1}(d-2)\right]^Q \left(x_{fi}^2\right)^{Q\left(\frac{d}{2}-1\right)}}. \quad (1.6.11)$$

From this expression, it follows that even in the double-scaling limit $\lambda_0 \to 0$ and $Q \to \infty$ with $\lambda_0 Q$ fixed, the expansion diverges for large Q. To overcome this problem, it is convenient to perform the following transformation $\phi \to \phi/\sqrt{Q}$

$$Z_Q^2 \left\langle \bar{\phi}^Q (x_f) \phi^Q (x_i) \right\rangle = Q^Q \frac{\int \mathcal{D}\phi \mathcal{D}\bar{\phi} e^{-Q\left[\int \partial\bar{\phi}\partial\phi + \frac{Q\lambda_0}{4}\left(\bar{\phi}\phi\right)^2 - \left(\ln \bar{\phi}(x_f) + \ln \phi(x_i)\right)\right]}}{\int \mathcal{D}\phi \mathcal{D}\bar{\phi} e^{-Q\left[\int \partial\bar{\phi}\partial\phi + \frac{Q\lambda_0}{4}\left(\bar{\phi}\phi\right)^2\right]}}. \quad (1.6.12)$$

From Eq.(1.6.12), the dependence on Q and λ_0 tell us that we can compute the path integral using the saddle-point approximation for large Q keeping $Q\lambda_0$ fixed. Thus, for large charge Q, the integral is dominated by a non-trivial saddle point of the following effective action

$$S_{eff} = \int d^4x \left[\partial\bar{\phi}\partial\phi + \frac{Q\lambda_0}{4} \left(\bar{\phi}\phi\right)^2 - \left(\ln \bar{\phi}(x_f) + \ln \phi(x_i)\right) \right]. \quad (1.6.13)$$

Independently of the specific details of the saddle-point, we can express the right-hand side of (1.6.12) as follows

$$Z_{\phi^Q}^2 \left\langle \left[\bar{\phi}^Q\right](x_f) \left[\phi^Q\right](x_i) \right\rangle = Q! e^{Q\Gamma_{-1}(Q\lambda_0, x_{fi}) + \Gamma_0(Q\lambda_0, x_{fi}) + \frac{1}{Q}\Gamma_1\left(Q\lambda_0, x_{fi}\right) + \ldots}. \quad (1.6.14)$$

We renormalize Eq.(1.6.14) by separating the UV divergence in each term of the exponent as follows

$$\frac{1}{Q^k}\Gamma_k(Q\lambda^*, x_{fi}) = \frac{1}{Q^k}\Gamma_k^{\text{div}}(Q\lambda) + \frac{1}{Q^k}\Gamma_k^{\text{ren}}(Q\lambda, x_{fi}, M), \quad (1.6.15)$$

where λ is the renormalized coupling constant and M is the energy scale. Then we can write Eq.(1.6.14) as

$$Z_Q^2 = \exp\left[\sum_{k=-1}^{\infty} Q^k \Gamma_k^{\text{div}}(Q) \right], \quad (1.6.16)$$

$$\left\langle [\bar{\phi}]^Q (x_f) [\phi^Q] (x_i) \right\rangle = Q! \exp\left[\sum_{k=-1}^{\infty} Q^k \Gamma_k^{\text{ren}}(Q\lambda, x_{fi}, M) \right]. \quad (1.6.17)$$

Therefore, using Eqs.(1.6.6)(1.6.5) the scaling dimension at large charge Q takes the following form

$$\Delta_Q = \sum_{k=-1} \frac{1}{Q^k} \Delta_k (Q\lambda^*), \quad (1.6.18)$$

where every term of the expansion Δ_k represents $k+1$-loop correction to the semiclassical expansion. This result, based on general assumptions, provides a rigorous proof that it is possible to compute the CFT data at large charge Q via a semiclassical expansion.

Semiclassics on the cylinder

As we mentioned in Sec.(1.5), at the fixed point we can exploit conformal symmetry by performing a Weyl map to the cylinder $\mathbb{R}\times S^{d-1}$ of radius R. By computing the ground state with charge E_q via a semiclassical expansion, we can use the state-operator correspondence to compute the first terms in (1.6.18). The new action on the cylinder read as

$$S_{\text{cyl}} = \int d^d x\sqrt{g}\left[g^{\mu\nu}\partial_\mu\bar{\phi}\partial_\nu\phi + m^2\bar{\phi}\phi + \frac{\lambda_0}{4}(\bar{\phi}\phi)^2\right], \tag{1.6.19}$$

where mass term $m^2 = \left(\frac{d-2}{2R}\right)^2$ arises from imposing conformal invariance on the cylinder. We can extract the scaling dimension Δ_q by studying the expectation value of the evolution operator e^{-HT} acting on an arbitrary state $|\psi_Q\rangle$ with charge Q. In the limit $T\to$ we obtain

$$\lim_{T\to\infty}\left\langle\psi_Q\left|e^{-HT}\right|\psi_Q\right\rangle = e^{-E_Q T}, \quad E_Q = \frac{\Delta_Q}{R} \tag{1.6.20}$$

where E_Q is the lowest state energy with charge Q. Parametrizing an arbitrary state of charge Q as

$$|\psi_Q\rangle = \int \mathcal{D}\chi \exp\left(i\frac{Q}{\Omega_{d-1}R^{d-1}}\int d\Omega_{d-1}\chi\right)|\rho,\chi\rangle, \tag{1.6.21}$$

we can then compute the left-hand side of Eq.(1.6.20) using the path integral representation, obtaining

$$\left\langle\psi_Q\left|e^{-HT}\right|\psi_Q\right\rangle = Z^{-1}\int \mathcal{D}\rho\mathcal{D}\chi e^{-S_{\text{eff}}}, \tag{1.6.22}$$

where the effective action S_{eff} read as follows

$$S_{\text{ eff}} = \int_{\frac{-T}{2}}^{\frac{T}{2}} d\tau\int d\Omega_{d-1}\left[\frac{1}{2}(\partial\rho)^2 + \frac{1}{2}\rho^2(\partial\chi)^2 + \frac{m^2}{2}\rho^2 + \frac{\lambda_0}{16}\rho^4 + i\frac{Q}{R^{d-1}\Omega_{d-1}}\dot{\chi}\right]. \tag{1.6.23}$$

The respective equations of motion are obtained by perfoming the variation of the action (1.6.23) concerning the fields ρ and χ

$$-\partial^2\rho + \left[(\partial\chi)^2 + m^2\right]\rho + \frac{\lambda_0}{4}\rho^3 = 0, \quad i\partial_\mu\left(\rho^2 g^{\mu\nu}\partial_\nu\chi\right) = 0 \tag{1.6.24}$$

in companion with the fixed charge condition,

$$i\rho^2\dot{\chi} = \frac{Q}{R^{d-1}\Omega_{d-1}}. \tag{1.6.25}$$

The solution with minimal energy and spatially homogeneous charge is given by

$$\rho = f, \quad \chi = -i\mu\tau \tag{1.6.26}$$

where f is a constant profile and μ is the chemical potential. These quantities are related via the equations of motion as follows

$$\left(\mu^2 - m^2\right) = \frac{\lambda_0}{4}f^2, \qquad \mu f^2 R^{d-1}\Omega_{d-1} = q. \tag{1.6.27}$$

Plugging this classical solution into the action we extract the leading order contribution to the scaling dimension

$$\frac{S_{\text{eff}}}{T} = \frac{Q}{2}\left(\frac{3}{2}\mu + \frac{1}{2}\frac{m^2}{\mu}\right). \tag{1.6.28}$$

Fluctuations

The next leading contribution to the scaling dimension requires considering fluctuations around the saddle point Eq.(1.6.26). Expanding the fields around Eq.(1.6.26) as

$$\rho = f + r(x); \quad \chi = -i\mu\tau + \frac{1}{f\sqrt{2}}\pi(x), \tag{1.6.29}$$

the quadratic action $S^{(2)}$ for the fluctuations is given by

$$S^{(2)} = \int_{\frac{T}{2}}^{-\frac{T}{2}} d\tau \int d\Omega_{d-1} \left[\frac{1}{2}(\partial r)^2 + \frac{1}{2}(\partial\pi)^2 - 2i\mu\tau r\partial_\tau\pi + \left(\mu^2 - m^2\right) r^2\right] \tag{1.6.30}$$

This action describes two modes with the following dispersion relations

$$\omega_\pm^2(\ell) = J_\ell^2 + 2\left(2\mu^2 - m^2\right) \pm 2\sqrt{J_\ell^2\mu^2 + \left(2\mu^2 - m^2\right)^2}, \tag{1.6.31}$$

here $J_\ell^2 = \ell(\ell + d - 2)/R^2$ is the quantized momentum on the S^{d-1} sphere. The first mode has a gap $\omega_+^2(0) = 6\mu^2 - 2m^2$ while the massless mode ω_- describes the Goldstone boson associated to the spontaneous breaking of $U(1)$ symmetry. The associated square sound speed is $\left(\frac{d\omega_-^2}{dJ_\ell^2}\right)_{\ell=0} = \frac{\mu^2 - m^2}{3\mu^2 - m^2}$, which approuches to $\frac{1}{3}$ for large μ. Using this information, we can compute the next leading contribution to the scaling dimension as

$$\ln \frac{\sqrt{\det S^{(2)}}}{\det\left(-\partial_\tau^2 - \Delta_{S^{d-1}} + m^2\right)} = \frac{T}{2}\sum_{\ell=0}^{\infty} n_\ell \left[\omega_+(\ell) + \omega_-(\ell) - 2\omega_0(\ell)\right] \tag{1.6.32}$$

where $n_\ell = \frac{(2\ell+d-2)\Gamma(\ell+d-2)}{\Gamma(\ell+1)\Gamma(d-1)}$ is the multiplicity on the S^{d-1} and $\omega_0(\ell) = J_\ell^2 + m^2 = \left(\ell + \frac{d-2}{2}\right)^2/R^2$ is the free dispersion relation on the cylinder. Finally, the semiclassical expansion of Eq.(1.6.22) read as

$$\lim_{T\to\infty} \left\langle \psi_n \left| e^{-HT} \right| \psi_n \right\rangle = e^{-S_{\text{eff}}} \frac{\int \mathcal{D}r\mathcal{D}\pi \exp\left[-S^{(2)}\right]}{\int \mathcal{D}\phi\mathcal{D}\bar{\phi} \exp\left[-\int_{-T/2}^{T/2}\left(\partial\phi\partial\bar{\phi} + m^2\phi\bar{\phi}\right)\right]} \tag{1.6.33}$$

$$= e^{-S_{\text{eff}} - \ln\left[\frac{\sqrt{\det S^{(2)}}}{\det(-\partial^2 + m^2)}\right]} = e^{-E_q T}. \tag{1.6.34}$$

Organizing our expansion as $E_q = \frac{\Delta_Q}{R} = \frac{1}{R}\left(Q\Delta_{-1} + \Delta_0 + \ldots\right)$, we indentify each term as

$$Q\Delta_{-1} = R\frac{S_{\text{eff}}}{T}, \tag{1.6.35}$$

$$\Delta_0 = \ln\left[\frac{\sqrt{\det S^{(2)}}}{\det\left(-\partial^2 + m^2\right)}\right]. \tag{1.6.36}$$

Setting $d = 4$ and $\lambda_0 = \lambda^*$, the solution for the chemical potential (1.6.27) read as

$$R\mu^* = \frac{3^{1/3} + \left[9\frac{\lambda^* Q}{(4\pi)^2} - \sqrt{81\frac{(\lambda Q)^2}{(4\pi)^4} - 3}\right]^{2/3}}{3^{2/3}\left[9\frac{\lambda^* Q}{(4\pi)^2} - \sqrt{81\frac{(\lambda^* Q)^2}{(4\pi)^4} - 3}\right]^{1/3}}. \tag{1.6.37}$$

Considering Eqs.(1.6.35) and (1.6.28), with the solution for the chemical potential (1.6.37), we obtain the leading correction to the scaling dimension given by

$$Q\Delta_{-1} = \frac{3\left[9x-\sqrt{81x^2-3}\right]^{1/3}+3^{2/3}\left[9x-\sqrt{81x^2-3}\right]}{\left[\left(9x-\sqrt{81x^2-3}\right)^{2/3}+3^{1/3}\right]^2}+\frac{9\times 3^{1/3}x\left[9x-\sqrt{81x^2-3}\right]^{2/3}}{2\left[\left(9x-\sqrt{81x^2-3}\right)^{2/3}+3^{1/3}\right]^2} \tag{1.6.38}$$

where $x=\frac{\lambda^* Q}{(4\pi)^2}$ is the 't Hooft coupling constant. Remarkably this quantity Eq.(1.6.38) resums an infinite number of Feynman diagrams in a close form. For small x reproduces standard perturbation theory, while for large x reproduces the large charge expansion

$$Q\Delta_{-1} = \begin{cases} Q\left[1+\frac{1}{2}\left(\frac{\lambda^* Q}{16\pi^2}\right)-\frac{1}{2}\left(\frac{\lambda^* Q}{16\pi^2}\right)^2+O\left(\frac{(\lambda^* Q)^3}{(4\pi)^6}\right)\right], & \text{for} \quad x\ll 1, \\ \frac{8\pi^2}{\lambda^*}\left[\frac{3}{4}\left(\frac{\lambda^* Q}{8\pi^2}\right)^{4/3}+\frac{1}{2}\left(\frac{\lambda^* Q}{8\pi^2}\right)^{2/3}+O(1)\right], & \text{for} \quad x\gg 1 \end{cases} \tag{1.6.39}$$

While (1.6.38) is a finite quantity, Eq.(1.6.36) is divergent and requires regularization. By performing dimensional regularization and subtracting the infinite part, we can write the final result as a finite sum, this results in the following expression

$$\Delta_0 = -\frac{15(R\mu^*)^4+6(R\mu^*)^2-5}{16}+\frac{1}{2}\sum_{\ell=1}^{\infty}\sigma(\ell)+\frac{\sqrt{3(R\mu^*)^2-1}}{\sqrt{2}}, \tag{1.6.40}$$

where $\sigma(\ell)$ is obtained by subtracting the divergent piece

$$\sigma(\ell) = (1+\ell)^2 R\left[\omega_+^*(\ell)+\omega_-^*(\ell)\right]-2\ell^3-6\ell^2-\left(2(R\mu^*)^2+4\right)\ell-2(R\mu^*)^2+\frac{5\left((R\mu^*)^2-1\right)^2}{4\ell}. \tag{1.6.41}$$

The star indicates that all quantities are evaluated setting $\lambda_0=\lambda^*$ and $d=4$. This computation shows explicitly that the scaling dimension of the lightest charge ϕ^Q operators in the $U(1)$ model at the W-F point in $d=4-\epsilon$ can be computed semiclassically for arbitrary values of $Q\epsilon$.

1.7 Dilaton Dressing

In this last section, we will introduce the notion of dilaton dressing, which is relevant to the study of near-conformal dynamics. Moreover, we will show how to employ the large charge expansion within this context. This framework is based on the observation that in certain regimes—such as at sufficiently high energies—the effects of terms that break conformal symmetry are negligible, allowing us to assume that scale transformation is an approximate symmetry. Under this assumption, it is possible to explore near-conformal theories by introducing a new light scalar degree of freedom known as the dilaton, which compensates for the terms that are not conformally invariant. Dilatation transformations are coordinate transformations of the form [40]

$$\alpha: \quad x\to e^{\alpha}x \tag{1.7.1}$$

where α is a real parameter. Assuming a near conformal behavior, we promote the theory to be scale-invariant by performing a dilaton dressing. Every operator $\mathcal{O}_k$ of mass dimension k is dressed as

$$\mathcal{O}_k \to e^{(k-4)\sigma f}\mathcal{O}_k, \tag{1.7.2}$$

where the dilaton σ is a field that transforms non-linearly under scale transformations

$$\sigma \to \sigma - \frac{\alpha}{f}. \tag{1.7.3}$$

being f a dimensionful constant that marks the scale of the breaking of conformal invariance. We will employ this technique to investigate the low-energy dynamics of a gauge-fermion theory near the conformal window. To illustrate this we consider a conformal theory with $U(1)$ global symmetry. Fixing the associated charge Q breaks the symmetry spontaneously and gives rise to a Goldstone boson. A two-derivative effective field theory for the associated Goldstone boson χ is the following

$$\mathcal{L} = \frac{f_\pi^2}{2}\partial_\mu\chi\partial^\mu\chi - C^4, \tag{1.7.4}$$

where f_π and C are constants related to the underlying theory. By applying the dressing (1.7.2) we obtain,

$$\mathcal{L}_{CFT} = \frac{f_\pi^2}{2}\partial_\mu\chi\partial^\mu\chi e^{-2\sigma f} - C^4 e^{-4\sigma f} + \frac{1}{2}\Big(\partial_\mu\sigma\partial^\mu\sigma - \frac{\xi R}{f^2}\Big)e^{-2\sigma f}, \tag{1.7.5}$$

where, additionally, we have applied a Weyl map to the cylinder in order to use the state-operator correspondence. We have included the conformal coupling $\xi = 1/6$ and the Ricci scalar R. Using this approach, we have obtained an EFT for two Goldstone bosons, χ and σ, arising from the spontaneous breaking of $U(1)$ and conformal symmetry, respectively. Is it possible to combine these two fields into a complex dilaton as

$$\Sigma = \sigma + i f_\pi \chi \tag{1.7.6}$$

and defining $\varphi = \frac{1}{\sqrt{2}f}e^{-f\Sigma}$. The action $\mathcal{L}_{CFT}$ can be recast in the form

$$\mathcal{L}[\varphi] = \partial_\mu\varphi^*\partial^\mu\varphi - \xi R\,\varphi^*\varphi - 4C^4 f^4(\varphi^*\varphi)^2\,. \tag{1.7.7}$$

We recognize that we have restored a $U(1)$ conformal theory in which the dilaton and the phonon appear, respectively, as the radial and the angular modes for φ. The three dimensionful constants f_π, C and f are combined into the two dimensionless quantities $b = f f_\pi$ and $u = 4C^4 f^4$. The parameter b, controls the deficit angle for the field φ, which covers the whole complex plane only if $b = 1$. Possible sources of explicit conformal breaking can be modeled by perturbing the underlying conformal theory via

$$\delta L_{\mathcal{O}} = \lambda_{\mathcal{O}}\mathcal{O}\ , \tag{1.7.8}$$

with $\mathcal{O}$ an operator with dimension $\Delta \neq 4$ and $\lambda_{\mathcal{O}}$ the associated coupling. The presence of such an operator generates the following effective dilaton potential [41, 42, 43, 44, 45, 46]

$$V(\sigma) = f^{-4}\, e^{-4\sigma f} \sum_{n=0}^{\infty} c_n\, e^{-n(\Delta-4)f\sigma}\ , \tag{1.7.9}$$

where the coefficients c_n depend on the microscopic theory and scale as $c_n \sim \lambda_{\mathcal{O}}^n$ [41, 43, 46, 45]. We are interested in cases where the explicit conformal breaking is small which, in turn, can be realized when $\lambda_{\mathcal{O}} \ll 1$ and/or $\Delta \to 4$. In the first case, one can truncate the expansion (3.5.4) and obtain [41, 43, 46, 45, 47]

$$V(\sigma) = \frac{m_\sigma^2 e^{-4f\sigma}}{4(4-\Delta)f^2}\left(1 - \frac{4}{\Delta}e^{-(\Delta-4)f\sigma}\right) + \mathcal{O}(\lambda_{\mathcal{O}}^2)\ , \tag{1.7.10}$$

where we introduced the dilaton mass m_σ and required that the ground state is realized for $\sigma = 0$. In the EFT spirit, the nature of the conformal breaking deformation and its conformal dimension Δ are left unspecified. When $\Delta = 2$ eq.(3.5.5) reduces to the usual ϕ^4 Higgs-like potential whereas when Δ vanishes the coefficient c_1 becomes parametrically larger than c_0 and the potential (3.5.5) diverges. On the other hand, by subtracting the infinite constant appearing in the expansion of Eq. (3.5.5) around $\Delta = 0$ one obtains the dilaton potential considered in the classic work of Coleman [48]

$$V^{(2)}_{\Delta\to 0}(\sigma) = -\frac{m_\sigma^2}{16 f^2}\left(1 - 4f\sigma - e^{-4f\sigma}\right) \,. \tag{1.7.11}$$

For the sake of completeness, we will also consider the traditional Coleman potential in the following analyses. We can induce a near conformal behavior by including a mass potential for the dilaton σ as follows

$$L_m[\chi, \sigma] = L_{CFT}[\chi, \sigma] - V^{(2)}_{\Delta\to 0}(\sigma) \tag{1.7.12}$$

It is through this deformation that one can continuously break conformal symmetry. Indeed, now the energy-momentum tensor is no longer traceless, its trace is proportional to the dilaton mass

$$T^\mu_\mu = \frac{m_\sigma^2}{f}\sigma \,. \tag{1.7.13}$$

The fixed-charge ground state is homogeneous and of the form

$$\chi = \mu t, \quad \sigma = \sigma_0, \tag{1.7.14}$$

using the equations of motion we find that energy on the cylinder is given by

$$r_0 E_{\text{cyl}} = \frac{c_{4/3}}{(4\pi^2)^{1/3}} Q^{4/3} + c_{2/3} Q^{2/3} + c_0 - \frac{\pi^2 m_\sigma^2 r_0^4}{3 f^2}\log Q + \dots \tag{1.7.15}$$

where $c_{4/3} = 3\left(C/\left(2f_\pi\right)\right)^{4/3}$, $c_{2/3} = \left(\pi/\left(f_\pi \Lambda^2\right)\right)^{2/3}/\left(2f^2\right)$ and c_0 is a Q-independent constant. Therefore, the dilaton mass m_σ leads to a characteristic logarithmic term $\log Q$. For $m_\sigma = 0$ this result reproduces the expected behavior of a four-dimensional CFT. This computation shows that it is possible to explore near-conformal dynamics using the large charge expansion via a dilaton field σ.

Chapter 2

The analytic structure of the large charge expansion

In Chapter 1, we have shown that it is possible to use the large charge expansion to investigate the conformal data of the $U(1)$-model at the W-F point in $d = 4 - \epsilon$. In particular, using a semiclassical expansion, is it possible to write the scaling dimension Δ_Q of charged operators ϕ^Q in the following way

$$\Delta_Q = \sum_{j=-1} \frac{1}{Q^j} \Delta_j (x) \,, \tag{2.0.1}$$

where x is the 't Hooft coupling. By expanding the Δ_j in the small x limit, one recovers the ordinary perturbative expansion [49], while for large x, Eq.(2.0.1) reproduces the general form of the large-charge expansion in generic non-supersymmetric relativistic CFTs [1] [11, 35, 38]

$$\Delta_Q = Q^{\frac{d}{d-1}} \left[\alpha_1 + \alpha_2 Q^{\frac{-2}{d-1}} + \dots\right] + Q^0 \left[\beta_0 + \beta_1 Q^{\frac{-2}{d-1}} + \dots\right] + \mathcal{O}\left(Q^{-\frac{d}{d-1}}\right), \tag{2.0.2}$$

In this chapter, we investigate the analytic properties of the fixed charge expansion for several conformal field theories in different space-time dimensions. The models of interest are $O(N)$ and QED_3. In [50], the authors considered the spectrum of charge Q operators for the critical $O(N)$ model in $d = 3$ dimensions in the double-scaling limit

$$Q \to \infty \,, \qquad N \to \infty \,, \qquad \frac{Q}{N} = \text{fixed} \,. \tag{2.0.3}$$

In this limit, the scaling dimensions of the lowest-lying operators with total charge Q assume the form [51]

$$\Delta_Q = \sum_{j=-1} \frac{1}{N^j} \Delta_j \left(\frac{Q}{N}\right) . \tag{2.0.4}$$

The small $\frac{Q}{N}$ expansion of Δ_{-1} is convergent with a radius of convergence related to the appearance of a zero-mode in the spectrum. On the other hand, the large $\frac{Q}{N}$ expansion of Δ_{-1} diverges $(2n)!$ factorially, and its Borel transform exhibits an infinite number of singularities on the positive real axis which, according to resurgence theory [2], indicate the

[1] When d is even, one needs to include in the expansion $Q^p \log(Q)$ terms, with p to be determined, induced by the cancellation of UV divergences [38].

[2] Notice that a priori is not known whether QFT observables satisfy the axiom of resurgence theory, i.e they are *resurgent functions*. In this work, we *assume* this condition. For a recent discussion on this point, including counterexamples, we refer the interested reader to [52].

emergence of non-perturbative corrections. The leading non-perturbative contributions scale as $e^{-\sqrt{Q}}$ and stem from worldline instantons describing the geodesic motion of a free particle with mass μ moving on close trajectories [53].

We aim to add information on the convergence properties of the large-charge expansion by addressing various models displaying very different large order behaviors. We will encounter convergent, asymptotic but Borel summable, and non-Borel summable series; in the first case, we will investigate what one can learn on the physics of the expansion from a finite number of coefficients. To this end, our main tool will be the Darboux's theorem [54, 55], which relates the behavior of a function around its non-analytical points to the rate of growth of the coefficients of its series expansion around regular points. Physical applications were explored in [54, 56, 57, 58, 59, 60, 61, 62, 63, 64].

First, we consider the critical $g^2(\phi_i\phi_i)^3$ theory in $d = 3-\epsilon$, which has been investigated in [12, 65] in the double-scaling limit

$$Q \to \infty\,, \qquad g \to 0\,, \qquad gQ = \text{fixed}\,. \tag{2.0.5}$$

resulting in the following semiclassical expansion

$$\Delta_Q = \sum_{j=-1}^{\infty} g^{*j}\Delta_j(g^*Q)\ , \tag{2.0.6}$$

where $g^* = g^*(\epsilon)$ is the coupling at the Wilson-Fisher fixed point. We discover that the small-charge (i.e. the small gQ) expansions of Δ_{-1} and Δ_0 are convergent and share the same radius of convergence. We observe that, as in [50], the leading singularity, which is an algebraic branch point, occurs when the mass of a certain mode vanishes. Moreover, the small gQ expansion of Δ_0 provides an interesting example of how the program of reconstructing the analytic structure of a function from a limited number of expansion coefficients can fail. In fact, even the precise identification of the radius of convergence requires more than one hundred expansion coefficients. However, we are able to make progress by identifying the source of the problem in the occurrence of two coincident singularities for which we can disentangle their contributions.

In $d = 3-\epsilon$ dimensions the contribution to the $O(N)$ fixed charge Q conformal dimensions obtained in the double scaling limit of large charge and vanishing ϵ is non-Borel summable, doubly factorial divergent, and with order $\sqrt{Q}$ optimal truncation order. By using resurgence techniques we show that the singularities in the Borel plane are related to worldline instantons that were discovered in the other double scaling limit of large Q and N of [50]. In $d = 4-\epsilon$ dimensions the story changes since in the same large Q and small ϵ regime the next order corrections to the scaling dimensions lead to a convergent series. The resummed series displays a new branch cut singularity which is relevant for the stability of the $O(N)$ large charge sector for negative ϵ. Although the QED_3 model shares the same large charge behaviour of the $O(N)$ model, we discover that at leading order in the large number of matter field expansion, the large charge scaling dimensions are Borel summable, single factorial divergent, and with order Q optimal truncation order.

Before going into a detailed analysis, we review some basic concepts of the theory of resurgence. This is based on the pedagogical book written by Marcos Mariño [66]

2.1 Resurgence Basics

In QM as well as QFT, there are few cases in which one is able to find an exact solution. Generally, we have to resort to perturbation theory, where we take an exact solution and

perturb it by some small coupling. This procedure results in an asymptotic power series that approximates our observable. Though these expansions provide good experimental agreement, many of these formal power series are divergent. Resurgence aims to make sense of these asymptotic series by extending them into trans-series, including non-analytic terms. The structure of these non-analytic terms is dictated by the large-order behavior of the perturbative expansion coefficients, which contain the non-perturbative physics. In summary, resurgence provides a framework to deal with asymptotic series by using the hidden non-perturbative information of the coefficients large order behavior.

Optimal truncation

Formally, we say that a power series is asymptotic to $\mathcal{O}(z)$ if for every N the remainder $N+1$ terms are much smaller as $z \to 0$

$$\left| \mathcal{O}(z) - \sum_{n=0}^{N} a_n z^n \right| \sim a_{N+1} z^{N+1} + \mathcal{O}\left(z^{N+2}\right), \quad z \ll 1. \tag{2.1.1}$$

Unlike a convergent series, the remainder does not go to zero as $N \to \infty$. One would expect that adding more terms to the power series would reproduce exactly $\mathcal{O}(z)$, however, this is not typically the case. This means that even if we add an infinite number of terms the result will be infinite. Dyson [67] first pointed out this fact in the context of QED. He argued that if observables were analytical in e^2, then it would imply that are convergent in a disk in $\mathbb{C}$. Since the physics for negative e^2 is completely different from that of positive values (the vacua is unstable), we should not expect an analytic continuation of QED for negative values of e^2. Thus, the series are not convergent. Technically the origin of this divergence relies on the fact that the asymptotic behavior coefficients of the perturbative expansion are of the form

$$a_n \sim A^{-n} n!. \tag{2.1.2}$$

which leads to a zero radius of convergence. This behavior implies that as we increase N the series will approuch to $\mathcal{O}(z)$ but, inevitably, will diverge for large N. Thus, it is natural to ask what is the optimal value $N = N^*$ such that the partial sum gives the best estimation of $\mathcal{O}(z)$. For a fixed z, minimizing the reminder of (2.1.1) we have

$$\partial_n \left| A^{-n} n! z^n \right| \Big|_{n=N^*} = 0, \tag{2.1.3}$$

using the Stirling approximation $n! \sim \mathrm{e}^{n(\log n - 1)}$ we get $N^* = \left|\frac{A}{z}\right|$ for $z \ll 1$. This procedure is called *optimal truncation* and determines the maximum resolution we can expect from the asymptotic expansion. Replacing the optimal value $N = N^*$ is in Eq. (2.1.1) we find that

$$\left| \mathcal{O}(z) - \sum_{n=0}^{N^*} a_n z^n \right| \sim e^{-|A/z|}, \quad z \ll 1. \tag{2.1.4}$$

This result shows that the error associated to the optimal value $N = N^*$ is given by a non-perturbative ambiguity $e^{-|A/z|}$. Moreover, we can see a relation between the leading order behavior of the perturbative expansion a_n and the non-analytic term that perturbation theory ignores. It follows that the asymptotic expansion does not determine the function $\mathcal{O}(z)$ uniquely, and some extra information is required. Though a finite number of coefficients provide a good estimate of the asymptotic expansion, it is possible to use all the terms of the perturbative expansion within a more rigorous framework. The idea is to promote formal power series to well-behaved functions by combining them with non-perturbative terms. This process is called Borel resummation.

Borel Resummation

The Borel transform is a standard tool used to make sense of asymptotic series and extend them into regular functions. Given an asymptotic series $\varphi(z)$ of the form

$$\varphi(z) = \sum_{n\geq 0} a_n z^n, \tag{2.1.5}$$

the Borel transform is defined as

$$B[\varphi](t) = \sum_{n=0}^{\infty} \frac{a_n}{n!} t^n. \tag{2.1.6}$$

If the coefficients a_n are of the form Eq. (2.1.2), the Borel transform Eq.(2.1.6) is analytic around $t = 0$ and its coefficients grow exponentially, the first singularity is located at the point $t = A$. If the real positive axis is free of singularities we can define the inverse Borel transforms as follows

$$s(\varphi)(z) = \int_0^{\infty} dt \mathrm{e}^{-t} B[\varphi](zt), \tag{2.1.7}$$

in such a case, we say that the power series φ is Borel summable. Both φ and $s(\varphi)$ are asymptotically equivalent to the same divergent series. In the case of singularities in the positive real axis, the integral defined in Eq.(2.1.7) is not longer well defined. We can deform the contour of integration passing above or below the poles using Borel lateral transform

$$s_{\pm}(\varphi)(z) = \frac{1}{z} \int_{\mathcal{C}_{\pm}} dt \mathrm{e}^{-t/z} B[\varphi](t), \tag{2.1.8}$$

here $\mathcal{C}_{\pm}$ denotes a contour passing above or below the pole respectively. Let us consider a perturbative behavior of the form (2.1.2) for $A > 0$. The associated Borel transform is given by

$$B[\varphi](t) = \sum_{n=0}^{\infty} A^{-n} t^n = \frac{1}{1 - t/A}, \tag{2.1.9}$$

which has a simple pole at $t = A$. The ambiguity of the lateral resummation is simply given by

$$\epsilon(z) = s_+(\varphi)(z) - s_-(\varphi)(z) = \frac{1}{z} \int_{\mathcal{C}_+ - \mathcal{C}_-} dt \mathrm{e}^{-t/z} B[\varphi](t) \tag{2.1.10}$$

$$= \frac{1}{z} \oint_{\mathcal{C}_A} dt \frac{e^{-t/z}}{1 - t/A} = \frac{2\pi i}{x} A e^{-A/x} \tag{2.1.11}$$

where $\mathcal{C}_A$ is a closed path around the pole $t = A$. In this simple example, non-perturbative corrections arise as ambiguities along rays where the poles in the Borel plane lie. Let us consider a more general behavior of the form

$$\varphi(z) = \sum_{n=0}^{\infty} \Gamma(n + b) A^{-n} z^n, \tag{2.1.12}$$

which leads to

$$B[\varphi](t) = \Gamma(b)\left(1 - \frac{t}{A}\right)^{-b} \tag{2.1.13}$$

In this case the discontinuity is no longer the residue on the pole, but rather the integral of the discontinuity along the branch cut $[A, \infty]$. This is given by

$$\epsilon(z) = \frac{\Gamma(b)}{t}\int_A^\infty dt e^{-t/z} \lim_{\epsilon\to 0}\left[\left(1 - \frac{e^{+i\epsilon}t}{A}\right)^{-b} - \left(1 - \frac{e^{-i\epsilon}t}{A}\right)^{-b}\right], \tag{2.1.14}$$

$$= 2\pi i A^b z^{-b} e^{-A/z}. \tag{2.1.15}$$

Trans-series

So far, we have seen that the large-order behavior of the perturbative expansion characterizes the analytic structure of the Borel plane. This, in turn, determines the non-perturbative ambiguity of the Borel resummation. We can cancel these non-perturbative ambiguities by incorporating them into a more general object called a trans-series. For simplicity, let us consider a trans-series of following form

$$\Phi(z) = \varphi^{(0)}(z) + \sum_{\ell=1}^{\infty} C_\ell \mathrm{e}^{-\frac{\ell A}{z}} \varphi^{(\ell)}(z), \tag{2.1.16}$$

where $\varphi^{(\ell)}$ are asymptotic series

$$\varphi^{(\ell)}(z) = \sum_{\ell=0}^{\infty} a_n^{(\ell)} z^n, \tag{2.1.17}$$

$\varphi^{(0)}$ is the original perturbative expansion and the constants C_ℓ are the trans-series parameters. These coefficients, play the important role of ensuring a well-behaved resummation. Given $B[\varphi^{(0)}](t)$, we expect it have singularities at $t = A\ell$ for $\ell \in \mathbb{N}$. It can be shown that the expansions around these singularities are related to the Borel transforms of the series of the other non-perturbative sectors. For logarithmic branch-cuts we have

$$B[\varphi^{(0)}](t)\Big|_{t=\ell A} = -\frac{\mathrm{S}^\ell}{2\pi\mathrm{i}} \log(t) B[\varphi^{(\ell)}](t) \tag{2.1.18}$$

where S is called Stokes constant. Since the singularities of the Borel transform are related to the large-order behavior of their associated asymptotic series we can rewrite the relation (2.1.18) in terms of the coefficients $a_n^{(j)}$

$$a_n^{(0)} \approx \Gamma(n) A^{-n} \sum_{\ell=1}^{\infty} \frac{\mathrm{S}^\ell}{2\pi\mathrm{i}} \ell^{-n} \sum_{k=0}^{\infty} (\ell A)^k \frac{\Gamma(n-k)}{\Gamma(n)} a_k^{(\ell)}. \tag{2.1.19}$$

In the following sections, we will study the large-order behavior of the large charge expansion for different models. We will identify the poles in the Borel plane and the non-perturbative contribution to the scaling dimension of charged operators.

2.2 The $O(N)$ model in $d = 3 - \epsilon$

In this section, we consider the sextic $O(N)$ CFT in $d = 3 - \epsilon$ with the Lagrangian

$$\mathcal{L} = \frac{1}{2}\partial^\mu \phi_i \partial_\mu \phi_i + \frac{g^2}{8 \times 3!}(\phi_i \phi_i)^3. \tag{2.2.1}$$

where ϕ_i, $i = 1, \ldots, N$, transforms as a $O(N)$-vector. This model exhibits an infrared stable fixed point at [68]

$$\frac{g^2}{(4\pi)^2} = \frac{2\epsilon}{22 + 3N} + \mathcal{O}\left(\epsilon^2\right) . \tag{2.2.2}$$

Interestingly, the beta function of the g coupling is non vanishing from two-loops, and the model is, therefore, conformally invariant in $d = 3$ at the one-loop level. This property will allow us to directly compare our results to those in [50] and link them to the large-charge effective theory describing the three-dimensional $O(N)$ CFT. In [65], the scaling dimension of the lowest-lying operators with total charge Q [3] has been computed in the double-scaling limit (2.0.5), where one can perform the semiclassical expansion of (2.0.6). The leading order Δ_{-1} is given by evaluating the action on the non-trivial classical trajectory induced by fixing the charge and it reads

$$\Delta_{-1}(gQ) = gQF_{-1}\left(\frac{g^2Q^2}{2\pi^2}\right) , \quad F_{-1}(x) = \frac{1 + \sqrt{1+x} + \frac{x}{3}}{\sqrt{2}(1+\sqrt{1+x})^{\frac{3}{2}}} , \quad x = \frac{g^2Q^2}{2\pi^2} . \tag{2.2.4}$$

At the next-to-leading order of the semiclassical expansion (2.0.6), one needs to compute the functional determinant of the fluctuations around the classical solution. This can be formally written as

$$\Delta_0(gQ) = \Delta_0^{(a)}(gQ) + \left(\frac{N}{2} - 1\right)\Delta_0^{(b)}(gQ) , \tag{2.2.5}$$

with

$$\Delta_0^{(a)}(gQ) = \frac{1}{2}\sum_{\ell=0}^{\infty} n_\ell [\omega_+(\ell) + \omega_-(\ell)] , \tag{2.2.6}$$

$$\Delta_0^{(b)}(gQ) = \sum_{\ell=0}^{\infty} n_\ell \, \omega_*(\ell) . \tag{2.2.7}$$

Here

$$\omega_\pm^2(\ell) = J_\ell^2 + 2\left(2\mu^2 - \frac{(d-2)^2}{4}\right) \pm 2\sqrt{J_\ell^2\mu^2 + \left(2\mu^2 - \frac{(d-2)^2}{4}\right)^2} , \qquad \omega_*(\ell) = \sqrt{J_\ell^2 + \mu^2} , \tag{2.2.8}$$

[3] It can be shown that in the perturbative regime, i.e. in absence of level-crossing, these operators transform as traceless symmetric $O(N)$ tensors and can be written as

$$T_Q = t_Q^{i_1 \ldots i_Q}(\phi_i) , \tag{2.2.3}$$

where $t_Q^{i_1 \ldots i_Q}(\phi_i)$ is a fully symmetric and traceless homogeneous polynomial of degree Q in the ϕ_i's. For instance $t_1^i(\phi) = \phi^i$ and $t_2^{ij}(\phi) = \phi^i\phi^j - \frac{1}{N}\delta^{ij}\phi_k\phi_k$. Physically, the Δ_Q control the critical behavior of $O(N)$-invariant systems subject to anisotropic perturbations, e.g. density-wave systems [69], magnets with a cubic crystal structure [70], and superconductors [71].

are the dispersion relations of the spectrum. The latter contains a massless mode ω_-, (the *conformal mode*), a gapped mode ω_+ with mass $\omega_+(0) = 2\sqrt{2\mu^2 - \frac{(d-2)^2}{4}}$ (the *radial mode*) as well as $(N-2)$ gapped modes ω_* with mass $\omega_*(0) = \mu$ (the *spectator modes*). The above expressions are explicit functions of the chemical potential μ, which is related to the 't Hooft coupling gQ through the equations of motion as [4]

$$\mu = \frac{1}{2\sqrt{2}}\sqrt{1+\sqrt{1+\frac{g^2Q^2}{2\pi^2}}}\,. \tag{2.2.9}$$

After regularizing the sums over ℓ in Eq.(2.2.7), one obtains the following final expression for the functional determinants [65]

$$\Delta_0^{(a)}(gQ) = \frac{1}{4} - 3\mu^2 + \tfrac{1}{2}\sqrt{8\mu^2-1} + \frac{1}{2}\sum_{\ell=1}^{\infty}\sigma^{(a)}(\ell)\,, \tag{2.2.10}$$

$$\Delta_0^{(b)}(gQ) = -\frac{1}{4} - \mu^2 + \mu + \frac{1}{2}\sum_{\ell=1}^{\infty}\sigma^{(b)}(\ell)\,, \tag{2.2.11}$$

where

$$\sigma^{(a)}(\ell) = (1+2\ell)[\omega_+(\ell)+\omega_-(\ell)] - 4l(l+1) - 6\mu^2 + \frac{1}{2}\,, \tag{2.2.12}$$

$$\sigma^{(b)}(\ell) = 2(1+2\ell)\omega_*(\ell) - 4l(\ell+1) - 2\mu^2 - \frac{1}{2}\,, \tag{2.2.13}$$

are convergent sums.

2.2.1 The small-charge expansion

Equipped with the basic setup above we can now study the convergence properties of the small gQ expansion of Δ_{-1} (2.2.4) and Δ_0 (2.2.5). In this limit, Δ_{-1} is convergent with a radius of convergence determined by the only non-analytical point at $x_0 = -1$. [5] It is therefore instructive to determine how many coefficients of the small gQ expansion are needed in order to fully characterize the singularity. This is achieved by making use of the Darboux's theorem which links the large order behaviour of the expansion coefficients about one point (which we take to be $x = 0$) to the behaviour of the function in the vicinity of its singularities. Concretely, if the perturbative coefficients of a function $\mathcal{O}(x) = \sum c_n x^n$ grow as

$$c_n \sim \frac{1}{x_0^n}\left[f(x_0)\binom{n+p-1}{n} - x_0 f'(x_0)\binom{n+p-2}{n} + \frac{x_0^2}{2!}f''(x_0)\binom{n+p-3}{n} - \dots\right] + \dots\,, \tag{2.2.14}$$

then x_0 corresponds to the closest singularity to the origin and further determines the radius of convergence of the expansion around $x = 0$. Moreover, in the vicinity of x_0, $\mathcal{O}(x)$ behaves as

$$\mathcal{O}(x) = f(x)\left(1 - \frac{x}{x_0}\right)^{-p} + \text{analytic}\,, \qquad x \to x_0\,, \tag{2.2.15}$$

[4] The chemical potential is measured in units of the compactification radius (which is fixed to unity) and is, therefore, dimensionless.

[5] Since $x_0 < 0$, one can trivially analytically continue the small-charge expansion to every positive value of x and continuously connect the small- and large-charge expansions for any real value of gQ.

	small $Q\epsilon$						large $Q\epsilon$	
	$O(N)$ in $d=3-\epsilon$			$O(N)$ in $d=4-\epsilon$			$O(N)$ in $d=3-\epsilon$	$O(N)$ in $d=4-\epsilon$
Δ_j	Δ_{-1}	$\Delta_0^{(a)}$	$\Delta_0^{(b)}$	Δ_{-1}	$\Delta_0^{(a)}$	$\Delta_0^{(b)}$	Δ_{-1}	Δ_{-1}
n	20	>100	22	25	>100	13	28	36

Table 2.2.1: Number of expansion coefficients needed to determine, with a 5 digits accuracy, the position (x_0), type (p), and amplitude ($f(x_0)$) of the leading singularity in the coefficient functions Δ_j in the $O(N)$ model in $d=3-\epsilon$ and $d=4-\epsilon$ dimensions. In the case of Δ_0, we separate the contribution of $\Delta_0^{(a)}$ and $\Delta_0^{(b)}$ as in Eq.(2.2.5). In order to accelerate the convergence, we made use of the Richardson extrapolation [73], which in all cases performed better than other series acceleration methods, e.g. Shanks transforms [74] and Padé approximants.

with $f(x)$ an analytic function near x_0. Given the c_n, the parameters entering Eq.(2.2.14) can be determined by considering various sequences which tend to them in the limit $n\to\infty$ and making use of acceleration methods to improve the convergence. For instance, the ratio of consecutive coefficients c_n/c_{n-1} converges to $1/x_0$ as $n\to\infty$ [6], whereas p and $f(x_0)$ can be found by considering the following sequences

$$p=1+\lim_{n\to\infty} n\left(x_0\frac{c_n}{c_{n-1}}-1\right)\,, \tag{2.2.16}$$

$$f(x_0)=\lim_{n\to\infty}\frac{c_n}{\left(\frac{1}{x_0}\right)^n\binom{n+p-1}{n}}\,. \tag{2.2.17}$$

In a similar manner, one can determine all the derivatives $f^{(n)}(x_0)$ and relevant parameters characterizing the subleading singularities [54, 55, 72]. As summarized in Table 2.2.1, by analyzing 20 coefficients of the small-charge expansion of Δ_{-1}, we learn that they satisfy Eq.(2.2.14) with $x_0=-1$, $p=-3/2$, $f(x_0)=-\frac{1}{12\sqrt{2}}$. With the same number of coefficients, we find also that $f'(x_0)=-0.051559(1)$, while computing higher derivatives of $f(x)$ requires an increasing number of coefficients. For instance, to obtain $f''(x_0)=-0.091150(1)$ and $f'''(x_0)=-0.2467(1)$, we had to consider 46 and 89 coefficients, respectively. .

Physically, when $x=x_0$ the chemical potential takes the value $\mu(x_0)=\frac{1}{2\sqrt{2}}$ and the mass of the radial mode ω_+ vanishes in $d=3$. Therefore, as in the large-N analysis of [50], the radius of convergence is dictated by the requirement of positive masses.

In order to study the small gQ expansion of Δ_0 we consider separately $\Delta_0^{(a)}=\sum_{n=0}a_n^{(a)}x^n$ and $\Delta_0^{(b)}=\sum_{n=0}a_n^{(b)}x^n$. In the $\Delta_0^{(a)}$ case, the ratio test to determine the radius of convergence exhibits a slow convergence while the sequence (2.2.17), fails to converge even with more than one hundred coefficients. The poor performance of the approach can be understood simply by inspecting the $\mu(x)$ dependence of $\Delta_0^{(a)}$ in Eq. (2.2.10). Here one immediately observes the emergence of two different singular behaviour at x_0, one coming from the square root term (3rd term) that has a branch cut that goes like $(1+x)^{1/4}$ (corresponding to $p=-1/4$) while the rest of the expression has an expected branch cut that goes like $(1+x)^{1/2}$ (corresponding to $p=-1/2$) . Making use of this knowledge we can accelerate the convergence process. We conclude that the slow convergence of Eq.(2.2.17)

[6] The radius of convergence can be found also by considering $\lim_{n\to\infty}|a_n|^{-1/n}=x_0$. However, for the series considered in this paper, the simple ratio test performs better.

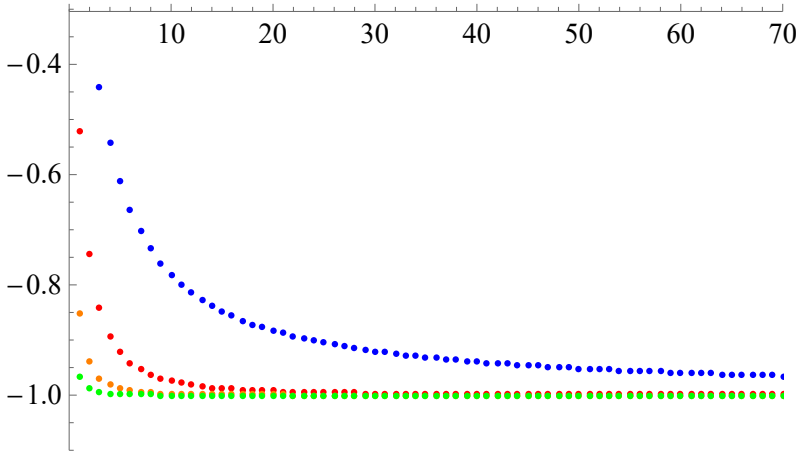

Figure 2.1: In this figure, we show the ratio of consecutive coefficients $\frac{b_n}{b_{n-1}}$ of the large gQ expansion of Δ_{-1} for growing n. The blue line represents the original coefficients, while the red, orange, and green lines denote, respectively, the first three Richardson extrapolations. The ratio tends to the value $1/x_0 = -1$.

when considering the full $a_n^{(a)}$ is due to the presence of two coincident singularities [7]. Being all the terms in Eq.(2.2.11), regular in $\mu(x_0)$ the convergence of the various ratio tests is much higher in the $\Delta_0^{(b)}$ case as shown in Table 2.2.1. We conclude that near $x_0 = -1$, Δ_0 behaves as

$$\Delta_0 = f(x)\,(1+x)^{1/4} + g(x,N)\,(1+x)^{1/2} + \text{analytic}\,. \tag{2.2.18}$$

2.2.2 The large-charge expansion

As shown above, the small gQ expansion of Δ_{-1} and Δ_0 is convergent. Here, we move to investigate the large gQ expansion, which, as we shall see, in the case of Δ_0 is asymptotic and non-Borel summable. The large gQ expansion of $\Delta_{-1} = gQx^{1/4}\sum_{n=-0} b_n x^{-n/2}$ is convergent as can be seen from the ratio of consecutive coefficients, which is depicted in Fig.2.1. The radius of convergence is again determined by the singularity at $x_0 = -1$. The number of coefficients one needs to precisely characterize the singularity is similar to the small gQ case, as shown in Table 2.2.1.

For the large gQ expansion of Δ_0 we focus on analytically determining the large-charge expansion of $\Delta_0^{(b)}$ and leave $\Delta_0^{(a)}$ for future work. As we shall see later, due to the factor of N in Eq.(2.2.5), our conclusions will not be affected by the inclusion of radial and conformal modes. In order to compute the large μ expansion of $\Delta_0^{(b)}$, we follow [65] and separate the positive powers of μ as

$$\Delta_0^{(b)} = a_{-3}\mu^3 + a_{-1}\mu + \sum_{l=0}(2\ell+1)\sqrt{\mu^2+\ell(\ell+1)}\,. \tag{2.2.19}$$

The value of $a_{-3} = -2/3$ and $a_{-1} = 1/3$ has been computed in [65] by performing a numerical fit to $\Delta_0^{(b)}$ and will be confirmed below via an analytical computation. By

[7] A possible strategy to deal with the lack of convergence due to nearby or coincident singularities consists in dividing out the strongest singularity and considering the obtained coefficients [54].

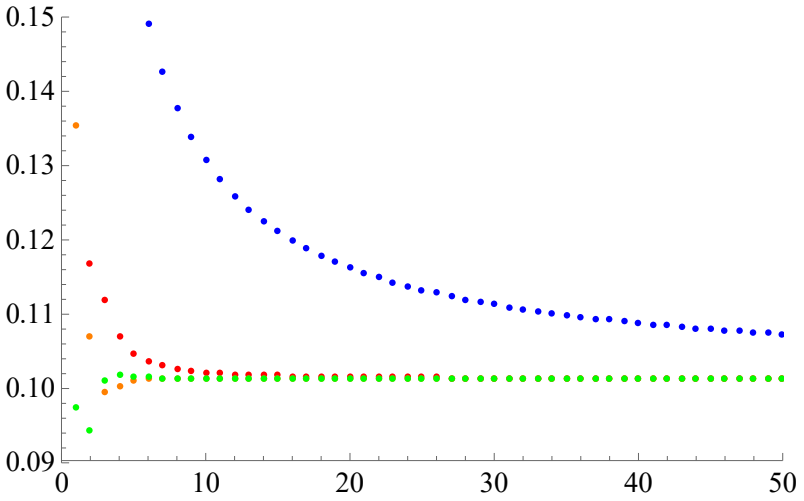

Figure 2.2: In this figure, we show the ratio $\frac{a_{k+1}}{k^2 a_k}$ (with a_k given by Eq.(2.2.22)) for growing k. The blue line represents the original ratio, while the red, orange, and green lines denote, respectively, the first three Richardson extrapolations. The ratio tends to the value $\frac{1}{\pi^2} = 0.101321\ldots$.

Taylor-expanding the square root and exchanging the two sums, we have

$$\begin{aligned}\Delta_0^{(b)} &= a_{-3}\mu^3 + a_{-1}\mu + \sum_{\ell=0}(2\ell+1)\sqrt{\mu^2+\ell(\ell+1)} \\ &= a_{-3}\mu^3 + a_{-1}\mu + \sum_{k=0}\frac{(-1)^k\mu^{-2k-1}\Gamma\left(k+\frac{1}{2}\right)}{2\sqrt{\pi}\Gamma(k+2)}\sum_{\ell=0}(2\ell+1)\ell^{k+1}(\ell+1)^{k+1} \\ &= a_{-3}\mu^3 + a_{-1}\mu + \frac{1}{\mu}\sum_{k=0}a_k\mu^{-2k}\,. \end{aligned} \tag{2.2.20}$$

By using that

$$\begin{aligned}\sum_{\ell=0}(2\ell+1)\ell^{k+1}(\ell+1)^{k+1} &= \sum_{n=0}^{k+2}\binom{k+2}{n}\sum_{\ell=0}\ell^{k+n+1} + \sum_{n=0}^{k+1}\binom{k+1}{n}\sum_{\ell=0}\ell^{k+n+2} \\ &= \sum_{n=0}^{k+2}\frac{(-1)^{k+n+1}B_{k+n+2}}{k+n+2}\binom{k+2}{n} + \sum_{n=0}^{k+1}\frac{(-1)^{k+n}B_{k+n+3}}{k+n+3}\binom{k+1}{n}\,,\end{aligned} \tag{2.2.21}$$

we obtain our final expression for the coefficients

$$a_k = \sum_{m=1}^{k+2}\frac{(-1)^{k+1}B_{2m}\Gamma\left(k+\frac{1}{2}\right)}{4\sqrt{\pi}m\Gamma(k+2)}\left[2\binom{k+1}{-k+2m-3} + \binom{k+1}{-k+2m-2}\right]. \tag{2.2.22}$$

The coefficients a_k diverge double-factorially, as can be seen from the ratio $\frac{a_{k+1}}{k^2 a_k}$, which is plotted in Fig.2.2. In fact, in the $k\to\infty$ limit, they behave as

$$a_k \approx -\pi^{-2k-5}\Gamma\left(k+\frac{1}{2}\right)\Gamma\left(k+\frac{5}{2}\right). \tag{2.2.23}$$

We can now employ resurgence arguments to infer the non-perturbative corrections to $\Delta_0^{(b)}$. According to resurgence theory, given an asymptotic series $\phi^{(0)}(z) = \sum a_k z^k$, we can promote it to a *transseries* of the form

$$\phi(z) = \phi^{(0)}(z) + \sum_{j\neq 0} \sigma_j e^{-A_j/z^{1/\beta_j}} z^{-b_j/\beta_j} \Phi^{(j)}(z), \qquad \Phi^{(j)}(z) \sim \sum_{i=0}^{\infty} a_i^{(j)} z^{i/\beta_j}\,, \tag{2.2.24}$$

where the parameters β_j, A_j and b_j are encoded in the large order behaviour of the a_k coefficients as [29, 30]

$$a_k \sim \sum_j \frac{S_j}{2\pi i} \frac{\beta_j}{A_j^{\beta_j k + b_j}} \sum_{i=0}^{\infty} a_i^{(j)} A_j^i \Gamma\left(\beta_j k + b_j - i\right)\,. \tag{2.2.25}$$

Therefore, the transseries can be mapped into the perturbative expansion up to a set of j-dependent constants σ_j, which are known as *transseries parameters* [30].

For our purposes, it is enough to focus on the dominant non-perturbative correction to the scaling dimension. The latter stems from the term with $m = k + 2$ in Eq.(2.2.22). Moreover, to ease the comparison with [50], we shift k as $k \to k - 2$ and introduce

$$\hat{a}_k \equiv a_k^{(m=k+2)}|_{k\to k-2} = -\pi^{-2k-1}\Gamma\left(k + \frac{1}{2}\right)\Gamma\left(k - \frac{3}{2}\right)\zeta(2k)\,. \tag{2.2.26}$$

To rewrite $\hat{a}_k$ in the form of Eq.(2.2.25), we resort to the following identity

$$2^{2k}\Gamma(k+\tfrac{1}{2})\Gamma(k-\tfrac{3}{2}) = \sqrt{\frac{\pi}{2}} \sum_{i=0}^{\infty} \gamma_i \Gamma\left(2k - \frac{3}{2} - i\right)\,, \tag{2.2.27}$$

where the coefficients γ_i diverge factorially and occur in Henkel's expansion of the modified Bessel function of the second kind. After some manipulations, we obtain

$$\hat{a}_k = -\frac{1}{4\pi^2} \sum_{j=1} \frac{j^{-3/2}}{(2\pi j)^{2k-3/2}} \sum_{i=0} \gamma_i \Gamma\left(2k - \frac{3}{2} - i\right)\,, \tag{2.2.28}$$

which agrees with Eq.(2.2.25) if

$$\beta_j = 2\,, \qquad b_j = -3/2\,, \qquad A_j = 2\pi j\,, \qquad \frac{S_j}{2\pi i} a_0^{(j)} = -\frac{\gamma_0}{j^{3/2} 8\pi^2}\,, \qquad a_{i>0}^{(j)} = \frac{a_0^{(j)}}{(2\pi j)^i}\frac{\gamma_i}{\gamma_0}\,. \tag{2.2.29}$$

Taking into account the shift in k performed before, we have that the dominant non-perturbative correction to $\Delta_0^{(b)}$ reads

$$\Delta_0^{(b)} \supset \sum_{j=1} e^{-2\pi j \mu} \mu^{3/2} \sum_{i=0} a_i^{(j)} \mu^{-i}\,. \tag{2.2.30}$$

By using Eq.(2.2.9), we can rewrite the above in terms of the charge as

$$\Delta_0^{(b)} \supset (gQ)^{5/4} \sum_{j=1} \exp\left(-\frac{\sqrt{\pi}}{2^{3/4}} j\sqrt{gQ}\right) \sum_{i=0} a_i \left(2^{7/4}\sqrt{\pi}\right)^i (gQ)^{-i/2}\,. \tag{2.2.31}$$

The leading non/perturbative contribution to the scaling dimension scales as $e^{-\sqrt{Q}}$, which is the same result obtained in [50] for the three-dimensional $O(N)$ model in the double-scaling (2.0.4). Of course, this is not surprising, since we, similarly to [50], consider the

same functional determinant (**??**), whose transseries representation is unique. Below we will make this connection more precise and explicitly show how Eq.(2.2.31) matches the contribution of worldline instantons computed in [50], corresponding to non-trivial saddle points of the geodesic equations on the two-sphere. This can be achieved by re-deriving our results using the Mellin representation of the functional determinant of the spectator modes. We, therefore, rewrite Eq.(2.2.7) as

$$\Delta_0^{(b)}(gQ) = \sum_{\ell=0}^{\infty} n_\ell\, \omega_*(\ell) = \sum_{\ell=0}^{\infty}(2\ell{+}1)\,\sqrt{\mu^2+\ell(\ell+1)} = \frac{1}{\Gamma(s)}\int_0^\infty dt\, t^{s-1}e^{-\mu^2 t}\mathrm{Tr}\left(e^{\Delta_{S^2}t}\right)\Big|_{s=-1/2}\,. \tag{2.2.32}$$

Since in the limit $\mu\to\infty$, the integral over t is dominated by the contribution at $t=0$, we proceed by studying the small t expansion of the heat kernel $\mathrm{Tr}\left(e^{\Delta_{S^2}t}\right)$. By using Poisson resummation and the asymptotic expansion of the Dawson function $F(z)$ for $z\to\infty$, we find

$$\begin{aligned}
\mathrm{Tr}\left(e^{\Delta_{S^2}t}\right) &= \sum_{\ell=0}^{\infty}(2\ell+1)\; e^{-\ell(\ell+1)t} \\
&= \frac{1}{2}\int_{-\infty}^{\infty}|\rho|\,d\rho e^{-\frac{1}{4}(\rho^2-1)t} + \frac{1}{2}\sum_{k=-\infty}^{\infty}(-1)^k\int_{-\infty}^{\infty}|\rho|\,d\rho e^{-\frac{1}{4}(\rho^2-1)t+i\pi k\rho} \\
&= \frac{e^{t/4}}{t} + \sum_{k=-\infty}^{\infty}\frac{(-1)^k e^{t/4}\left(\sqrt{t}-2\pi k F\left(\frac{k\pi}{\sqrt{t}}\right)\right)}{t^{3/2}} = \frac{1}{t}\sum_{k=0}c_k t^k\,,
\end{aligned} \tag{2.2.33}$$

where

$$c_k = \sum_{n=0}^{k}\frac{2^{-2k}(-1)^{k+n+1}\left(4^{k-n}-2\right)B_{2(k-n)}}{n!(k-n)!}\,. \tag{2.2.34}$$

By taking the integral over t in Eq.(2.2.32), one recovers the correct a_k coefficients (2.2.22), including the coefficients of the positive powers of μ (a_{-3} and a_{-1}) in Eq.(2.2.20). Moreover, the above shows that our expansion coefficients a_k in Eq.(2.2.22), stems from the Cauchy product of the asymptotic expansion of [50] with the Taylor series of $e^{t/4}$. We again focus on the leading non-perturbative correction to the heat kernel and consider

$$c_k^{n=0} = \frac{(-1)^{k+1}\left(1-2^{1-2k}\right)B_{2k}}{k!}\,, \tag{2.2.35}$$

which, as expected, matches exactly the (*full*) coefficients of the heat kernel expansion in [50]. In particular, by using Eq.(2.2.25), we have that the leading non-perturbative corrections to the heat kernel have the following form

$$\mathrm{Tr}\left[e^{\Delta_{S^2}t}\right] \supset 2i\left(\frac{\pi}{t}\right)^{\frac{3}{2}}(-1)^{k+1}|k|e^{-(k\pi)^2/t}\,, \tag{2.2.36}$$

which, of course, precisely matches the contribution of the worldline instantons calculated in [50]. A few remarks are in order:

- Due to the mismatch in N of the contributions of $\Delta_0^{(a)}$ and $\Delta_0^{(b)}$ to Δ_0, the non-perturbative corrections to $\Delta_0^{(b)}$ found here, survive in the full Δ_0 for every value of N (except obviously $N=2$ and at most another value of N for which there is an exact cancellation with Δ_0^a). In addition, there may be additional non-perturbative effects coming from $\Delta_0^{(a)}$, which may reduce the optimal truncation order below $n_{\mathrm{opt}} = \mathcal{O}\left(\sqrt{Q}\right)$.

- Both the authors of Ref. [50] and we start from the functional determinant of the spectator modes in $d = 3$ (2.2.7). However, due to the different double-scaling limits considered, we obtain *two distinct expansions*. Technically, we expanded Eq. (2.2.7) in powers of μ which is the mass with respect to the Laplacian operator Δ_{S^2}, which can, in turn, be expressed as a (convergent) powers series in $Q\epsilon$ via Eq.(2.2.9). Conversely, in [50], Eq.(2.2.7) is expanded in powers of the mass $m = \sqrt{\mu^2 - \frac{(d-2)^2}{4}}$ with respect to the conformal Laplacian $\Delta_{S^2} - \frac{(d-2)^2}{4}$, which, in turn, can be expressed as an (asymptotic) power series in $\frac{Q}{N}$. However, the transseries representation of $\Delta_0^{(b)}$ derived in [50] via Borel resummation does not depend on such considerations and can be obtained from Eq.(2.2.32) by rewriting the heat kernel expansion as $\mathrm{Tr}\left(e^{\Delta_{S^2} t}\right) = \frac{e^{t/4}}{t} \sum_k c_k^{n=0} t^k$.

- Unlike [50], where the large-charge expansion is asymptotic already at the leading order of the semiclassical expansion (2.0.4), in our case, the $(2k)!$ factorial growth shows up only at the next-to-leading order of the semiclassical expansion (2.0.6), i.e. in Δ_0. In fact, due to the factor on N in Eq.(2.2.5), the spectator modes contribute to the leading order of the expansion (2.0.4) and to the NLO of (2.0.5).

- Our results strengthen the idea that the non-perturbative effects found in [50] stem from the geometry of the compactification manifold and, therefore, do not depend on the particular double-scaling limit considered. In the next section, we will, therefore, change the manifold and study the $O(N)$ model on $\mathbb{R} \times S^{3-\epsilon}$. This case is particularly interesting since the heat kernel on odd-spheres is known to be convergent [75]. Moreover, in Sec.2.4, we will study the large-charge expansion in $QED_3 - GN$ (Gross-Neveu) on $\mathbb{R} \times S^2$. Interestingly, we will show that, due to properties of the fixed-charge operators considered, the expansion is asymptotic but Borel summable.

2.3 The $O(N)$ model around four dimensions

In this section, we continue analysing the convergence of the large-charge expansion in the $O(N)$ model by moving from $d = 3 - \epsilon$ to $d = 4 - \epsilon$, where we consider the renormalizable action

$$\mathcal{S} = \int d^d x \left(\frac{(\partial \phi_i)^2}{2} + \frac{(4\pi)^2 g_0}{4!} (\phi_i \phi_i)^2 \right) . \tag{2.3.1}$$

It is well-known that this model exhibits a Wilson-Fisher infrared fixed point which is weakly coupled when $\epsilon \ll 1$. At the 1-loop level, the value of the coupling at the FP reads

$$g^*(\epsilon) = \frac{3\epsilon}{8+N} + \mathcal{O}(\epsilon^2) . \tag{2.3.2}$$

As in the previous section, we consider the double-scaling limit (2.0.5) and write Δ_Q as in Eq.(2.0.6). The first two coefficients of the expansion (2.0.6) have been computed in [26] (generalizing the $O(2)$ result of [13]). The leading order reads

$$\frac{4\Delta_{-1}}{g^* Q} = \frac{3^{\frac{2}{3}} \left(x + \sqrt{-3 + x^2}\right)^{\frac{1}{3}}}{3^{\frac{1}{3}} + \left(x + \sqrt{-3 + x^2}\right)^{\frac{2}{3}}} + \frac{3^{\frac{1}{3}} \left(3^{\frac{1}{3}} + \left(x + \sqrt{-3 + x^2}\right)^{\frac{2}{3}}\right)}{\left(x + \sqrt{-3 + x^2}\right)^{\frac{1}{3}}} , \qquad x \equiv 6 g^* Q , \tag{2.3.3}$$

while Δ_0 is given by

$$\Delta_0 = \frac{R}{2}\sum_{\ell=0}^{\infty} n_\ell \left[\omega_+(\ell) + \omega_-(\ell) + (N-2)(\omega_*(\ell))\right] , \tag{2.3.4}$$

where

$$\omega_\pm(l) = \sqrt{J_\ell^2 + 3\mu^2 - \frac{1}{4}(d-2)^2 \pm \sqrt{4J_\ell^2\mu^2 + \left(3\mu^2 - \frac{1}{4}(d-2)^2\right)^2}} , \tag{2.3.5}$$

and

$$\omega_*(l) = \sqrt{J_\ell^2 + \mu^2} , \tag{2.3.6}$$

are the dispersion relations of the fluctuations. J_ℓ^2 and n_ℓ have been given in Eq.(**??**). The spectrum is analogous to the $d = 3-\epsilon$ case, with one conformal mode ω_-, one radial mode ω_+ with mass $\sqrt{6\mu^2 - \frac{1}{2}(d-2)^2}$, and $(N-2)$ spectator modes ω_*. Notice that the dispersion relation of the spectators does not depend on d and is the same in the $d = 3-\epsilon$ and $d = 4-\epsilon$ cases, i.e. its functional determinant is given by Eq.(**??**) evaluated in $d = 4-\epsilon$. The chemical potential μ is related to the 't Hooft coupling gQ as

$$\mu = \frac{3^{\frac{1}{3}} + \left(x + \sqrt{-3+x^2}\right)^{\frac{2}{3}}}{3^{\frac{2}{3}}\left(x + \sqrt{-3+x^2}\right)^{\frac{1}{3}}} . \tag{2.3.7}$$

For later convenience, we separate the contribution of the various modes as

$$\Delta_0(gQ) = \Delta_0^{(a)}(gQ) + \left(\frac{N}{2} - 1\right)\Delta_0^{(b)}(gQ) , \tag{2.3.8}$$

where, after performing regularization and renormalization, $\Delta_0^{(a)}$ and $\Delta_0^{(b)}$ can be written in terms of convergent sums as [26]

$$\Delta_0^{(a)}(g^*\bar{Q}) = -\frac{15\mu^4 + 6\mu^2 - 5}{16} + \frac{1}{2}\sum_{\ell=1}^{\infty}\sigma^{(a)}(\ell) + \frac{\sqrt{3\mu^2-1}}{\sqrt{2}} , \tag{2.3.9}$$

$$\Delta_0^{(b)}(g^*\bar{Q}) = -\frac{1}{16}\left[7 + \mu\left(-16 + 6\mu + 3\mu^3\right)\right] + \frac{1}{2}\sum_{\ell=1}^{\infty}\sigma^{(b)}(\ell) , \tag{2.3.10}$$

with

$$\sigma^{(a)}(\ell) = (1+\ell)^2\left[\omega_+(\ell) + \omega_-(\ell)\right] - 2\ell^3 - 6\ell^2 - 2\mu^2 - 2\left(\mu^2+2\right)\ell + \frac{5\left(\mu^2-1\right)^2}{4\ell} , \tag{2.3.11}$$

$$\sigma^{(b)}(\ell) = 2(1+\ell)^2\omega_*(\ell) - 2\ell^3 - 6\ell^2 - (\mu^2+1) - \left(\mu^2+5\right)\ell + \frac{\left(\mu^2-1\right)^2}{4\ell} . \tag{2.3.12}$$

In the following, we will unveil the large order behaviour of the small-gQ and large-gQ expansions of Δ_{-1} and Δ_0. In particular, we will show that, when neglecting $\Delta_0^{(a)}$, both expansions are convergent as opposed to the three-dimensional case considered in the previous section.

2.3.1 The small-charge expansion

The small gQ expansion of Δ_{-1} is convergent and its radius of convergence is determined by the only non-analytical point $x = x_0 = -\sqrt{3}$. Notice that, being x_0 negative, one can smoothly connect the small- and large-charge expansions via analytic continuation. On the other hand, as observed in [76], if one considers the model in $4-\epsilon$ (with $\epsilon < 0$) dimensions, where the FP occurs in the UV at negative values of g, then the non-analytical point lies on the positive Q axis and analytic continuing to large values of Q yields a complex Δ_Q. The onset of complex dynamics in the large-charge sector of the quartic $O(N)$ theory above four dimensions has been previously observed in the literature. In fact, in [77, 76], it has been pointed out the existence of a critical value of the charge Q_c above which Δ_Q has a non-vanishing imaginary part. In $d = 4-\epsilon$ ($\epsilon < 0$), and using $x = 6g^*Q$ supplemented by Eq.(2.3.2) we have

$$Q_c\big|_{1-\text{loop}} = x_0 \frac{(N+8)}{18\epsilon} = -\frac{N+8}{6\sqrt{3}\epsilon}\,, \tag{2.3.13}$$

in agreement with [77, 76].

By studying the coefficients of the small gQ expansion of Δ_{-1} we have that they satisfy Eq.(2.2.14) with $x_0 = -\sqrt{3}$, $p = -3/2$, $f(x_0) = \frac{1}{9}\sqrt{\frac{2}{3}}$ (obtained with 25 terms), $f'(x_0) = 0.0014549(1)$ (with 60), and $f''(x_0) = 0.000256(1)$ (with 45). Therefore, in the vicinity of the point $x = -\sqrt{3}$, Δ_{-1} behaves as

$$\Delta_{-1} = f(x)\left(1+\frac{x}{\sqrt{3}}\right)^{3/2} + \text{analytic}\,. \tag{2.3.14}$$

As in the $d = 3-\epsilon$ case, the radius of convergence occurs when the radial mode becomes massless as can be seen from Eqs.(2.3.5) and (2.3.7).

By investigating the small-charge expansion of the next orders in the semiclassical expansion we now test the claim made in [13] according to which the coefficients of the small gQ expansion of Δ_j, i.e. $a_{j,n}$ (i.e. $\Delta_j = \sum_n a_{j,n}(gQ)^n$), should obey the following large-order relation

$$\frac{a_{j+1,n-1}}{a_{j,n}} \approx n\,. \tag{2.3.15}$$

If the above were true it would imply the following large order behaviour:

$$a_{j,n} = b_j \left(\frac{1}{-\sqrt{3}}\right)^n \binom{n+j-3/2}{n}\left[1+\mathcal{O}\left(\frac{1}{n}\right)\right], \tag{2.3.16}$$

where b_j are real numbers. Then, according to the Darboux's theorem, all the Δ_j would be non-analytic in $x = -\sqrt{3}$ and in the vicinity of this point would behave as

$$\Delta_j = f_j(x)\left(1+\frac{x}{\sqrt{3}}\right)^{1/2-j} + \text{analytic}\,. \tag{2.3.17}$$

However, already for Δ_0 the analysis of the coefficients of the small gQ expansion reveals that the above is incorrect. In fact, as for the case with $d = 3-\epsilon$, near the singularity Δ_0 reads

$$\Delta_0 = f(x)\left(1+\frac{x}{\sqrt{3}}\right)^{1/4} + g(x,N)\left(1+\frac{x}{\sqrt{3}}\right)^{1/2} + \text{analytic}\,. \tag{2.3.18}$$

In other words the arguments of [13] capture only, for Δ_0, the essence of the second term in Eq. (2.3.18) but not the full singularity structure.

Interestingly, the nature of the leading non-analytical structure characterized by p in both Δ_{-1} and Δ_0 is identical in $d = 3 - \epsilon$ and $d = 4 - \epsilon$ dimensions for $O(N)$ theories. Intrigued by this observation, we studied the small $Q\epsilon$ expansion of Δ_{-1} in other two theories which have been previously investigated in the double-scaling limit (2.0.5), namely the cubic $O(N)$ model in $d = 6 - \epsilon$ [76] and the $U(N) \times U(M)$ model in $d = 4 - \epsilon$ [78, 79]. In both cases, we find that the leading singularity $Q = Q_c$ is tied to a vanishing mass for the "radial modes" of the models. Around this point Δ_{-1} behaves as

$$\Delta_{-1} = f(Q\epsilon)\left(1 + \left(\frac{Q}{Q_c}\right)^{\beta}\right)^{3/2} + \text{analytic}\,, \tag{2.3.19}$$

where $\beta = 2$ for $O(N)$ in $d = 3 - \epsilon$ and $\beta = 1$ for the other theories we investigated. The difference in β should be traced, not in the space-time dimension, but in the fact that the model investigated in $3 - \epsilon$ dimensions has one-loop vanishing beta function. Our results hint at new universal behaviours in quantum field theories.

2.3.2 The large-charge expansion

The large gQ expansion of Δ_{-1} is convergent with a radius of convergence determined by the non-analytical point at $x = -\sqrt{3}$. The number of expansion coefficients needed to accurately characterize the singularity is larger (≈ 35) when compared to the small gQ case, as shown in Table 2.2.1.

To analyze the large μ expansion of Δ_0, we focus on the contribution of the spectator fields defining $\Delta_0^{(b)}$. In particular, our goal is to prove that the large gQ expansion is convergent. We use the following Mellin representation to investigate the convergence for $\Delta_0^{(b)}$

$$\begin{aligned}\Delta_0^{(b)}(gQ) &= \sum_{\ell=0}^{\infty} n_\ell\, \omega_*(\ell) = \sum_{\ell=0}^{\infty}(\ell+1)^2\, \sqrt{\mu^2 + \ell(\ell+2)} \\ &= \frac{1}{\Gamma(s)}\int_0^\infty dt\; t^{s-1}e^{-\mu^2 t}\mathrm{Tr}\left(e^{\Delta_{S^{3-\epsilon}}t}\right)\Big|_{s=-1/2} = \sum_{k=0} a_k \frac{\Gamma(-1/2+k-\frac{3-\epsilon}{2})}{-2\sqrt{\pi}}\mu^{4-\epsilon-2k}\,,\end{aligned} \tag{2.3.20}$$

where the a_k are the heat kernel coefficients on $S^{3-\epsilon}$, i.e. $\mathrm{Tr}\left(e^{\Delta_{S^{3-\epsilon}}t}\right) = \sum_{k=0} a_k t^{k+\frac{3-\epsilon}{2}}$. For a given manifold, the heat kernel coefficients depend only on its geometrical properties, e.g. $a_0 = \dfrac{\mathrm{Vol}(S^{3-\epsilon})}{(4\pi)^{\frac{3-\epsilon}{2}}}$. Due to the gamma function in the numerator of the equation above, the terms with $k = 0, 1, 2$ diverge in the limit $\epsilon \to 0$ and need to be renormalized. For example, the term with $k = 0$ reads

$$-a_0\frac{\Gamma(-2+\epsilon/2)}{2\sqrt{\pi}}\mu^{4-\epsilon} = \left[-\frac{1}{8\epsilon} + \frac{1}{32}(4\gamma_E - 5 - 4\log(2)) + \frac{1}{8}\log(\mu) + \mathcal{O}(\epsilon)\right]\mu^4\,. \tag{2.3.21}$$

We checked that the $1/\epsilon$ divergence cancels against a term arising from the renormalization of Δ_{-1}. As usual, the renormalization is connected with a logarithm of the relevant scale that here is given by the chemical potential. By renormalizing the first three coefficients, we obtain

$$\begin{aligned}\Delta_0^{(b)}(gQ) = {}& \frac{1}{32}\mu^4(-5 + 4\gamma_E - 4\log(2)) + \frac{1}{24}\mu^2(1 - 6\gamma_E + 6\log(2)) \\ & + \frac{1}{80}(11 + 10\gamma_E - 10\log(2)) + \frac{1}{8}\left(\mu^2 - 1\right)^2\log(\mu) + \mu^4\sum_{k=3} b_k\mu^{-2k}\end{aligned} \tag{2.3.22}$$

in agreement with the numerical results of [80]. The coefficients b_k with $k \geq 3$ can be computed directly in $d = 4$. The heat kernel coefficients on the 3-sphere can be obtained as

$$\begin{aligned}\mathrm{Tr}\left(e^{\Delta_{S^3-\epsilon}t}\right) &= \sum_{l=0}(l+1)^2 e^{-l(l+2)t} \\ &= \frac{1}{2}e^t \sum_{p=-\infty}^{\infty} p^2 e^{-p^2 t} = \frac{\sqrt{\pi}e^t}{4t^{3/2}} + \mathcal{O}\left(e^{-1/t}\right) = t^{-3/2}\sum a_k t^k + \mathcal{O}\left(e^{-1/t}\right),\end{aligned} \tag{2.3.23}$$

with $a_k = \frac{\sqrt{\pi}}{4k!}$. Unlike the $d = 3 - \epsilon$ case, the heat kernel expansion has an infinite radius of convergence. By plugging the above in Eq.(2.3.20), we obtain the coefficients of the large μ expansion of $\Delta_0^{(b)}$

$$b_{k\geq 3} = -\frac{1}{4k(k-1)(k-2)}\,. \tag{2.3.24}$$

Interestingly, we can resum the series and obtain a closed-form expression for $\Delta_0^{(b)}$ not involving infinite sums. We have

$$\Delta_0^{(b)} = -\frac{5\mu^4}{32} + \frac{\mu^2}{6} - \frac{1}{20} + \frac{1}{8}\left(\mu^2-1\right)^2\left(\log\left(\mu - \frac{1}{\mu}\right) + \gamma_E - \log(2)\right)\,. \tag{2.3.25}$$

The analytic structure of $\Delta_0^{(b)}$ is as follows: there is an essential singularity at $\mu = 0$ and two logarithmic branch cuts which run, respectively, from $\mu = -1$ to $\mu = -\infty$ and from $\mu = 1$ to $\mu = 0$. However, from Eq.(2.3.7), we see that $\mu \neq 0$ for any value of gQ. Moreover, $\mu(gQ = 0) = 1$, and Δ_0 is complex for any Q when $g < 0$, i.e. at the (metastable) UV FP of the quartic $O(N)$ theory in $4 < d < 6$. Therefore, while the small-gQ expansion of Δ_{-1} reveals the existence of a critical value of the charge above which Δ_Q is complex, the analytic structure of Δ_0 suggests a stronger statement, i.e. in $4 < d < 6$ Δ_Q is complex for *any* value of Q. Away from four dimensions the situation can change due to different asymptotic behaviours for even and odd dimensions of the $O(N)$ CFT [81].

We have observed that the large gQ expansion of the $\Delta_0^{(b)}$ is convergent, in net contrast with the $(2n)!$ factorial growth found in three dimensions. Hence our result strengthens the idea that the non-perturbative contributions to the functional determinant of spectator fields (i.e. of free particles of mass equal to μ) have a geometrical origin and are, therefore, absent on $\mathbb{R} \times S^3$, where the WKB expansion of the heat kernel is exact [75].

2.4 Monopoles in QED_3

Here we consider the large-charge expansion in fermionic gauge theories. In particular, we study the QED_3 model with Euclidean action given by

$$S = \int d^3x \left[\frac{1}{4e^2}F_{\mu\nu}F^{\mu\nu} + \overline{\psi}^i\left(\partial\!\!\!/ + iA\!\!\!/\right)\psi^i\right]\,, \tag{2.4.1}$$

where the flavor index runs over $i = 1, ..., N_f$ and A_μ is a $U(1)$ gauge field with field strength $F_{\mu\nu}$. The theory has a $SU(N_f)$ flavor symmetry and a $U(1)$ global symmetry associated with the current

$$J_\mu = \frac{1}{4\pi}\epsilon_{\mu\nu\rho}F^{\nu\rho}\,, \tag{2.4.2}$$

which is conserved due to the Bianchi identity $dF = 0$. One can define the monopole operators as the operators carrying the corresponding conserved charge $Q = \int d^2x J_0$, which

is subject to the Dirac quantization condition $Q \in \mathbb{Z}/2$. For large enough N_f, the theory is believed to flow to a conformal field theory in the infrared [82, 83]. In this phase we can relate the scaling dimension of the lowest-lying monopole operators to the ground state energy on the cylinder as

$$\Delta_Q = E_Q \equiv -\log Z_{S^2\times\mathbb{R}}\left[A^Q\right] . \tag{2.4.3}$$

Here Δ_Q corresponds to the scaling dimension of a monopole operator carrying the charge Q, E_Q is the ground state energy on the cylinder when there is $4\pi Q$ units of magnetic flux across S^2, A^Q the associated background gauge field, and $Z_{S^2\times\mathbb{R}}$ is the partition function of the theory. For large N_f, Δ_Q can be computed via a semiclassical expansion in $1/N_f$ yielding Eq.(**??**). The leading order corresponds to the action evaluated on the classical field configuration and reads [84, 85]

$$\Delta_{-1} = 4\sum_{\ell=Q+1}^{\infty} \ell\sqrt{\ell^2 - Q^2}\,, \tag{2.4.4}$$

where ℓ labels the eigenvalues of the Laplacian on a 2-sphere with a charge Q at the center. The corresponding eigenfunctions are the monopole harmonics [86, 87] and the presence of the background monopole field bounds ℓ as $\ell \geq Q+1$. The above expression can be regularized and computed numerically, as explained in detail in [84, 85].

2.4.1 The large-charge expansion

Here we focus on the large Q expansion of Δ_{-1} (2.4.4). By shifting the sum over ℓ, we can rewrite Δ_{-1} as

$$\begin{aligned}
\Delta_{-1} &= 4\sum_{n=0}^{\infty}(n+Q+1)\sqrt{(n+1)(n+2Q+1)} \\
&= 4\sqrt{2}Q^{3/2}\sum_{n=0}^{\infty}\sqrt{n+1}\left(\frac{n+1}{Q}+1\right)\sqrt{\frac{n+1}{2Q}+1} \\
&= 4\sqrt{2}Q^{3/2}\sum_{k=0}^{\infty}\frac{(-1)^{k-1}8^{-k}(2k)!}{(2k-1)(k!)^2}\left[\sum_{n=0}^{\infty}(n+1)^{k+\frac{1}{2}}\left(\frac{n+1}{Q}+1\right)\right]\left(\frac{1}{Q}\right)^k \\
&= 4\sqrt{2}Q^{3/2}\sum_{k=0}^{\infty}\frac{(-1)^{k-1}8^{-k}(2k)!}{(2k-1)(k!)^2}\left[\frac{\zeta\left(-k-\frac{3}{2}\right)}{Q}+\zeta\left(-k-\frac{1}{2}\right)\right]\left(\frac{1}{Q}\right)^k .
\end{aligned} \tag{2.4.5}$$

Rearranging the terms of the expansion, we obtain

$$\Delta_{-1} = Q^{3/2}\sum_{k=0}^{\infty} a_k \frac{1}{Q^k}\,, \tag{2.4.6}$$

where the a_k coefficients are given by

$$a_k = \frac{2}{\pi^2 k!}(-1)^{k+1}\frac{1}{(4\pi)^k}\Gamma\left(k-\frac{3}{2}\right)\Gamma\left(k+\frac{5}{2}\right)\sin\left(\frac{\pi}{4}(2k+1)\right)\zeta\left(k+\frac{3}{2}\right) . \tag{2.4.7}$$

Analysing the ratio of consecutive coefficients, which we show in Fig.2.3, we find that the series is asymptotic and, therefore, requires a summation prescription such as Borel resummation. The Borel transform of Eq.(2.4.6) is given by

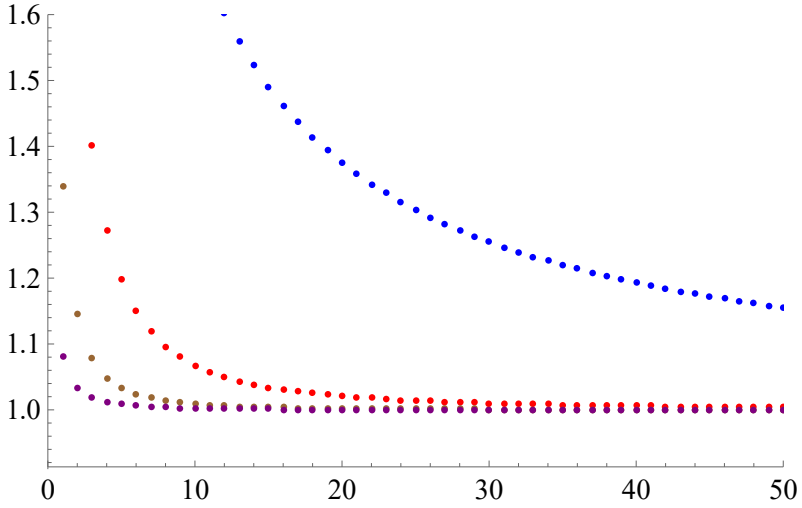

Figure 2.3: In this figure, we show the ratio $\frac{4\pi}{k(-1)^{k+1}}\frac{a_k}{a_{k-1}}$, where the a_k are given by Eq.(2.4.7). The blue line represents the original coefficients, while the red, brown, and purple lines denote, respectively, the first three Richardson extrapolations.

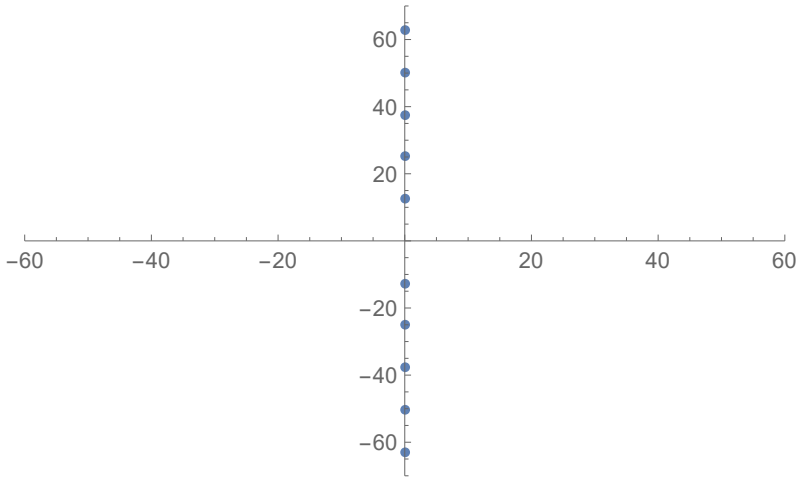

Figure 2.4: The singularity structure of the Borel transform of Δ_{-1} (2.4.8). There are branch points at $t = 4\pi i m$, $m \in \mathbb{Z}$.

$$\mathcal{B}\left[\frac{\Delta_{-1}}{Q^{3/2}}\right](t) = \sum_{k=0}^{\infty}\frac{a_k}{k!}t^k = \sum_{m=1}^{\infty}\frac{(i-1)}{\sqrt{2}\pi m^{3/2}}\left[{}_2F_1\left(-\frac{3}{2},\frac{5}{2};1;-\frac{it}{4m\pi}\right) + i\ {}_2F_1\left(-\frac{3}{2},\frac{5}{2};1;\frac{it}{4m\pi}\right)\right]. \tag{2.4.8}$$

Here ${}_2F_1(a,b;c;x)$ denotes the Hypergeometric function, which can be analytically continued in the complex plane along any path avoiding the branch points at $x = 1$ and $x = \infty$. Hence $\mathcal{B}\left[\frac{\Delta_{-1}}{Q^{3/2}}\right](t)$ features an infinite series of branch points at $t = 4\pi i m$, $m \in \mathbb{Z}$, as shown in Fig.2.4. As a consequence, the series (2.4.6) is Borel summable and both lateral

Borel summations coincide

$$\Delta_{-1} = Q^{5/2} \int_0^\infty dt\ e^{-Qt} \mathcal{B}\left[\frac{\Delta_{-1}}{Q^{3/2}}\right](t) = \sum_{m=1} \frac{2iQ^2}{\pi m} \left[e^x K_2(x) - e^{-x} K_2(-x)\right] , \quad x \equiv 2i\pi m Q \,, \tag{2.4.9}$$

where K_2 is the modified Bessel function of the second kind. Finally, the optimal truncation order corresponds to the value of k such that a_k/Q^k has a minimum and reads

$$k_{\text{opt}} \approx 4\pi Q \,, \tag{2.4.10}$$

with an error of order $\mathcal{O}\left(e^{-4\pi Q}\right)$. We conclude that, even if the QED_3 model shares the same universal large-charge behaviour (2.0.2) of the three-dimensional $O(N)$ model, its large-charge expansion behaves better than $O(N)$, having a higher optimal truncation order (i.e. $\approx Q$ rather than $\approx \sqrt{Q}$) and being Borel summable. Notice that, since at the leading order in $1/N_f$ the scaling dimensions are not affected by the inclusion of a Gross-Neveu interaction term, our results apply also to $QED_3 - GN$ [88].

Chapter 3

QCD-like theories at finite charge

Quantum Chromodynamics (QCD) constitutes one of the pillars of the standard model of particle physics. Featuring three colors and several flavors, its dynamics become strongly coupled at low energies while weak at high energies. It is often assumed that analyzing the strong sector of QCD is not fruitful and, consequently, numerical methods are commonly used.

Several relevant questions remain unanswered about its dynamics, from its spectrum to the interplay between chiral symmetry breaking and confinement, to its phase structure as a function of light-matter fields (conformal window), temperature, and matter density. An important unsolved puzzle is the absence or unexplained strong suppression [89, 90] of the presence in the theory of the topological term responsible for strong CP violation. Its possible resolutions in terms of either the axion physics [91, 92, 93, 94, 95, 96, 97, 98] or its alternatives such as the ones in which CP is broken spontaneously [99, 100, 101].

Reducing the number of colors from three to two provides a number of theoretical advantages and increases potential phenomenological applications beyond the QCD template. This is due, to the symplectic nature of the matter representation that enhances the quantum global symmetries for the light flavors from the $SU(N_f)\times SU(N_f)\times U(1)_B$ to $SU(2N_f)$. When discussing non-zero baryon charge the model allows for well-defined lattice simulations because the action remains real, differently from ordinary QCD. For a review of the various applications of the theory we refer to [102, 103]. Last but not least this model together with ordinary QCD has been one of the most studied theories on the lattice as function of light flavors in the hunt for the predicted lower edge of the conformal window [104, 105, 106, 107] and its dynamical properties [108, 109, 110, 111, 112, 113, 114, 115, 108, 116, 117, 118, 119, 120], finite baryon density [121, 122, 123, 124, 125, 126, 127, 128, 129, 130, 131, 132, 133, 134, 135, 136, 137, 138, 139, 140, 141].

In this chapter, we investigate the θ-angle and axion physics at non-zero baryon chemical potential of two-color QCD outside and near the conformal window. In the first Section. 3.1 we discuss general aspects of the QCD phase diagram as function of the number of colors and flavors. In the following Section 3.2 we introduce the two-color effective pion Lagrangian at non-zero baryon charge, including both the θ-angle term as well as the axion field. In Section 3.3 we will determine the vacuum structure of the theory both in the normal and superfluid phase as a function of the different number of matter fields. We will show how new phases emerge due to the interplay of the θ-angle term, quark masses, and baryon chemical potential. We will also characterize the type of phase transitions for $N_f = 2, 3, 6, 7, 8$ flavors and discuss general properties depending on the even versus odd number of flavors. Then, in Section 3.5 we investigate the near-conformal strongly coupled dynamics of two-color QCD by introducing a dilaton state. Then, using the state-operator

correspondence we compute the dependence of near-conformal scaling dimensions of charged operators, including the impact of the θ angle.

3.1 QCD phase diagram

In this section we will discuss some features of Quantum Chromodynamics in presence of a general number of colors and flavors. The object of study is the β function of the theory. We can identify three different scenarios

- For $\beta > 0$, the theory is weakly coupled at low energies while the coupling increases at high energies, resulting in a Landau pole. QED is an example of this.
- For $\beta < 0$, the coupling becomes large at low energies, implying that the theory becomes strongly coupled. Conversely, the coupling constant approaches zero in the ultraviolet regime. This phenomenon is known as *asymptotic freedom*. An example of this is QCD.
- If $\beta = 0$ in this case the coupling constant is independent of the energy scale and the theory becomes conformal. Theories with this behavior do not contain any ultraviolet divergences. An example of this is $N = 4$ Super-Yang-Mills.

Let us start with pure Yang-Mill with internal gauge group $SU(N_c)$. The Lagrangian is the following

$$\mathcal{L} = -\frac{1}{4}F^a_{\mu\nu}F^{\mu\nu}_a, \quad F^a_{\mu\nu} = \partial_\mu A^a_\nu - \partial_\nu A^a_\mu + g_0 f^{abc} A^b_\mu A^c_\nu \tag{3.1.1}$$

here $F^a_{\mu\nu}$ is gluon field strength tensor and g_0 is the bare gauge coupling constant. The index algebra runs from $a = 1, ..., N_c^2 - 1$ and f_{abc} are the structure constants of the $su(N_c)$ algebra, defined by the commutation relation

$$[T^a, T^b] = f^{abc}T^c. \tag{3.1.2}$$

where T^a denotes the generators of $su(N_c)$ in the adjoint representation. Indicating by g the renormalized coupling constant, the associated beta function $\beta(g)$ at one-loop read as

$$\beta(g) = \mu\frac{\partial g}{\partial \mu} = -\frac{g^3}{(4\pi)^2}\frac{11}{3}N_c < 0. \tag{3.1.3}$$

In this case the β function is negative for all values of g, thus the theory becomes free at high energies while at low energies the theory becomes strongly coupled. It follows from the running of the coupling that the one-loop scale

$$\Lambda = \mu e^{-1/\left(2\beta g^2\right)} \tag{3.1.4}$$

is independent of the scale μ and therefore defines an RG- invariant scale. The fact that a theory with dimensionless coupling g_0 generates a scale Λ is called dimensional transmutation. We can extend the previous result by including N_f Dirac fermions transforming in the fundamental representation of $SU(N_c)$, now the beta function β read as follows

$$\beta(g) = -\frac{g^3}{(4\pi)^2}\left[\frac{11}{3}N_c - \frac{2}{3}N_f\right]. \tag{3.1.5}$$

Depending on the number of colors and flavors (N_f, N_c), we can have three different phases

- Non-Abelian QED-phase: $\beta > 0$ for $N_f > \frac{11}{2}N_c$
- Asymptotically free phase: $\beta < 0$ for $N_f < \frac{11}{2}N_c$
- Non-Abelian Coulomb-phase: $\beta = 0$ for $N_f = \frac{11}{2}N_c$

If $N_f > \frac{11}{2}N_c$ then the beta functions changes sign, we lose asymptotic freedom, and the theory exhibits a Landau regime and becomes infrared-free, like QED with massless electrons. For $N_f = \frac{11}{2}N_c$, the beta function is zero for any value of g leading to scale-invariant QCD. At two-loop, the beta function β read as

$$\beta(g) = -\frac{g^3}{(4\pi)^2}\beta_0 - \frac{g^5}{(4\pi)^4}\beta_1 + \dots \tag{3.1.6}$$

where the first two coefficients are universal and independent of the renormalization group scheme [142]

$$\beta_0 = \frac{11}{3}N_c - \frac{2}{3}N_f, \tag{3.1.7}$$

$$\beta_1 = \frac{34}{3}N_c^2 - \frac{N_f}{3N_c}\left(13N_c^2 - 3\right). \tag{3.1.8}$$

Let us define the value of $N_f = N_f^I$ for which asymptotically freedom is lost as $\beta_0(N_f^I) = 0$. Below this number of flavors, the theory develops a Bank-Zaks fixed point. It appear soon as the coefficients β_1 change of sign, it happens for $N_f = N_f^{II}$ such that $\beta_1(N_f^{II}) = 0$. The respective values are

$$N_f^I = \frac{11}{2}N_c, \tag{3.1.9}$$

$$N_f^{II} = \frac{34N_c^3}{13N_c^2 - 3}. \tag{3.1.10}$$

Therefore, in the region $N_f^{II} < N_f < N_f^I$ the two coefficients of the beta function will have a different sign and thus, a non-trivial an infrared fixed point $g = g^*$ will emerge. The respective fixed point is

$$\frac{g_*^2}{16\pi^2} = -\frac{\beta_0}{\beta_1}, \tag{3.1.11}$$

here there are no localized particle-like states in the spectrum, rather, we find massless unconfined interacting quarks and gluons. Since we are sure that below N_f^I we are in the conformal phase, there must be a critical number of flavors N_f^* for which the theory is still conformal at the infrared. The region

$$N_f^* < N_f < N_f^I \tag{3.1.12}$$

is known as *conformal window*. The task of identifying the lower bound N_f^* is highly non-trivial, as it may be in the strongly coupled regime in general, and non-perturbative effects might emerge. When the transition is sufficiently smooth, close to the lower end of the conformal window, the theory exhibits a near-conformal phase characterized by the existence of a region of the renormalization group (RG) flow in which the coupling remains nearly constant signaling the occurrence of *walking dynamics* [143, 144, 145]. The infrared dynamics of the near-conformal theory can be modeled by augmenting the standard chiral Lagrangian via the introduction of a new light scalar degree of freedom

with the same quantum numbers of the vacuum which is commonly referred to as the *dilaton*. In this scenario, the dilaton is the Goldstone boson stemming from the spontaneous breaking of scale invariance whereas sources of explicit conformal breaking leading to the near-conformal phase can be encoded in the effective dilaton potential. The aforementioned phenomenological applications have motivated several investigations of the resulting dilaton effective field theory (EFT) [105, 146, 147, 148, 149, 150, 151, 152, 153, 47, 154, 155, 156, 44, 46, 157, 45, 158].

3.2 Two-color chiral Lagrangian

The Lagrangian of N_f Dirac fermions transforming according to the fundamental representation of two-color QCD reads:

$$\mathcal{L} = -\frac{1}{4g^2}\vec{G}_{\mu\nu}\cdot\vec{G}^{\mu\nu} + i\bar{\mathcal{Q}}\bar{\sigma}^{\nu}\left[\partial_\nu - i\vec{G}_\nu\cdot\frac{\vec{\tau}}{2}\right]\mathcal{Q} - \frac{1}{2}m_q\mathcal{Q}^T\tau_2 E\mathcal{Q} + \text{h.c.}\ . \tag{3.2.1}$$

Here $G^a_{\mu\nu}$ and G^a_μ with $a = 1, 2, 3$ are respectively the gluon field strength and the field itself, τ^a are the Pauli matrices for the $SU(2)$ color group, and $\mathcal{Q}^{c,i}_\alpha$ is a two-spinor fermion field transforming according to the fundamental representation of color with $c = 1, 2$ and $i = 1, \cdots, 2N_f$. In terms of $q_{L,R}$, which are the original left and right handed quarks stemming from the Dirac notation it reads

$$\mathcal{Q} = \begin{pmatrix} q_L \\ i\sigma_2\tau_2 q_R^* \end{pmatrix}\ . \tag{3.2.2}$$

At zero fermion mass (i.e. $m_q = 0$) the theory exhibits the classical $U(2N_f)$ symmetry broken at the quantum level by the Adler-Bell-Jackiw anomaly to $SU(2N_f)$. The Dirac mass term breaks explicitly the symmetry to $Sp(2N_f)$ and the $2N_f \times 2N_f$ matrix E reads:

$$E = \begin{pmatrix} 0 & 1 \\ -1 & 0 \end{pmatrix} \otimes \mathbb{1}_{N_f}\ . \tag{3.2.3}$$

At small number of flavors the dynamics is expected to be strong enough for a fermion condensate to form breaking the $SU(2N_f)$ global symmetry spontaneously to a smaller subgroup expected to be the maximal diagonal one. However, only recently, first-principle lattice simulations have been able to demonstrate this pattern of chiral symmetry breaking in [111] which has been further confirmed in [113] for two Dirac flavors. Increasing the number of flavors the dynamics can change and one expects the existence of a critical number of flavors N_f^* above which an IR interacting conformal fixed point emerges. This dynamics has been investigated theoretically [107] and via first principle lattice simulations [159]. A recent up-to-date review can be found in [103]. In fact, even the dynamics at very large number of flavours is extremely interesting both theoretically and phenomenologically. It is also being investigated on the lattice [160] searching for the existence of an interacting non-perturbative UV fixed point [161] similar to the one shown to exist in [162, 163] for gauge-Yukawa theories. For any $2 < N_f < N_f^*$ it is therefore natural to expect the pattern of spontaneous symmetry breaking to be $SU(2N_f) \to Sp(2N_f)$. The associated chiral Lagrangian embodying the previous pattern of symmetry breaking reads [164, 102] :

$$\mathcal{L}_{\text{eff}} = \nu^2 Tr\{\partial_\mu\Sigma\partial^\mu\Sigma^\dagger\} + m_\pi^2\nu^2 Tr\{M\Sigma + M^\dagger\Sigma^\dagger\}\ , \tag{3.2.4}$$

with Σ transforming linearly under a chiral rotation as

$$\Sigma \to u\Sigma u^T\ , \qquad u \in SU(2N_f)\ , \tag{3.2.5}$$

and the democratic mass matrix M being

$$M = -i\sigma_2 \otimes \mathbb{1}_{N_f} = \begin{pmatrix} 0 & -1 \\ 1 & 0 \end{pmatrix} \otimes \mathbb{1}_{N_f} \ . \tag{3.2.6}$$

3.2.1 Baryon charge

We can take into account a non-vanishing baryon charge by coupling it to a chemical potential μ. The latter can be introduced as the zero component of a background gauge field via the covariant derivative

$$\partial_\mu \mapsto D_\mu = \partial_\mu - i\mu\delta^0_\mu B \,, \qquad B \equiv \begin{pmatrix} 1/2 & 0 \\ 0 & -1/2 \end{pmatrix} \otimes \mathbb{1}_{N_f} \tag{3.2.7}$$

which reproduces the usual coupling of the chemical potential to the Noether charge in the Dirac notation. In fact

$$\bar{q}\gamma^0 q = \begin{pmatrix} q_L^* \\ q_R^* \end{pmatrix}^T \begin{pmatrix} 1 & 0 \\ 0 & 1 \end{pmatrix} \otimes \mathbb{1}_{N_f} \begin{pmatrix} q_L \\ q_R \end{pmatrix} = \mathcal{Q}^\dagger \underbrace{\begin{pmatrix} 1 & 0 \\ 0 & -1 \end{pmatrix} \otimes \mathbb{1}_{N_f}}_{\equiv 2B} \mathcal{Q} = 2\mathcal{Q}^\dagger B \mathcal{Q} \ . \tag{3.2.8}$$

Notice that the baryon charge generator belongs to the $su(2N_f)$ algebra being proportional to the third Pauli matrix.

From the form of the B matrix, we see that for non-zero μ the Lagrangian is no longer invariant under $SU(2N_f)$ transformations. To fix the ideas, when the mass term is zero the $SU(2N_f)$ symmetry is explicitly broken as

$$SU(2N_f) \xrightarrow{m=0,\ \mu\neq 0} SU(N_f)_L \times SU(N_f)_R \times U(1)_B \ , \tag{3.2.9}$$

conversely, for $m \neq 0$ one has

$$SU(2N_f) \xrightarrow{m\neq 0,\ \mu\neq 0} SU(N_f)_V \times U(1)_B \ . \tag{3.2.10}$$

By using the covariant derivative (3.2.7) into eq.(3.2.4), we obtain the effective Lagrangian describing the theory at non-zero baryon charge

$$\begin{aligned} \mathcal{L}_B = {} & \nu^2 Tr\{\partial_\mu \Sigma \partial^\mu \Sigma^\dagger\} + 4\mu\nu^2 Tr\{B\Sigma^\dagger \partial_0 \Sigma\} + m_\pi^2 \nu^2 Tr\{M\Sigma + M^\dagger \Sigma^\dagger\} \\ & + 2\mu^2\nu^2 \left[Tr\{\Sigma B^T \Sigma^\dagger B\} + Tr\{BB\} \right] \ . \end{aligned} \tag{3.2.11}$$

3.2.2 The θ-angle and the U(1) problem

In order to discuss the physics of the θ-angle and of the axial anomaly [165, 166, 167], we introduce the topological charge density

$$q(x) = \frac{g^2}{64\pi^2} \epsilon^{\mu\nu\rho\sigma} F^a_{\mu\nu} F^a_{\rho\sigma} \ , \tag{3.2.12}$$

which we incorporate in the effective Lagrangian as

$$\mathcal{L}_{q(x)} = \frac{i}{4} q(x) \mathrm{Tr}\{\log\Sigma - \log\Sigma^\dagger\} - \theta q(x) + \frac{q(x)^2}{4a\nu^2} \ . \tag{3.2.13}$$

Here the new Σ is related to the old one that transforms only under $SU(2N_f)$ via [168]

$$\Sigma \to \Sigma e^{i\frac{S}{\sqrt{2N_f}}\mathbb{1}_{2N_f}}, \tag{3.2.14}$$

with the S-field a singlet of $SU(2N_f)$ transforming under the anomalous $U(1)_A$, and it is parent to the η' particle in ordinary QCD.

The minimal choice to neglect orders higher than $q^2(x)$ is justified at large number of colors, see discussion in [168, 169]. Here, to keep the same pattern of chiral symmetry breaking the $SU(2)$ of color generalizes to $Sp(2N)$ and not $SU(N)$. The linear term allows accommodating for the $U(1)_A$ anomaly. The coefficient of the quadratic term in $q(x)$ is known as the topological susceptibility of the Yang-Mills theory. The coefficients of these terms are coherently chosen such that we reproduce the axial anomaly $\partial_\mu J^\mu_5 = 4N_f q(x)$ in two-color QCD with quarks in the fundamental representation [168]. Notice that $q(x)$ is a background auxiliary field introduced to implement the anomalous transformation at the action level in linear fashion. It can, therefore,be integrated out via its equations of motion, yielding the following effective Lagrangian

$$\begin{aligned}\mathcal{L}_\theta &= \nu^2 Tr\{\partial_\mu \Sigma \partial^\mu \Sigma^\dagger\} + 4\mu\nu^2 Tr\{B\Sigma^\dagger \partial_0 \Sigma\} + m_\pi^2 \nu^2 Tr\{M\Sigma + M^\dagger \Sigma^\dagger\} \\ &+ 2\mu^2\nu^2 \left[Tr\{\Sigma B^T \Sigma^\dagger B\} + Tr\{BB\}\right] - a\nu^2 \left(\theta - \frac{i}{4} Tr\{\log\Sigma - \log\Sigma^\dagger\}\right)^2 . \end{aligned} \tag{3.2.15}$$

The action of the symmetry groups is summarised in Table 3.2.1 where the axial generator A in our notation is

$$A = \frac{1}{2}\begin{pmatrix} 1 & 0 \\ 0 & 1 \end{pmatrix} \otimes \mathbb{1}_{N_f} . \tag{3.2.16}$$

	$[SU(2)]$	$SU(N_f)_L$	$\times$	$SU(N_f)_R$	$\times$	$U(1)_V$	$\times$	$U(1)_A$
q_L	$\square$	$\square$		$\mathbf{1}$		$+1$		$+1$
$i\sigma_2\tau_2 q_R^*$	$\square$	$\mathbf{1}$		$\bar{\square}$		-1		$+1$

	$[SU(2)]$	$SU(2N_f)$	$\times$	$U(1)_A$
$\mathcal{Q}$	$\square$	$\square$		$+1$

Table 3.2.1: Transformation properties of q_L, $i\sigma_2\tau_2 q_R^*$ and $\mathcal{Q}$ under the action of the symmetry groups.

3.2.3 The axion and the baryon charge

For the Standard Model three colors QCD there is no experimental evidence of strong CP violation. This constrains the associated value of the effective theta angle $\bar{\theta} = \theta + \arg\det(M)$, with M the physical quark mass matrix, to be $\bar{\theta} < 10^{-10}$. The limit comes from the bound on the neutron electric dipole moment $|d_n| = C_{\rm EDM} e\, \bar{\theta} < 1.8 \times 10^{-26} e$ cm [89, 90], where $C_{\rm EDM} = 2.4(1.0) \times 10^{-16}$ cm [170] is related to the effective nucleon interactions with the axion explained in the Appendix of [168]. From a theoretical viewpoint, a tiny value of a physical parameter unprotected by any symmetry requires an explanation. One solution for the so-called strong CP problem was proposed in the 70s by R. Peccei and H. Quinn [91, 92].

The proposal makes use of an additional $U(1)_{PQ}$ symmetry which is quantum mechanically anomalous and spontaneously broken leading to the axion as an extra (pseudo-)Goldstone boson. Axion physics has led to a great deal of both theoretical and phenomenological work including active experimental searches beyond the original QCD axion [171]. An alternative solution to the strong CP problem featuring new composite dynamics and heavier (if not completely absent) axions was proposed in [172] and reconsidered in [173] and applied extensively in model building in [174, 175, 176].

Of course, when discussing the θ-angle physics here, depending on the physical application of the model, we can allow for new sources of CP breaking, perhaps relevant for some models of dark matter or Standard Model secluded sectors [171]. Nevertheless, it is interesting to entertain the possibility that an axion is present in the theory and therefore explore its finite chemical potential dynamics and impact. We denote by ν_{PQ} the scale of $U(1)_{PQ}$ spontaneous symmetry breaking and by a_{PQ} the coefficient of the $U(1)_{PQ}$ anomalous term. We include the axion in our theory by extending (3.2.15) to the following effective Lagrangian

$$\begin{aligned}\mathcal{L}_{\hat{a}} &= \nu^2 Tr\{\partial_\mu \Sigma \partial^\mu \Sigma^\dagger\} + \nu_{PQ}^2 \partial_\mu N \partial^\mu N^\dagger + 4\mu\nu^2 Tr\{B\Sigma^\dagger \partial_0 \Sigma\} + m_\pi^2 \nu^2 Tr\{M\Sigma + M^\dagger \Sigma^\dagger\} \\ &+ 2\mu^2\nu^2 \left[Tr\{\Sigma B^T \Sigma^\dagger B\} + Tr\{BB\}\right] - a\nu^2 \left(\theta - \frac{i}{4} Tr\{\log\Sigma - \log\Sigma^\dagger\} - \frac{i}{4} a_{PQ}(\log N - \log N^\dagger)\right)^2 .\end{aligned} \tag{3.2.17}$$

The details on how to construct the extended effective theory can be found in [168].

3.3 Determining the Vacuum

In this section, we focus on the vacuum structure of theory (3.2.15) in the presence of the θ-angle and finite baryon charge. In particular, we will first study the general conditions determining the classical vacuum solution as a function of θ and μ. Armed with these results, we then carefully analyze the properties of the vacuum in the concrete cases $N_f = 2, 3, 6, 7, 8$ and N_f arbitrary. To begin with, we notice that for vanishing θ the vacuum is determined by the competition of mass and baryon chemical potential. In other words, the ground state can be written as [177]

$$\Sigma_c = \begin{pmatrix} 0 & \mathbb{1}_{N_f} \\ -\mathbb{1}_{N_f} & 0 \end{pmatrix} \cos\varphi + i \begin{pmatrix} \mathcal{I} & 0 \\ 0 & \mathcal{I} \end{pmatrix} \sin\varphi \qquad \text{where} \qquad \mathcal{I} = \begin{pmatrix} 0 & -\mathbb{1}_{N_f/2} \\ \mathbb{1}_{N_f/2} & 0 \end{pmatrix} , \tag{3.3.1}$$

where the angle φ is determined by the equations of motion.

To study the effect of θ on the vacuum solutions it is convenient to introduce the Witten variables α_i as [178]

$$\Sigma_0 = U(\alpha_i)\Sigma_c , \qquad U(\alpha_i) \equiv \text{diag}\{e^{-i\alpha_1}, \dots, e^{-i\alpha_{N_f}}, e^{-i\alpha_1}, \dots, e^{-i\alpha_{N_f}}\} . \tag{3.3.2}$$

These variables reflect the possibility to generalize the mass matrix in (3.2.6) by replacing the $\mathbb{1}_{N_f}$ with $\text{diag}\{e^{-i\alpha_1}, \dots, e^{-i\alpha_{N_f}}\}$. Each phase is the overall axial transformation for each left-right quark pair. The reason why we cannot consider a single (odd number of) Weyl fermion(s) at the time (as is the case for real gauge representations) is that one cannot write a mass term in this case and the theory overall suffers from a topological anomaly [179].

We take the above to be the general ansatz for the vacuum. The Lagrangian evaluated on this ansatz reads

$$\mathcal{L}_\theta[\Sigma_0] = \nu^2 \left[4m_\pi^2 X \cos\varphi + 2\mu^2 N_f \sin^2\varphi - a\bar{\theta}^2\right] \tag{3.3.3}$$

where for later convenience we introduced

$$\bar{\theta} = \theta - \sum_i^{N_f} \alpha_i \,, \qquad X = \sum_i^{N_f} \cos\alpha_i \tag{3.3.4}$$

where $\bar{\theta}$ is the effective theta angle that enters physical observables. The equations of motion read

$$\sin\varphi \left(N_f \cos\varphi - \frac{m_\pi^2}{\mu^2} X \right) = 0 \tag{3.3.5}$$

$$2m_\pi^2 \sin\alpha_i \cos\varphi = a\bar{\theta} \,, \quad i = 1, .., N_f \tag{3.3.6}$$

and the energy of the system is

$$E = -\nu^2 \left[4m_\pi^2 X - a\bar{\theta}^2 \right] \,, \qquad \text{normal phase } (\varphi = 0) \tag{3.3.7}$$

$$E = -\nu^2 \left[2\frac{N_f^2\mu^4 + m_\pi^4 X^2}{N_f \mu^2} - a\bar{\theta}^2 \right] \,, \qquad \text{superfluid phase } \left(\cos\varphi = \frac{m_\pi^2}{N_f\mu^2} X \right) \,. \tag{3.3.8}$$

Note that when $a \gg m_\pi$ all the θ-dependence is contained in an effective pion mass $m_\pi^2(\theta) \equiv \frac{m_\pi^2 X}{N_f}$. For $\theta = 0$ (i.e. $U(\alpha_i) = \mathbb{1}$) one has $X = N_f$ and $\bar{\theta} = 0$, and we recover the results in [177]. In this case, a normal to superfluid phase transition occurs when $\mu = m_\pi$, i.e. when $\cos\varphi = 1$. For $\theta \neq 0$ the θ-dependence of the energy may be different in the two phases. Therefore, to find the conditions for the onset of the superfluid phase we first need to determine the θ vacuum in both phases. To this end, we observe that in the normal (superfluid) phase the energy is minimized when X (X^2) is maximized. In the former case, the Witten variables are related to θ by the well-known equation

$$2m_\pi^2 \sin\alpha_i = a\bar{\theta} = a \left(\theta - \sum_i^{N_f} \alpha_i \right) \,. \tag{3.3.9}$$

For the general solution we must have for any $\bar{\theta}$ fixed $\sin\alpha_i = \sin\alpha_j$. To solve for the α_i we consider the expansion in the parameter $\frac{m_\pi^2}{a}$ that we take to be small. Concretely, at the leading order one needs to solve for $\bar{\theta} = 0$ and the angles α_i satisfy

$$\alpha_i = \begin{cases} \pi - \alpha, & i = 1, \ldots, n \\ \alpha, & i = n+1, \ldots, N_f \end{cases} \tag{3.3.10}$$

where α is the solution of the following modular equation

$$n(\pi - \alpha) + (N_f - n)\alpha = \theta \text{ Mod } 2\pi \,. \tag{3.3.11}$$

The modulo comes from the fact that if a solution $\{\alpha_i\}$ of eq.(3.3.9) is found, then it is possible to build another solution as follows

$$\alpha_1(\theta + 2\pi) = \alpha_1(\theta) + 2\pi \,, \qquad \alpha_i(\theta + 2\pi) = \alpha_i(\theta) \,, \quad i = 2, \ldots, N_f \,. \tag{3.3.12}$$

However, since the physics depends only on $e^{-i\alpha_i}$, the dynamics is invariant under $\theta \to \theta + 2\pi$. The solution of eq.(3.3.11) can be written as

$$\alpha = \frac{\theta + (2k - n)\pi}{(N_f - 2n)}, \quad k = 0, \ldots, N_f - 2n - 1 \,, \quad n = 0, ..., \left[\frac{N_f - 1}{2} \right] \,. \tag{3.3.13}$$

The range for k above emerges because for $k \geq N_f - 2n$ we repeat the solution for a given n. Note that when $n \neq 0$, the vacuum spontaneously breaks $Sp(2N_f)$ because of the different phases for each quark flavour.

It is well-known that CP is preserved when $\bar{\theta} = 0$. For equal mass quarks as considered here, this happens when $m_\pi = 0$ or $\theta = 0$. On the other hand, for $\theta = \pi$ the Lagrangian (3.2.15) possess CP symmetry but in the normal phase the latter is spontaneously broken by the vacuum [180, 168, 181, 182] [1], leading to a strong θ-dependence near $\theta = \pi$. In fact, assuming that the ground state does not break $Sp(2N_f)$ spontaneously (i.e. $n = 0$), the vacua lie at [181]

$$U(\alpha_i) = e^{i\frac{\theta+2\pi k}{N_f}} \mathbb{1}_{2N_f} \,. \tag{3.3.14}$$

For $\theta = \pi$ one has $X = \cos\left(\frac{(2k+1)\pi}{N_f}\right)$, which is maximized when $k = 0$ and $k = N_f - 1$, that is

$$U(\alpha_i) = e^{\frac{i\pi}{N_f}} \mathbb{1}_{2N_f} \,, \qquad U(\alpha_i) = e^{-\frac{i\pi}{N_f}} \mathbb{1}_{2N_f} \,. \tag{3.3.15}$$

The two solutions are related by a CP transformation $U \to U^\dagger$ and thus CP is spontaneously broken. For $N_f > 2$ the minima are separated by an energy barrier while for $N_f = 2$ the leading order quark-mass induced potential vanishes[2], apparently leading to a paradoxical situation according to which one has massless pions and no explicit breaking of chiral symmetry. The paradox is simply resolved by going to higher orders in the mass for the chiral Lagrangian. Once these corrections are taken into account they lift, as expected, the vacuum degeneracy yielding two minima separated by a barrier [183, 184]. The spontaneous breaking of CP at $\theta = \pi$ is known as Dashen's phenomenon [180] and has been thoroughly studied in the literature [178, 185, 183, 184, 181, 182, 186]. As we shall see, in the superfluid phase CP may be violated or not at $\theta = \pi$ depending on the value of N_f. Once determined the α_i to the leading order in $\frac{a}{m_\pi^2}$, subleading corrections can be more easily computed. Note that in the superfluid phase the equation of motion (3.3.6) becomes

$$\frac{2m_\pi^4}{N_f \mu^2} X \sin\alpha_i = a\bar{\theta} \,, \qquad i = 1, .., N_f. \tag{3.3.16}$$

Hence, in this case the natural expansion parameter is $\frac{m_\pi^4}{a\mu^2}$ leading to an enhanced suppression compared to the normal phase.

We now consider specific values of N_f to cover most of the phase diagram for which chiral symmetry is expected to break spontaneously. In the companion paper [**?**] we will re-examine the values of N_f that are expected to cover the near-conformal dynamics.

3.3.1 $N_f = 2$

We now focus on the case $N_f = 2$ which has been previously considered in [187] at the leading order in $\frac{m_\pi^2}{a}$. In this limit, the two angles $\{\alpha_1, \alpha_2\}$ satisfy $\alpha_1 + \alpha_2 = \theta + 2k\pi$. Additionally, because $\sin\alpha_1 = \sin\alpha_2$ we have

$$\sin\alpha_1 = \sin\left(\theta + 2k\pi - \alpha_1\right) \tag{3.3.17}$$

[1] See also the discussion about the impact on the $\theta = \pi$ solution due to quark masses ordering provided in the appendix of [168].

[2] As well explained in the work by Smilga [183] this phenomenon occurs because the trace of $SU(2)$ matrices are real.

yielding the solutions

$$\sin\alpha_1 = \sin\alpha_2 = \sin\left(\frac{\theta}{2} + k\pi\right). \tag{3.3.18}$$

Only $k = 0$ and $k = 1$ are independent solutions of the equations of motion and agree with the general result in equation (3.6.17) for the α_i for $N_f = 2$ that has the two solutions corresponding to $n = 0$ and $k = 0, 1$ (i.e. $\{\alpha_1, \alpha_2\} = \{\frac{\theta}{2}, \frac{\theta}{2}\}$ and $\{\alpha_1, \alpha_2\} = \{\frac{\theta+2\pi}{2}, \frac{\theta+2\pi}{2}\}$).

To determine the solution corresponding to the ground state for any value of θ we need to consider the ground state energy. In the normal phase, the energy is linear in X and therefore the original equation of motion solutions cross at $\theta = \pi$ where Dashen's phenomenon occurs stemming from spontaneous CP symmetry breaking. Because in the superfluid phase we have that the ground state energy is proportional to X^2 the two solutions are identical yielding a degenerate ground state. Interestingly this degeneracy is not lifted by higher order corrections in $\frac{m_\pi^2}{a}$. The θ-dependence in the two phases is shown in Fig.3.1. Additionally, when $\theta = \pi$ the effective mass $m_\pi^2(\theta) \sim m_\pi^2 \left|\cos\left(\frac{\theta}{2}\right)\right|$ vanishes up to correction of order $cO\left(\frac{m_\pi^2}{a}\right)$. Therefore, the mass term disappears from the Lagrangian and the global flavor symmetry is again $SU(4)$ consequently leading to massless Goldstones when it spontaneously breaks to $Sp(4)$ [187]. Nevertheless, there is no chiral symmetry restoration in the fundamental Lagrangian. As mentioned, this apparent paradox is solved by realising that $SU(4)$ is still broken by higher order mass terms in the effective Lagrangian also for $a \to \infty$ [183, 187, 181]. By including the first two subleading

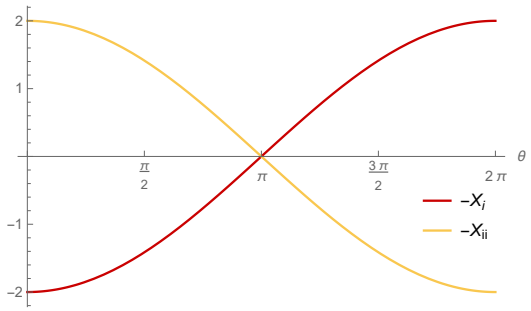

(a) θ-dependence of the energy in the normal phase for $N_f = 2$.

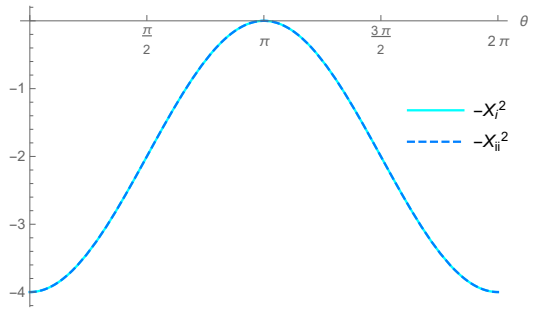

(b) θ-dependence of the energy in the superfluid phase for $N_f = 2$.

Figure 3.1: θ-dependence of the energy for $N_f = 2$.

corrections in $\frac{m_\pi^2}{a}$, the energy in the two phases reads

$$E(\theta) = -8m_\pi^2\nu^2\left(\left|\cos\frac{\theta}{2}\right| + \frac{1}{2}\frac{m_\pi^2}{a}\sin^2\frac{\theta}{2} - \frac{1}{4}\frac{m_\pi^4}{a^2}\left|\sin\frac{\theta}{2}\sin\theta\right|\right), \quad \text{normal phase} \tag{3.3.19}$$

$$E(\theta) = -\nu^2\left(\frac{4\left(m_\pi^4\cos^2\frac{\theta}{2} + \mu^4\right)}{\mu^2} + \frac{m_\pi^8\sin^2\theta}{a\mu^4} - \frac{m_\pi^{12}\sin^2\theta\cos\theta}{a^2\mu^6}\right), \quad \text{superfluid phase}\,. \tag{3.3.20}$$

At fixed quark masses, the superfluid phase transition occurs at a critical value of the chemical potential given by

$$\mu_c = m_\pi(\theta) = m_\pi\left[\sqrt{\left|\cos\frac{\theta}{2}\right|} + \mathcal{O}\left(\frac{m_\pi^2}{a}\right)\right], \tag{3.3.21}$$

implying that it can be realized for tiny values of the chemical potential when $\theta \sim \pi$. To estimate μ_c in the region $\theta \sim \pi$, we introduce $\phi \equiv \theta - \pi$ and take into account the leading correction in $\frac{m_\pi^2}{a}$. As a result, we have that for small $|\phi|$ the critical chemical potential in the region $\theta \sim \pi$ reads

$$\mu_c \sim m_\pi \sqrt{\frac{m_\pi^2}{a} + \frac{|\phi|}{2}}\,, \tag{3.3.22}$$

and vanishes for $a \to \infty$ and $\phi \to 0$.

Still, in the superfluid phase the energy is an analytic function of θ. This can be better appreciated by analyzing the CP order parameter $\left\langle F\tilde{F} \right\rangle \propto -\frac{\partial E}{\partial \theta}$ shown in Fig. 3.2 for the two phases. The normal phase is characterized by a discontinuous CP order parameter at $\theta = \pi$ while it is clear from the right-hand panel of the figure that the superfluid phase displays a smooth behavior for any value of the θ-angle and vanishes for $\theta = \pi$.

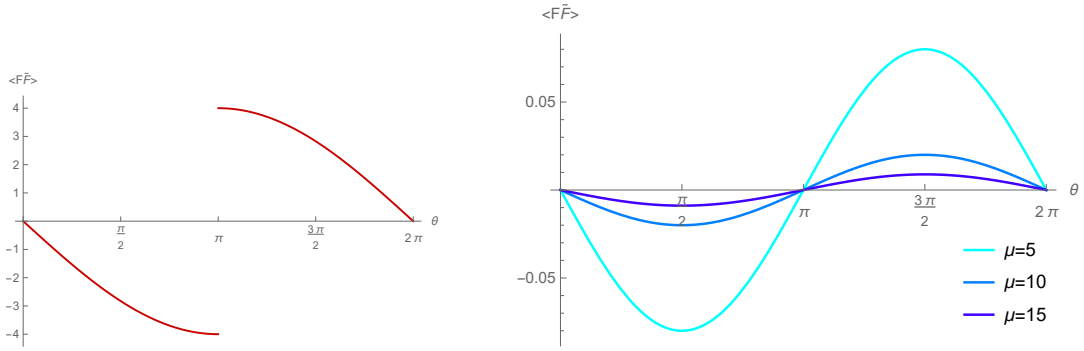

(a) CP order parameter for $N_f = 2$ in the normal phase.

(b) CP order parameter for $N_f = 2$ in the superfluid phase.

Figure 3.2: CP order parameter as a function of θ both in the normal and superfluid phase for $N_f = 2$.

The discontinuity of the CP order parameter in the normal phase translates into a divergent topological susceptibility $\chi = \dfrac{\partial^2 E}{\partial \theta^2}$ at $\theta = \pi$. Note that the presence of the baryon chemical potential suppresses CP violation for every value of θ as can be seen from the right panel of Fig. 3.2. Finally, we study the effective $\bar{\theta}$ angle for $\theta = \pi$ at higher orders in $\frac{m_\pi^2}{a}$ for the solutions of the equations of motion. We find

$$\bar{\theta} = \frac{2m_\pi^2}{a} \sin\frac{\theta}{2} \underset{\theta=\pi}{=} \frac{2m_\pi^2}{a} + \mathcal{O}\left(\frac{m_\pi^6}{a^3}\right), \qquad \text{normal phase} \tag{3.3.23}$$

$$\bar{\theta} = \frac{m_\pi^4}{a\mu^2} \sin\theta \underset{\theta=\pi}{=} 0\,, \qquad \text{superfluid phase}\,. \tag{3.3.24}$$

Note that eq.(3.3.24) is exact to all orders in $\frac{m_\pi^4}{a\mu^2}$ since the equation of motion (3.3.16) becomes

$$\frac{m_\pi^4}{a\mu^2} \sin(2\alpha) = \pi - 2\alpha\,, \tag{3.3.25}$$

and has the solution $\alpha = \pi/2$ (equivalent to $\alpha = 3\pi/2$ under a shift $\theta \to \theta + 2\pi$). Therefore to the present order in the chiral expansion, there is no spontaneous CP symmetry breaking in the superfluid phase for $\theta = \pi$.

3.3.2 $N_f = 3$

Compared to the previous subsection, the $N_f = 3$ case leads to a richer vacuum structure as has been first pointed out in [183], who studied the physics in the normal phase. In fact, we find the following four solutions for the set $\{\alpha_i\} = \{\alpha_1\,, \alpha_2\,, \alpha_3\}$

$$\textbf{i.}\left\{\frac{\theta}{3}, \frac{\theta}{3}, \frac{\theta}{3}\right\}, \quad \textbf{ii.}\left\{\frac{\theta+2\pi}{3}, \frac{\theta+2\pi}{3}, \frac{\theta+2\pi}{3}\right\}, \quad \textbf{iii.}\left\{\frac{\theta+4\pi}{3}, \frac{\theta+4\pi}{3}, \frac{\theta+4\pi}{3}\right\}, \quad \textbf{iv.}\left\{\theta-\pi\,, \theta-\pi\,, 2\pi-\theta\right\}. \tag{3.3.26}$$

In Fig.3.3.(a) we show the value of the variable $-X$ as a function of θ. Recalling that in the normal phase, the energy is minimized when X is maximized, we observe that the physical vacuum is ruled by the solutions **i.** and **iii.** which cross at $\theta = \pi$ where Dashen's phenomenon occurs [183]. In the superfluid phase the story changes since now the minimum of the energy is achieved when X^2 is maximized. The situation is depicted in Fig. 3.3.(b): here the relevant solutions are **i.**, **ii.**, **iii.**. Solutions **i.** and **ii.** cross at $\theta = \frac{\pi}{2}$ whereas **ii.** and **iii.** cross at $\theta = \frac{3\pi}{2}$. Therefore, at $\theta = \pi$ we have a unique minimum and CP is conserved. In other words, Dashen's phenomenon at $\theta = \pi$ is again absent in the superfluid region. However, two new non-analytic points occur, one at $\theta = \frac{\pi}{2}$ and the other at $\theta = \frac{3\pi}{2}$. These are indications of two novel first-order phase transitions because the derivative of the free energy (corresponding to the CP order parameter $\left\langle F\widetilde{F}\right\rangle$) jumps at these two values of θ.

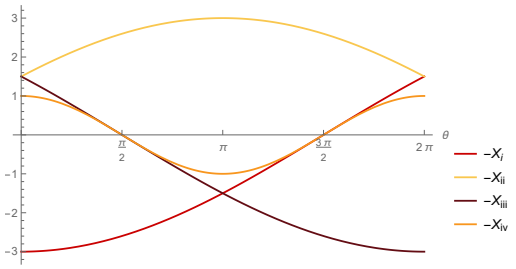

θ-dependence of the energy in the normal phase for $N_f = 3$.

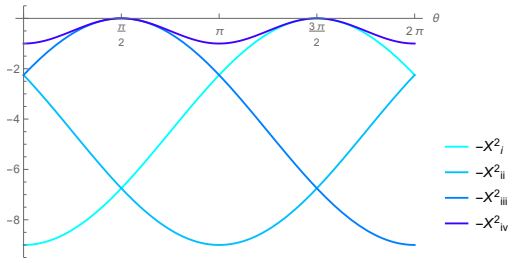

θ-dependence of the energy in the superfluid phase for $N_f = 3$.

Figure 3.3: θ-dependence of the energy for $N_f = 3$.

Having determined the θ-vacuum in the two regions, we proceed by studying the transition between the normal and superfluid phases. Since the $U(\alpha_i)$ that minimizes the energy depends on θ and differs in the two phases, one should determine the critical μ by comparing the energies (3.3.7) and (3.3.8) in the given intervals of θ. We find that when the superfluid solution exists (i.e. $\cos\varphi \leq 1$) it is always realized. In turn, the critical chemical potential is $\mu_c = m_\pi(\theta)$, which is displayed in Fig.3.4. Differently from the $N_f = 2$ case, μ_c exhibits a mild dependence on θ and oscillates near the value $\mu_c = m_\pi$.

The CP order parameter is plotted for the normal and superfluid phases in Fig.3.5 (a) and Fig. 3.5 (b), respectively. Finally, we show the value of $\bar{\theta}$ at $\theta = \pi$ for the ground state energy. The expression in the $\frac{m_\pi^2}{a}$ expansion is

$$\bar{\theta} = \frac{\sqrt{3}m_\pi^2}{a} - \frac{m_\pi^4}{\sqrt{3}a^2} - \frac{m_\pi^6}{6\sqrt{3}a^3} + \mathcal{O}\left(\frac{m_\pi^8}{a^4}\right), \qquad \text{normal phase} \tag{3.3.27}$$

$$\bar{\theta} = 0, \qquad \text{superfluid phase}\,. \tag{3.3.28}$$

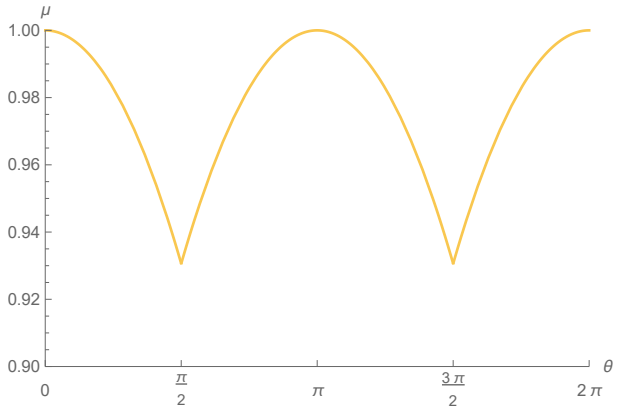

Figure 3.4: Normalized critical chemical potential ($m_\pi = \nu = 1$) above which the superfluid phase is realized as a function of θ for $N_f = 3$.

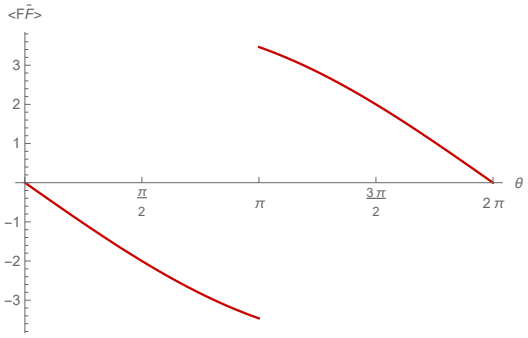

(a) The CP order parameter $\left\langle F\tilde{F}\right\rangle$ as a function of θ in the normal phase. We consider $m_\pi = \nu = 1$.

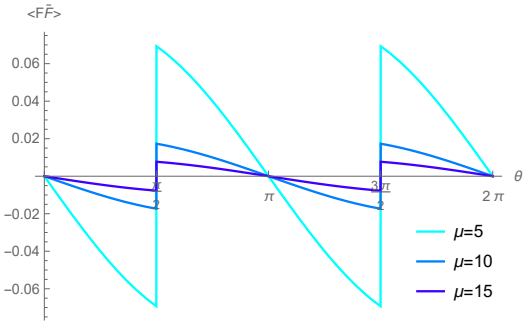

(b) The CP order parameter $\left\langle F\tilde{F}\right\rangle$ as a function of θ in the superfluid phase for different values of the chemical potential: $\mu = 5, 10, 15$. We consider $m_\pi = \nu = 1$.

Figure 3.5: θ-dependence of the CP order parameter for $N_f = 3$.

3.3.3 $N_f = 6$

The full set of solutions is given by

$$\begin{aligned}
&\text{Solutions i-vi}: \alpha_1 = \alpha_2, \cdots = \alpha_6 = \frac{\theta + 2\pi k}{6}, && k = 0, \ldots, 5 \\
&\text{Solutions vii-ix}: \alpha_1 = \alpha_2 = \cdots = \alpha_5 = \frac{\theta - \pi + 2\pi k}{4}, \quad \alpha_6 = \pi - \alpha_1\,, && k = 0, \ldots, 3 \\
&\text{Solutions x-xii}: \alpha_1 = \alpha_2 = \cdots = \alpha_4 = \frac{\theta - 2\pi + 2\pi k}{2}, \quad \alpha_5 = \alpha_6 = \pi - \alpha_1, && k = 0, 1\ .
\end{aligned} \tag{3.3.29}$$

Here the relevant solutions for $U(\alpha_i)$ have $\alpha_1 = \alpha_2 = \cdots = \alpha_6 = \alpha$. Moreover, all the solutions appear in pairs of degenerate energy in the superfluid phase as already observed in the $N_f = 2$ case. This can be understood by noting that when N_f is even, then from a given solution α of eq.(3.6.17) it is possible to build another solution as $\alpha + \pi$ that will lead to the same $-X^2$. As displayed in Fig. 3.6.(a), in the normal phase the minimum of the energy is achieved for $\alpha = \frac{\theta}{6}$ (defined as solution i) and $\alpha = \frac{\theta + 10\pi}{6}$ (solution iii) with the two solutions crossing at $\theta = \pi$. This occurs also in the superfluid phase but now solution i and iii are degenerate for every value of θ with $\alpha = \frac{\theta}{6} + \pi$ and $\alpha = \frac{\theta + 4\pi}{6}$, respectively. In

Fig. 3.6.(b) we show the phase diagram of the theory as a function of θ and μ. Differently from $N_f = 2$ we still observe a Dashen phenomenon at $\theta = \pi$ and therefore CP breaks spontaneously for this value.

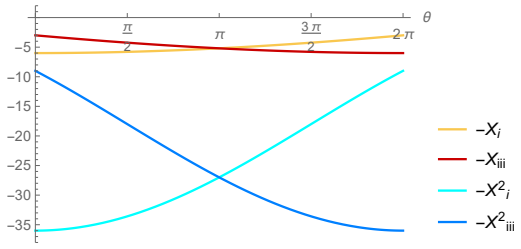

(a) θ-dependence of the energy for $N_f = 6$ both in the normal and superfluid phase.

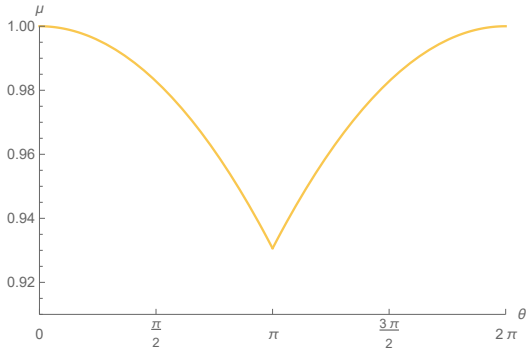

(b) Normalized critical chemical potential ($m_\pi = \nu = 1$) above which the superfluid phase is realized as a function of θ.

Figure 3.6: θ-dependence of the energy and of the critical chemical potential for $N_f = 6$.

In the $N_f = 6$ case we therefore have spontaneous breaking of CP at $\theta = \pi$ in both phases as can be seen considering the CP order parameter represented in Fig.3.7.(a) and Fig. 3.7.(b).

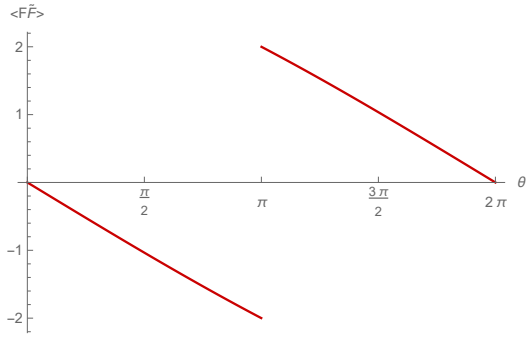

(a) The CP order parameter $\left\langle F\tilde{F}\right\rangle$ as a function of θ in the normal phase. We consider $m_\pi = \nu = 1$.

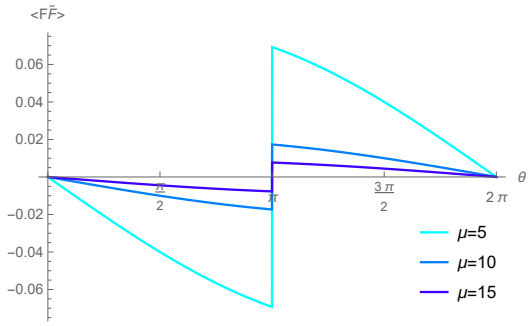

(b) The CP order parameter $\left\langle F\tilde{F}\right\rangle$ as a function of θ in the superfluid phase for different values of the chemical potential: $\mu = 5, 10, 15$. We consider $m_\pi = \nu = 1$.

Figure 3.7: θ-dependence of the CP order parameter for $N_f = 6$.

Finally, we report the value of $\bar{\theta}$ at $\theta = \pi$ expanded in $\frac{m_\pi^2}{a}$

$$\bar{\theta} = \frac{m_\pi^2}{a} - \frac{m_\pi^4}{2\sqrt{3}a^2} + \frac{5m_\pi^6}{72a^3} + \mathcal{O}\left(\frac{m_\pi^8}{a^4}\right), \qquad \text{normal phase} \quad (3.3.30)$$

$$\bar{\theta} = -\frac{\sqrt{3}m_\pi^4}{2a\mu^2} + \frac{m_\pi^8}{4\sqrt{3}a^2\mu^4} + \frac{m_\pi^{12}}{48\sqrt{3}a^3\mu^6} + \mathcal{O}\left(\frac{m_\pi^{16}}{a^4\mu^8}\right), \qquad \text{superfluid phase .} \quad (3.3.31)$$

3.3.4 $N_f = 7$

For the $N_f = 7$ case we have thus 16 solutions of eq.(3.6.17) which are given by

$$\begin{aligned}
&\text{Solutions i-vii}: \alpha_1 = \alpha_2, \cdots = \alpha_7 = \frac{\theta + 2\pi k}{7}, && k = 0, \ldots, 6 \\
&\text{Solutions viii-xii}: \alpha_1 = \alpha_2 = \cdots = \alpha_5 = \frac{\theta - \pi + 2\pi k}{5}, \quad \alpha_6 = \alpha_7 = \pi - \alpha_1\,, && k = 0, \ldots, 4 \\
&\text{Solutions xiii-xv}: \alpha_1 = \alpha_2 = \alpha_3 = \frac{\theta - 2\pi + 2\pi k}{3}, \quad \alpha_4 = \alpha_5 = \alpha_6 = \alpha_7 = \pi - \alpha_1, && k = 0, \ldots, 2 \\
&\text{Solution xvi}: \alpha_1 = \theta - 3\pi, \quad \alpha_2 = \alpha_3 = \cdots = \alpha_7 = \pi - \alpha_1\,. && (3.3.32)
\end{aligned}$$

The solution that minimizes the energy and their corresponding θ-dependence in the two phases is shown in Fig.3.8. As in the previous cases, the solutions that minimize the energy have all equal angles, corresponding here to the first set of solutions in (3.3.32). In particular, in the normal phase the minimum of the energy is achieved for $\alpha = \frac{\theta}{7}$ and $\alpha = \frac{\theta+12\pi}{7}$ with the two solutions crossing at $\theta = \pi$ (in Fig.3.8.(a)). The θ-dependence in the superfluid phase is analogous to the $N_f = 3$ case. In fact, the relevant solutions are $\alpha = \frac{\theta}{7}$, $\alpha = \frac{\theta+6\pi}{7}$, and $\alpha = \frac{\theta+12\pi}{7}$ with the first two crossing at $\theta = \frac{\pi}{2}$ while the second and the third at $\theta = \frac{3\pi}{2}$. As already described in the $N_f = 3$ section, the energy is characterised by a unique minimum and CP intact symmetry at $\theta = \pi$.

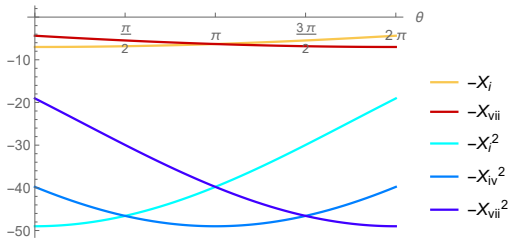

(a) θ-dependence of the energy for $N_f = 6$ both in the normal and superfluid phase.

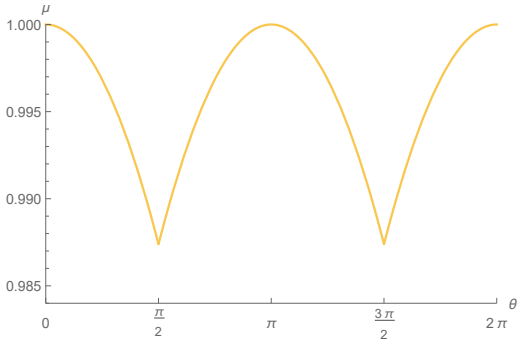

(b) Normalized critical chemical potential ($m_\pi = \nu = 1$) above which the superfluid phase is realized as a function of θ.

Figure 3.8: θ-dependence of the energy and of the critical chemical potential for $N_f = 7$.

The critical chemical potential is displayed in Fig.3.8.(b). It oscillates with period 2π between the values $\mu_c = m_\pi$ and $\mu_c = m_\pi(\theta)$. Fig. 3.8 leads us to further investigate the physical meaning of the $\theta = \frac{\pi}{2}$ and $\theta = \frac{3\pi}{2}$ points. As a consequence, we analysed the CP order parameter which we show in Fig.3.9 as a function of θ. As can be seen from the figure, the aforementioned points are actually points of discontinuity of the CP order parameter therefore it signals the occurrence of a first-order phase transition.
Finally, we provide the values of $\bar{\theta}$ at $\theta = \pi$ in the $\frac{m_\pi^2}{a}$ expansion

$$\bar{\theta} = \frac{2m_\pi^2 \sin\frac{\pi}{7}}{a} - \frac{2m_\pi^4 \cos\frac{3\pi}{14}}{7a^2} + \frac{2m_\pi^6 \sin\frac{\pi}{7}\left(1 + 3\sin\frac{3\pi}{14}\right)}{49a^3} + \mathcal{O}\left(\frac{m_\pi^8}{a^4}\right), \qquad \text{normal phase} \tag{3.3.33}$$

$$\bar{\theta} = 0, \qquad \text{superfluid phase}\,. \tag{3.3.34}$$

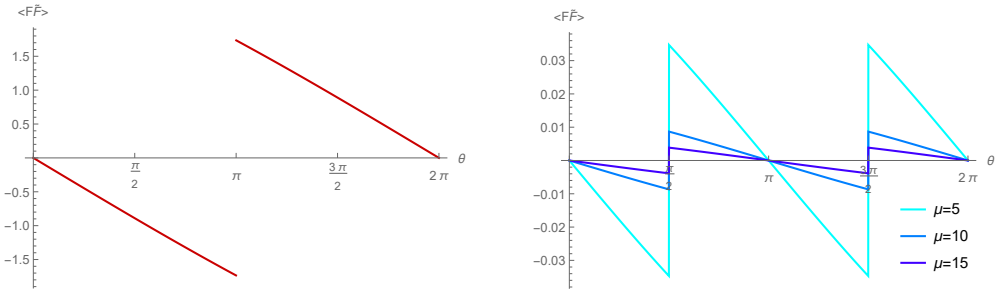

(a) The CP order parameter $\left\langle F\tilde{F}\right\rangle$ as a function of θ in the normal phase. We consider $m_\pi = \nu = 1$.

(b) The CP order parameter $\left\langle F\tilde{F}\right\rangle$ as a function of θ in the superfluid phase for different values of the chemical potential: $\mu = 5, 10, 15$. We consider $m_\pi = \nu = 1$.

Figure 3.9: θ-dependence of the CP order parameter for $N_f = 7$.

3.3.5 $N_f = 8$

We proceed with the general expression for the solutions of (3.6.17) for the $N_f = 8$ case

$$\text{Solutions i-viii}: \alpha_1 = \cdots = \alpha_8 = \frac{\theta + 2\pi k}{8}, \qquad k = 0, \ldots, 7 \tag{3.3.35}$$

$$\text{Solutions ix-xiv}: \alpha_1 = \cdots = \alpha_6 = \frac{\theta - \pi + 2\pi k}{6}, \quad \alpha_7 = \alpha_8 = \pi - \alpha_1, \qquad k = 0, \ldots, 5 \tag{3.3.36}$$

$$\text{Solutions xv-xviii}: \alpha_1 = \cdots = \alpha_4 = \frac{\theta - 2\pi + 2\pi k}{4}, \quad \alpha_5 = \cdots = \alpha_8 = \pi - \alpha_1, \qquad k = 0, \ldots, 3 \tag{3.3.37}$$

$$\text{Solutions xix-xx}: \alpha_1 = \alpha_2 = \frac{\theta - 3\pi + 2\pi k}{2}, \quad \alpha_3 = \cdots = \alpha_8 = \pi - \alpha_1, \qquad k = 0, 1\ . \tag{3.3.38}$$

In line with our previous analyses, the θ-dependence of the energy is minimized by the solutions with all equal angles. Fig. 3.10 displays the behavior of this minimum in the range $\theta \in [0, 2\pi]$ as well as the phase diagram of the theory. The θ-dependence is analogous to $N_f = 6$ case as it can be further deduced by studying the CP order parameter with its behavior shown in Fig.3.11 The value of $\bar{\theta}$ at $\theta = \pi$ in an $\frac{m_\pi^2}{a}$ expansion reads

$$\bar{\theta} = \frac{2m_\pi^2 \sin\frac{\pi}{8}}{a} - \frac{m_\pi^4}{4\sqrt{2}a^2} + \frac{\left(1 + \frac{3}{\sqrt{2}}\right) m_\pi^6 \sin\frac{\pi}{8}}{32a^3} + \mathcal{O}\left(\frac{m_\pi^8}{a^4}\right), \qquad \text{normal phase} \tag{3.3.39}$$

$$\bar{\theta} = \frac{m_\pi^4}{\sqrt{2}a\mu^2} - \frac{m_\pi^8}{8a^2\mu^4} + \frac{m_\pi^{12}}{64\sqrt{2}a^3\mu^6} + \mathcal{O}\left(\frac{m_\pi^{16}}{a^4\mu^8}\right), \qquad \text{superfluid phase}\ . \tag{3.3.40}$$

3.3.6 Considerations for general N_f

Having analyzed in detail the physics for different values of N_f away from the conformal window, we take a step back and consider the emerging structure hinting at structural differences between the even/odd N_f cases in the superfluid phase. We start by noting

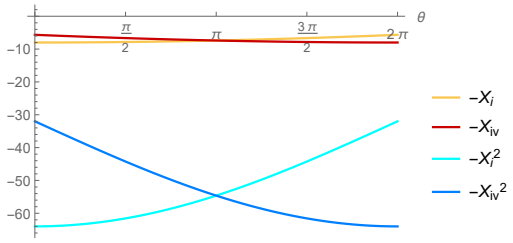

(a) θ-dependence of the energy for $N_f = 8$ both in the normal and superfluid phase.

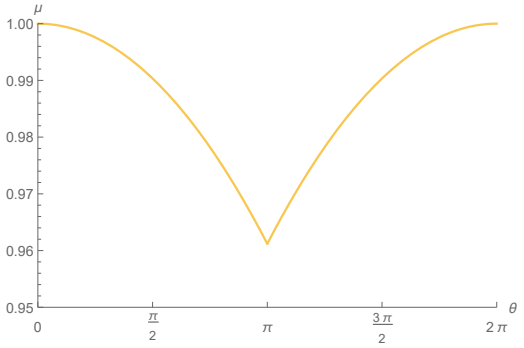

(b) Normalized critical chemical potential ($m_\pi = \nu = 1$) above which the superfluid phase is realized as a function of θ.

Figure 3.10: θ-dependence of the energy and of the critical chemical potential for $N_f = 8$.

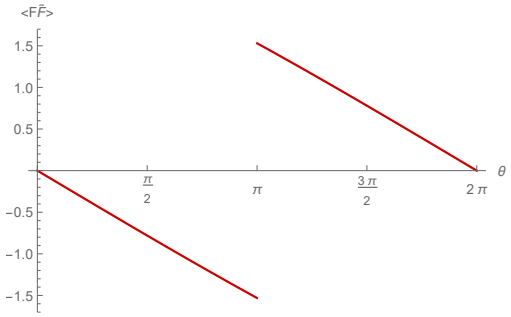

(a) The CP order parameter $\left\langle F\tilde{F} \right\rangle$ as a function of θ in the normal phase. We consider $m_\pi = \nu = 1$.

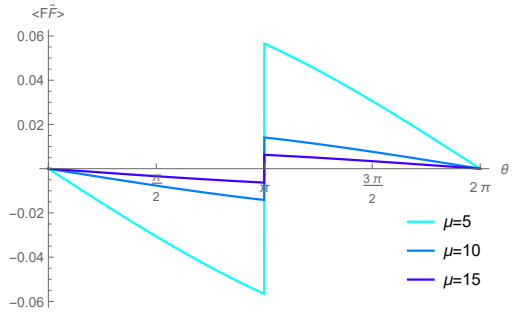

(b) The CP order parameter $\left\langle F\tilde{F} \right\rangle$ as a function of θ in the superfluid phase for different values of the chemical potential: $\mu = 5, 10, 15$. We consider $m_\pi = \nu = 1$.

Figure 3.11: θ-dependence of the CP order parameter for $N_f = 8$.

that solutions of the EOM are generally not periodic of 2π for θ. In fact, the periodicity condition can be satisfied only if at least two solutions cross in the interval $\theta \in [0, 2\pi]$. Taking $U = e^{-i\alpha} \mathbb{1}_{2N_f}$, one can ask when two different solutions of the equation of motion can have the same energy. This corresponds to requiring

$$\cos\left(\frac{\theta + 2\pi k_1}{N_f}\right) = \cos\left(\frac{\theta + 2\pi k_2}{N_f}\right) , \qquad \text{normal phase} \tag{3.3.41}$$

$$\cos^2\left(\frac{\theta + 2\pi k_1}{N_f}\right) = \cos^2\left(\frac{\theta + 2\pi k_2}{N_f}\right) , \qquad \text{superfluid phase .} \tag{3.3.42}$$

Both conditions are satisfied when $k_1 = -\frac{\theta}{\pi} - k_2 + N_f$. Since k_1, k_2 are integers, it follows that the energy can only be non-trivially equal for $\theta = \pi$. Therefore to find the two different solutions, in the normal phase, covering the full $[0, 2\pi]$ interval for θ it is sufficient to consider the case $k_1 = 0$ that for $[0, \pi]$ interval corresponds to the ground state energy, furthermore at $\theta = \pi$ it forces the second solution to be $k_2 = N_f - 1$. This result is in agreement with the findings for the specific cases above for the normal phase.

In the superfluid phase, we have two additional solutions to the second condition (3.3.42):

- When N_f is even we have the solution $k_1 = k_2 + \frac{N_f}{2}$ which does not depend on θ. This corresponds to the observation that the solutions for even N_f organize themselves in pairs (α and $\alpha + \pi$) with the same energy for every θ. Additionally, of course, we still have the normal phase solution $k_1 = 0$ and $k_2 = N_f - 1$ together with their superfluid degenerate partners. These two classes of solutions cross at $\theta = \pi$ except for the special $N_f = 2$ case for which the crossing disappears. Note that the pairs of completely degenerate solutions remain such to all orders in $\frac{m_\pi^2}{a}$. In fact, given the EOM for a certain α

$$\frac{m_\pi^4}{a\mu^2}\sin(2\alpha) = \theta - N_f\alpha\,, \tag{3.3.43}$$

  we have the same EOM for $\alpha + \pi$, upon shifting the θ-angle as $\theta \to \theta + N_f\pi$. Being N_f even, this corresponds to a shift by an integer multiple of 2π.

- When N_f is odd we have the solution $k_1 = -k_2 + \frac{N_f}{2} - \frac{\theta}{\pi}$ which can be realized for $\theta = \frac{\pi}{2}$ and $\theta = \frac{3\pi}{2}$. Since the solution that minimizes the energy near $\theta = 0$ is $\alpha = \frac{\theta}{N_f}$, then it will cross at $\theta = \frac{\pi}{2}$ with the solution for $\theta > \frac{\pi}{2}$ that becomes $\alpha = \frac{\theta+2\pi k_2}{N_f} = \frac{\theta-\pi}{N_f} + \pi$. The latter solution represents the minimum till $\theta = \frac{3\pi}{2}$ where its energy crosses with $\alpha = \frac{\theta-2\pi}{N_f}$. As a consequence, the vacuum is always non degenerate at $\theta = \pi$ where CP is conserved. In particular, for $\theta = \pi$, $\bar{\theta}$ vanishes to all orders in $\frac{m_\pi^4}{a\mu^2}$ since the equation of motion (3.3.16) admits the minimum energy solution $\alpha = \theta = \pi$. On the other hand, we have two novel first-order phase transitions at $\theta = \frac{\pi}{2}\,, \frac{3\pi}{2}$ due to a jump of the physical vacuum between the two minima and characterized by a discontinuous CP order parameter.

Finally, we estimate the tension of the domain wall between the two degenerate vacua at $\theta = \pi$ for even N_f in the superfluid phase. To this end, we consider the Lagrangian (3.2.15) and look for solutions $\alpha_i = \alpha_i(x)$ that interpolate between the two degenerate ground states(3.3.15) at $\theta = \pi$ with x the coordinate orthogonal to the domain wall. By considering the ansatz (3.3.2), we obtain the tension of the wall as

$$T = 2\nu^2 \int_{-\infty}^{\infty} dx \left[\sum_{i=1}^{N_f} \alpha_i'(x)^2 - \frac{m_\pi^4}{\mu^2 N_f}\left(\sum_{i=1}^{N_f}\cos\left(\frac{\pi}{N_f} + \alpha_i(x)\right)\right)^2\right] \tag{3.3.44}$$

where we have shifted α_i as $\alpha_i \to \alpha_i + \frac{\pi}{N_f}$ such that the boundary conditions are $\alpha(-\infty) = 0$ and $\alpha(\infty) = \pi$. As discussed in [181], the boundary condition fixes $\alpha_i = \alpha$ for $i = 1, \ldots, N_f - 1$ and $\alpha_{N_f} = -(N_f - 1)\alpha$, leading to

$$T = 2\nu^2 \int_{-\infty}^{\infty} dx \left[(N_f - 1)\, N_f \alpha'(x)^2 - \frac{m_\pi^4}{\mu^2 N_f}\left((N_f - 1)\cos\left(\alpha(x) + \frac{\pi}{N_f}\right) + \cos\left(\frac{\pi}{N_f} - (N_f - 1)\,\alpha(x)\right)\right)^2\right] \tag{3.3.45}$$

By introducing dimensionless coordinates as $\bar{x} = x\frac{m_\pi^2}{\mu}$, we obtain that regardless of the exact form of the wall's profile, its tension scales as

$$T \approx \frac{\nu^2 m_\pi^2}{\mu} \tag{3.3.46}$$

and shows a suppression by a factor or $\frac{m_\pi}{\mu}$ compared to the normal phase result $T \approx \nu^2 m_\pi$ [181].

3.3.7 Ground state energy with the axion

The effective action for two-color QCD at finite baryon number in the presence of the Peccei-Quinn axion field N is

$$L_{\text{eff}} = -a\nu^2 \left(\theta - \sum_{i=1}^{N_f} \alpha_i - \delta \right)^2 - \Lambda^4 + 4\nu^2 m_\pi^2 X \cos\varphi + 2\mu^2\nu^2 N_f \sin^2\varphi \,, \qquad \langle N \rangle = e^{-i\delta/a_{PQ}} \,, \tag{3.3.47}$$

whose equation of motion $\theta - \sum_{i=1}^{N_f} \alpha_i - \delta = 0$ is solved for $\delta = \theta$ and $\alpha_i = 0$. This solution minimizes the energy and leads to $X = N_f$. Hence, the superfluid ground state energy in presence of the axion corresponds to the known result at $\theta = 0$ [177]

$$E = -\frac{2\nu^2 N_f}{\mu^2} \left(m_\pi^4 + \mu^4 \right) \,. \tag{3.3.48}$$

3.4 Symmetry-breaking pattern and spectrum

In the section above we concentrated on determining the vacuum structure of the theory. We now move to establish the associated symmetry-breaking pattern starting with the theory without an axion. The pattern will allow us to disentangle the light degrees of freedom of the theory. We will keep the analysis as general as possible so that it is applicable to the near-conformal phase Sec.3.5.

3.4.1 Symmetry-breaking pattern without the axion

The dynamics of the theory at hand depends on three parameters: the mass of the quarks m, the chemical potential μ, and the scale of the axial anomaly a. The latter corresponds to the energy at which the pseudo-Goldstone (the S-particle) emerging from the spontaneous symmetry breaking of the axial symmetry acquires an anomalous mass. We are interested in the low energy theory where S is kept into the spectrum. We, therefore, consider the following hierarchy [3]

$$m \ll \sqrt{a} \leq \mu \ll 4\pi\nu \,, \tag{3.4.1}$$

where the last inequality implies the validity of the chiral EFT. For $m = \mu = 0$ and in absence of the singlet S, the infrared spectrum consists of massless Goldstone bosons of the spontaneously broken chiral symmetry as

$$SU\left(2N_f\right) \rightsquigarrow Sp\left(2N_f\right) , \tag{3.4.2}$$

implying the existence of $2N_f^2 - N_f - 1$ Goldstones transforming under the antisymmetric representation of $Sp(2N_f)$. When setting to zero the anomaly, and in the absence of the quark mass, the S-field becomes the Goldstone boson of the $U(1)_A$.

We now provide the full spectrum of light particles in the following limits

1. $\mathbf{m \neq 0, \mu = 0}$ **and** $\mathbf{\sqrt{a} \ll 4\pi\nu}$
   In this case, the presence of mass term m at the Lagrangian level explicitly break the global symmetry $SU(2N_f)$ to the residual subgroup $Sp(2N_f)$

$$SU(2N_f) \to Sp(2N_f) \tag{3.4.3}$$

[3] This hierarchy of scales is typical when modelling neutron stars in 2-color QCD at finite isospin chemical potential [188].

therefore $2N_f^2 - N_f$ pseudo-Goldstone bosons acquire masses via the non-zero quark mass.

2. $\mathbf{m = 0, \mu \neq 0}$ **and** $\mathbf{\sqrt{a} \ll 4\pi\nu}$
The introduction of the chemical potential breaks explicitly $SU(2N_f)$ to $SU(N_f)_L \times SU(N_f)_R \times U(1)_B$ while the anomaly breaks $U(1)_A$. The relativistic Bose-Einstein condensation leads to the spontaneous symmetry breaking $SU(N_f)_L \times SU(N_f)_R \times U(1)_B \rightsquigarrow Sp(N_f)_L \times Sp(N_f)_R$. Therefore, the final spectrum is composed of $N_f^2 - N_f - 1$ massless Goldstone bosons the massive S state due to the anomaly, and N_f^2 modes with mass proportional to the chemical potential. The latter belong to the (N_f, N_f) irreducible representation of $Sp(N_f)_L \times Sp(N_f)_R$ whereas the true Goldstones arrange themselves into three different irreducible representations: a singlet $(1,1)$, the $\left(\frac{N_f(N_f-1)}{2} - 1, 1\right)$ representation and the $\left(1, \frac{N_f(N_f-1)}{2} - 1\right)$. The sum of the degrees of freedom adds to $2N_f^2 - N_f$.

$$SU\left(2N_f\right) \to SU\left(N_f\right)_L \times SU\left(N_f\right)_R \times U(1)_B \rightsquigarrow Sp\left(N_f\right)_L \times Sp\left(N_f\right)_R . \tag{3.4.4}$$

3. $\mathbf{m \neq 0, \mu \neq 0}$ **and** $\mathbf{\sqrt{a} \ll 4\pi\nu}$
The situation here is involved due to the competition between the quark mass term and the baryon chemical potential. The chemical potential breaks $Sp(2N_f)$ down to $SU(N_f)_L \times SU(N_f)_R \times U(1)_B$, which, in turn, is explicitly broken by the mass term to its vectorial subgroup $SU(N_f)_V \times U(1)_B$. Finally, the superfluid vacuum breaks the latter symmetry group to $Sp(N_f)_V$ yielding to $\frac{N_f^2 - N_f}{2}$ massless Goldstone bosons as shown below

$$SU\left(2N_f\right) \to SU\left(N_f\right)_V \times U(1)_B \rightsquigarrow Sp\left(N_f\right)_V \tag{3.4.5}$$

The case of our interest is the last one, where we have $\frac{N_f^2 - N_f}{2}$ Goldstones transforming according to the antisymmetric representation of $Sp(N_f)_V$ plus a singlet. Additionally, there's the η' like state S with mass of order $\sqrt{a}$.

The naive counting above of the number of Goldstone bosons holds correct here since there are no Goldstone bosons of type II [189] in this case. The reason is that the dimension of the representation of the Goldstone bosons is identical to the number of broken generators (see discussion in [19]).

3.4.2 Symmetry-breaking pattern with the axion

In this section, we analyse the symmetry-breaking pattern for $m \neq 0$, $\mu \neq 0$, $a \ll 4\pi\nu$ but including the presence of the additional $U(1)_{PQ}$ symmetry discussed at the end of Sec.3.2. The latter is classically exact but quantum mechanically anomalous and spontaneously broken, leading to the existence of a new pseudo-Goldstone boson (the axion) with the mass of the order of the scale of the anomaly. We summarize below the pattern of symmetry breaking

$$SU\left(2N_f\right) \times U(1)_A \times U(1)_{PQ} \to SU\left(N_f\right)_V \times U(1)_B \rightsquigarrow Sp\left(N_f\right)_V \tag{3.4.6}$$

From the picture is clear that the spectrum of Goldstones remains the same as in the case without the axion with an additional singlet massive state.

In the next section, we will study the dispersion relations of the light modes describing the infrared dynamics by explicitly expanding the Lagrangian at the quadratic order in the fluctuations around the ground state.

3.4.3 Fluctuations spectrum

To analytically determine the dispersion relations of the different relevant states around the vacuum we consider the large a/m_π^2 expansion and stop at the leading order. We recover eqs. (69) and (84) of [177] for $\theta = 0$, and generalize them to include the θ-angle by taking it into account via an effective quark mass matrix. We obtain

$$\omega_1^2 = k^2 + \mu^2\,, \qquad \square\square \qquad \frac{1}{2}N_f(N_f+1) \tag{3.4.7}$$

$$\omega_2^2 = k^2 + \frac{m_\pi^4 X^2}{\mu^2 N_f^2}\,, \qquad \begin{array}{|c|}\hline\\\hline\\\hline\end{array} \qquad \frac{1}{2}N_f(N_f-1)-1 \tag{3.4.8}$$

$$\omega_3^2 = k^2 + \frac{2\left(\mu^4 N_f^2 + 3m_\pi^4 X^2\right)}{N_f^2\mu^2} + A\,, \qquad \bullet + \begin{array}{|c|}\hline\\\hline\\\hline\end{array} \qquad \frac{1}{2}N_f(N_f-1) \tag{3.4.9}$$

$$\omega_4^2 = k^2 + \frac{2\left(\mu^4 N_f^2 + 3m_\pi^4 X^2\right)}{N_f^2\mu^2} - A\,, \qquad \bullet + \begin{array}{|c|}\hline\\\hline\\\hline\end{array} \qquad \frac{1}{2}N_f(N_f-1) \tag{3.4.10}$$

$$\omega_5^2 = k^2 + M_S^2\,, \qquad \bullet \qquad 1 \tag{3.4.11}$$

where

$$A = \frac{2}{N_f^2\mu^2}\sqrt{\left(N_f^2\mu^4 + 3m_\pi^4 X^2\right)^2 + 4N_f^2\mu^2 m_\pi^4 k^2 X^2}\,, \tag{3.4.12}$$

$$M_S^2 = \frac{a\mu^4 N_f^3 + 2\mu^2 m_\pi^4 X^2}{2\mu^4 N_f^2 - 2m_\pi^4 X^2}\left(1 - \frac{m_\pi^4 X^2}{\mu^2 N_f^2}\right)\,. \tag{3.4.13}$$

The Young tableaux describe the irreducible representations of $Sp(N_f)$ according to which the states transform with $\bullet$ denoting the singlet representation. The number of degrees of freedom sum to $\dim\left(\frac{U(2N_f)}{Sp(2N_f)}\right) = N_f(2N_f-1)$, i.e the number of pseudo-Goldstones of the chiral symmetry breaking plus the η' like S-particle. For $\theta = 0$ the first four dispersion relations reduce to the ones found in [177]. ω_4 describes true Goldstone modes with speed $v_G = 1$ which parametrize the coset $\frac{SU(N_f)}{Sp(N_f)}$ and correspond to the π modes considered in [19]. These are the modes in which we will be mainly interested in the companion paper of this work since they dominate the large-charge dynamics. In addition, we have modes with a mass of order μ (ω_1 and ω_3) and modes with mass $\frac{m_\pi^2 X}{\mu N_f}$. If we include the axion in our theory, the dispersion relations of the modes described by eqs.(3.4.7)-(3.4.10) remain the same with $X = N_f$, i.e. we have the spectrum at $\theta = 0$ as expected from the Peccei-Quinn mechanism. On top of that, we have the modes stemming from the mixing between the singlet S and the axion, which is described by the following

inverse propagator

$$D^{-1} = \begin{pmatrix} \frac{\omega^2-k^2}{\sin^2\varphi} - M_S^2 & -\frac{a\sqrt{N_f}a_{PQ}}{4\sqrt{2}\nu_{PQ}\sin^2\varphi} \\ -\frac{a\sqrt{N_f}a_{PQ}}{4\sqrt{2}\nu_{PQ}\sin^2\varphi} & \frac{\omega^2-k^2}{4\nu^2\sin^2\varphi} - M_{\hat{a}}^2 \end{pmatrix} , \tag{3.4.14}$$

where

$$M_S^2 = \frac{\left(a\mu^4 N_f + 2\mu^2 m_\pi^4\right)}{2\mu^4 - 2m_\pi^4} \tag{3.4.15}$$

$$M_{\hat{a}}^2 = \frac{a\mu^4 a_{PQ}^2}{16\nu_{PQ}^2\left(\mu^4 - m_\pi^4\right)} . \tag{3.4.16}$$

The dispersion relations read

$$\omega_{6,7} = \frac{1}{2}\sqrt{4k^2 + 8\nu^2 M_{\hat{a}}^2\sin^2\varphi + 2M_S^2\sin^2\varphi \pm \frac{1}{\nu_{PQ}}\sqrt{2a^2\nu^2 N_f a_{PQ}^2 + 4\nu_{PQ}^2\sin^4\varphi\ \left(M_S^2 - 4\nu^2 M_{\hat{a}}^2\right)^2}} . \tag{3.4.17}$$

As can be seen from the inverse propagator, the S particle and the axion decouple in the anomaly-free limits $a \to 0$ and $a_{PQ} \to 0$. In the former case, the S-particle describes a pseudo-Goldstone mode with mass of order $M_S^2 = \frac{\mu^2 m_\pi^4}{\mu^4 - m_\pi^4}$, while for $a_{PQ} \to 0$ we have $M_S^2 = \frac{aN_f}{2}$ for $\mu \gg m_\pi$, in agreement with the Witten-Veneziano relation [165, 166]. On the other hand, in the limit of vanishing anomalies, the axion is massless being the $U(1)_{PQ}$ symmetry exact.

3.5 Conformal Window

In the previous sections, we have characterized the spectrum, the pattern of chiral symmetry breaking, and the dispersion relations at low energy of two-color QCD as a function of the baryon chemical potential, the topological term responsible for strong CP breaking as well as the quark masses. We considered different from two, three, six, seven and eight light matter flavors and determined the normal and superfluid ground state. We analysed these phases, studied the dependence of the critical chemical potential on the θ angle, delineating the boundary between the normal phase and the superfluid phase

In this section, we present the natural extension, near the conformal window [18, 19], of [2] in which we study the impact of the CP violating topological term [167] and axion field [92, 91, 93, 94, 95, 96, 97, 98] on the ground-state dynamics and low energy spectrum of *non* near conformal two-color QCD as function of matter fields both in the normal and superfluid phases of the theory [181, 177, 123, 190, 183]. There are two main ingredients that we use here to upgrade the analysis of [2] to describe near conformal dynamics. The first, is the introduction of a dilaton-like state ensuring (near) conformal dynamics following [191]. For fixed charge physics the introduction of the dilaton was considered in [19, 18] in absence of the topological θ term. The second ingredient is the interpretation via state-operator correspondence [192, 193] of the ground state energy on the cylinder as the lowest conformal dimension of the operators carrying nonzero baryon charge. Under a scale transformation $x \mapsto e^\alpha x$, each operator $\mathcal{O}_k$ of dimension k is assumed to transform as follows

$$\mathcal{O}_k \mapsto e^{(k-4)\sigma f}\ \mathcal{O}_k , \tag{3.5.1}$$

where f is the order parameter of the spontaneous scale symmetry breaking whose pseudo-Goldstone boson transforms as

$$\sigma \mapsto \sigma - \frac{\alpha}{f} \ . \tag{3.5.2}$$

We consider the fermion-induced mass term operator to have dimension $y = 3 - \gamma$, with γ being the anomalous dimension of the fermion condensate constrained to be $0 < \gamma < 2$ by the unitarity bound. However, around $\gamma \simeq 1$ the underlying four fermion operator becomes near-marginal and therefore we will concentrate our analysis in the interval $0 < \gamma < 1$.

In the absence of the underlying quark mass, the underlying conformal symmetry can break due to the emergence of another operator $\mathcal{O}$ with $\Delta_{\mathcal{O}}$ scaling dimensions just below the critical number of matter fields below which conformality is lost. This dynamics is encoded in the dilaton potential. This amounts to adding to the CFT the following Lagrangian term:

$$\delta L_{\mathcal{O}} = \lambda_{\mathcal{O}} \mathcal{O} \ . \tag{3.5.3}$$

Here $\lambda_{\mathcal{O}}$ is the associated coupling to the Lagrangian. One expects this operator to be, for example, related to the emergence of a quasi-relevant four-fermion interaction [145, 194, 195, 196, 197]. The general form of the dilaton potential is

$$V(\sigma) = f^{-4}\, e^{-4\sigma f} \sum_{n=0}^{\infty} c_n\, e^{-n(\Delta_{\mathcal{O}}-4)f\sigma} \ , \tag{3.5.4}$$

as can be shown by introducing a spurion field taking into account the explicit breaking of conformal symmetry [42, 41, 43, 198]. Here $\Delta_{\mathcal{O}}$ is the scaling dimension of $\mathcal{O}$ while the c_n depend on the given theory. Since we are interested in describing near-conformal dynamics we assume that the explicit breaking is small. This can be realized when $\lambda_{\mathcal{O}} \ll 1$ and/or $\mathcal{O}$ is near marginal. In the former case one expects $c_n \sim \lambda_{\mathcal{O}}^n$.

Inspired by the above ordering one could truncate the expansion (3.5.4) to the first two terms and obtain [41]

$$V(\sigma) = \frac{m_\sigma^2 e^{-4f\sigma}}{4(4-\Delta_{\mathcal{O}})f^2}\left(1 - \frac{4}{\Delta_{\mathcal{O}}} e^{-(\Delta_{\mathcal{O}}-4)f\sigma}\right) + \mathcal{O}(\lambda_{\mathcal{O}}^2) \ . \tag{3.5.5}$$

Here the first two unknown coefficients have been fixed by requiring that the ground state occurs for $\sigma = 0$ and that the mass squared of σ on the ground state is m_σ^2. These constraints link the c_0 and c_1 coefficients as follows

$$\frac{c_1}{c_0} = -\frac{4}{\Delta_{\mathcal{O}}} \ , \quad \text{with} \quad c_0 = \frac{f^2\, m_\sigma^2}{4(4-\Delta_{\mathcal{O}})} \ . \tag{3.5.6}$$

The coefficient of the cosmological constant c_0 is thereby forced to be of the same order as the first coefficient of the series $c_1 \sim \lambda_{\mathcal{O}}$. This potential has been employed in recent investigations [198] including comparisons with lattice simulations [199]. Assuming $\Delta_{\mathcal{O}} = 2$ one recovers the usual ϕ^4 Higgs-like potential while in the $\Delta_{\mathcal{O}} \to 0$ limit one obtains

$$V_{\Delta_{\mathcal{O}}\to 0}(\sigma) = -\frac{m_\sigma^2}{4\Delta_{\mathcal{O}} f^2} - \frac{m_\sigma^2}{16 f^2}\left(-4f\sigma - e^{-4f\sigma} + 1\right) + \mathcal{O}\left(\Delta_{\mathcal{O}}\right) \tag{3.5.7}$$

The order $\mathcal{O}\left(\Delta_{\mathcal{O}}^0\right)$ term in the above expression coincides with the dilaton potential considered in the pioneering work of Coleman [48].

Another interesting limit is the one for which the deformation itself is nearly marginal $\Delta_{\mathcal{O}} \to 4$. Here one expands eq.(3.5.4) in powers of $\Delta_{\mathcal{O}} - 4$ obtaining

$$V(\sigma) = -\frac{m_\sigma^2 e^{-4f\sigma}}{16 f^2}(1 + 4f\sigma) + \mathcal{O}\left((\Delta_{\mathcal{O}} - 4)^2\right) \ . \tag{3.5.8}$$

In fact, here one can abide the conditions that the potential is minimized for $\sigma = 0$ and that at the leading order in $\Delta_{\mathcal{O}} - 4$ the mass for the dilaton is m_σ without assuming an expansion in $\lambda_{\mathcal{O}}$. The same potential can be derived from (3.5.5) in the double limit $\Delta_{\mathcal{O}} \to 4$ and $\lambda_{\mathcal{O}} \to 0$.

The potential in (3.5.8) acquired central stage in a series of interesting papers by Golterman and Shamir [150, 151, 153, 200, 154, 201, 156]. In these works the authors considered a dilaton EFT featuring the following counting in the parameters $p^2 \sim m \sim N_f - N_f^* \sim 1/N_c$. N_f^* is taken to be the critical number of fermions marking the onset of the IR fixed point, and m is the quark mass.

In this work, we consider the established potentials for $\Delta_{\mathcal{O}} \to 4$, $\Delta_{\mathcal{O}} = 2$, and $\Delta_{\mathcal{O}} \to 0$. In the latter case we disregard the divergent constant in eq.(3.5.7).

3.5.1 Baryon charging the Dilaton-θ-Axion-Chiral Lagrangian

To access the (near) conformal dynamics of large charge operators we consider our system on a manifold $\mathcal{M}$ with volume V and curvature R such that the underlying new scale of the theory is $\Lambda_Q = (Q/V)^{1/3}$ where Q is the fixed baryon charge. Concretely, we will take our manifold to be $\mathcal{M} = \mathbb{R} \times S^{d-1}$ such that we consider an approximate state-operator correspondence implying:

$$\Delta_Q = \tilde{V}^{1/3} E_Q \,, \qquad E_Q = \mu Q - \mathcal{L} \,, \tag{3.5.9}$$

where Δ_Q is the scaling dimension of the lowest-lying operator with baryon charge Q, E_Q is the ground state energy on $\mathbb{R} \times S^{d-1}$ at fixed charge, $\tilde{V}^{1/3}$ is the radius of S^{d-1}, and μ is the baryon chemical potential.

As customary, we introduce the chemical potential into the covariant derivative as the zero component of a gauge field. The dynamics of the theory is controlled by various energy scales. These are the chemical potential μ, the mass of the quarks m, the scale of the axial anomaly a, the scales of chiral and conformal symmetry breaking ν and f, respectively, and the explicit conformal symmetry breaking scale m_σ. One can envision different counting schemes respecting the following hierarchy

$$m_\pi \,, m_\sigma \ll \mu \ll 4\pi\nu \,, \tag{3.5.10}$$

The first inequality implies that the theory is in the broken phase where pion condensation occurs [2] while the last inequality ensures the applicability of the chiral EFT at finite chemical potential.

After taking into account the background geometry and the dressing with the dilaton we arrive at the following two Lagrangians [35, 202, 11, 48, 18]

$$\begin{aligned}\mathcal{L}_{\theta,\sigma} = {} & \nu^2 Tr\{\partial_\mu \Sigma \partial^\mu \Sigma^\dagger\}\, e^{-2\sigma f} + 4\mu\nu^2 Tr\{B\Sigma^\dagger \partial_0 \Sigma\}\, e^{-2\sigma f} + m_\pi^2 \nu^2 Tr\{M\Sigma + M^\dagger \Sigma^\dagger\}\, e^{-y\sigma f} + \\ & + 2\mu^2\nu^2 \left[Tr\{\Sigma B^T \Sigma^\dagger B\} + Tr\{BB\}\right]\, e^{-2\sigma f} - a\nu^2 \left(\theta - \frac{i}{4} Tr\{\log\Sigma - \log\Sigma^\dagger\}\right)^2\, e^{-4\sigma f} + \\ & + \frac{1}{2}\left(\partial_\mu\sigma\partial^\mu\sigma - \frac{R}{6f^2}\right)\, e^{-2\sigma f} - V(\sigma) - \Lambda_0^4\, e^{-4\sigma f} \,,\end{aligned} \tag{3.5.11}$$

and

$$\begin{aligned}\mathcal{L}_{\hat{a},\sigma} &= \nu^2 Tr\{\partial_\mu \Sigma \partial^\mu \Sigma^\dagger\}\ e^{-2\sigma f} + 4\mu\nu^2 Tr\{B\Sigma^\dagger \partial_0 \Sigma\}\ e^{-2\sigma f} + m_\pi^2 \nu^2 Tr\{M\Sigma + M^\dagger \Sigma^\dagger\}\ e^{-y\sigma f} \\ &+ 2\mu^2\nu^2 \left[Tr\{\Sigma B^T \Sigma^\dagger B\} + Tr\{BB\}\right]\ e^{-2\sigma f} + \nu_{PQ}^2 \partial_\mu N \partial^\mu N^\dagger\ e^{-2\sigma f} + \\ &- a\nu^2 \left(\theta - \frac{i}{4} Tr\{\log\Sigma - \log\Sigma^\dagger\} - \frac{i}{4} a_{PQ}(\log N - \log N^\dagger)\right)^2\ e^{-4\sigma f} + \\ &+ \frac{1}{2}\left(\partial_\mu\sigma\partial^\mu\sigma - \frac{R}{6f^2}\right)\ e^{-2\sigma f} - V(\sigma) - \Lambda_0^4\ e^{-4\sigma f}\ ,\end{aligned} \tag{3.5.12}$$

where for later convenience we included the bare cosmological constant Λ_0.

3.6 The vacuum structure and semiclassical expansion

In this section, we study the classical ground state energy of the theory which, according to the state-operator correspondence, gives the leading order in the large-charge expansion for the scaling dimension of the lowest-lying operator with baryon charge Q. As discussed in detail in [2] the ground state takes the following form

$$\Sigma_0 = U(\alpha_i)\Sigma_c \tag{3.6.1}$$

with

$$\begin{aligned}&U(\alpha_i) = \text{diag}\{e^{-i\alpha_1}, \dots, e^{-i\alpha_{N_f}}, e^{-i\alpha_1}, \dots, e^{-i\alpha_{N_f}}\} \quad \text{and} \\ &\Sigma_c = \begin{pmatrix} 0 & \mathbb{1}_{N_f} \\ -\mathbb{1}_{N_f} & 0 \end{pmatrix} \cos\varphi + i \begin{pmatrix} \mathcal{I} & 0 \\ 0 & \mathcal{I} \end{pmatrix} \sin\varphi \quad \text{with} \quad \mathcal{I} = \begin{pmatrix} 0 & -\mathbb{1}_{N_f/2} \\ \mathbb{1}_{N_f/2} & 0 \end{pmatrix}\ ,\end{aligned} \tag{3.6.2}$$

where the alignment angle φ and the Witten variables α_i are determined by the equations of motion (EOMs).

Replacing this vacuum ansatz, the Lagrangian (3.5.11) becomes

$$\begin{aligned}\mathcal{L}_{\theta,\sigma}\left[\Sigma_0, \sigma_0\right] = &-e^{-4f\sigma_0}\Lambda_0^4 - V(\sigma_0) - \frac{R\ e^{-2f\sigma}}{12f^2} + 4m_\pi^2\nu^2 X\cos\varphi\ e^{-f\sigma_0 y} \\ &+ 2\mu^2 N_f \nu^2 e^{-2f\sigma_0}\sin^2\varphi - a\nu^2 e^{-4f\sigma_0}\bar{\theta}^2\ ,\end{aligned} \tag{3.6.3}$$

where

$$\bar{\theta} \equiv \theta - \sum_i^{N_f} \alpha_i\,, \qquad X \equiv \sum_i^{N_f} \cos\alpha_i\ . \tag{3.6.4}$$

The respective equations of motion are

$$N_f\mu^2 e^{-2f\sigma_0}\cos\varphi - m_\pi^2 X e^{-f\sigma_0 y} = 0 \tag{3.6.5}$$

$$a e^{-4f\sigma_0}\bar{\theta} - 2m_\pi^2 \sin\alpha_i \cos\varphi e^{-f\sigma_0 y} = 0\,, \qquad i = 1, .., N_f \tag{3.6.6}$$

$$\begin{aligned}&\frac{R e^{-2f\sigma_0}}{6f} + 4af\nu^2 e^{-4f\sigma_0} Y^2 + 4f\Lambda_0^4 e^{-4f\sigma_0} - \left.\frac{\partial V(\sigma)}{\partial\sigma}\right|_{\sigma=\sigma_0} + \\ &-4f\mu^2 N_f \nu^2 e^{-2f\sigma_0}\sin^2\varphi - 4fm_\pi^2\nu^2 yX\cos\varphi e^{-f\sigma_0 y} = 0\end{aligned} \tag{3.6.7}$$

$$4\mu N_f \nu^2 e^{-2f\sigma_0}\sin^2\varphi = \frac{Q}{V}\ . \tag{3.6.8}$$

We solve these equations in the large Q expansion; focusing on the two extreme cases $\gamma \ll 1$ and $1-\gamma \ll 1$, we find the following expressions for the ground state energy

- $\mathbf{V_{\Delta_{\mathcal{O}}\to 0}}(\sigma)$

$$
\begin{aligned}
E^{\gamma\ll 1} =& \frac{c_{4/3}Q^{4/3}}{\tilde{V}^{1/3}} + Q^{2/3}\tilde{V}^{1/3}\left\{c_{2/3}\tilde{R} - \frac{X_{00}^2}{4\pi^2 N_f^3 c_{4/3}^4}\left(\frac{9m_\pi^2}{32\nu}\right)^2\left[1-\gamma\left(\frac{2}{3}\log Q - \log\left(\frac{32N_f\nu^2\pi^2 c_{4/3}\tilde{V}^{2/3}}{3}\right)\right.\right.\right. \\
&\left.\left.\left. -\frac{X_{10}}{X_{00}}\right) + \mathcal{O}\left(\gamma^2\right)\right]\right\} - \tilde{V}\log Q\left\{\frac{16\pi^2}{9}N_f c_{2/3}c_{4/3}\nu^2 m_\sigma^2 - \frac{\gamma}{3\pi^2 N_f^4 c_{4/3}^5}\left(\frac{9m_\pi^2}{32\nu}\right)^2\left[\frac{5}{8\pi^2 c_{4/3}^4 N_f^2}\left(\frac{9m_\pi^2}{32\nu}\right)^2 X_{00}^4\right.\right. \\
&\left.\left. - c_{2/3}\tilde{R}N_f X_{00}^2 + \frac{9X_{00}X_{01}}{32c_{4/3}}\right] + \mathcal{O}\left(\gamma^2\right)\right\} + \mathcal{O}\left(Q^0\right), \\
E^{1-\gamma\ll 1} =& \frac{c_{4/3}Q^{4/3}}{\tilde{V}^{1/3}} + c_{2/3}Q^{2/3}\tilde{R}\tilde{V}^{1/3} - \left[\frac{16}{9}\pi^2 m_\sigma^2 N_f c_{2/3}c_{4/3}\nu^2 + \frac{9(1-\gamma)X_{00}^2 m_\pi^4}{64c_{4/3}^3 N_f^2} + \mathcal{O}\left((1-\gamma)^2\right)\right]\tilde{V}\log Q + \mathcal{O}\left(Q^0\right)
\end{aligned}
\tag{3.6.9}
$$

- $\mathbf{V_{\Delta_{\mathcal{O}}=2}}(\sigma)$

$$
\begin{aligned}
E^{\gamma\ll 1} =& \frac{c_{4/3}Q^{4/3}}{\tilde{V}^{1/3}} + Q^{2/3}\tilde{V}^{1/3}\left\{c_{2/3}\tilde{R} - \frac{1}{2}c_{2/3}m_\sigma^2 - \frac{X_{00}^2}{4\pi^2 N_f^3 c_{4/3}^4}\left(\frac{9m_\pi^2}{32\nu}\right)^2\left[1-\gamma\left(\frac{2}{3}\log Q - \frac{X_{10}}{X_{00}}\right.\right.\right. \\
&\left.\left.\left. - \log\left(\frac{32N_f\nu^2\pi^2 c_{4/3}\tilde{V}^{2/3}}{3}\right) + \mathcal{O}\left(\gamma^2\right)\right)\right]\right\} + \left\{\frac{\gamma}{3\pi^2 N_f^4 c_{4/3}^5}\left(\frac{9m_\pi^2}{32\nu}\right)^2\left[\frac{5}{8\pi^2 c_{4/3}^4 N_f^2}\left(\frac{9m_\pi^2}{32\nu}\right)^2 X_{00}^4\right.\right. \\
&\left.\left. -c_{2/3}\tilde{R}N_f X_{00}^2 + \frac{9X_{00}X_{01}}{32c_{4/3}}\right] + \mathcal{O}\left(\gamma^2\right)\right\}\tilde{V}\log Q + \mathcal{O}\left(Q^0\right), \\
E^{1-\gamma\ll 1} =& \frac{c_{4/3}}{\tilde{V}^{1/3}}Q^{4/3} + c_{2/3}Q^{2/3}\tilde{R}\tilde{V}^{1/3} - \frac{m_\sigma^2 c_{2/3}Q^{2/3}\tilde{V}^{1/3}}{2} - \left[\frac{9(1-\gamma)m_\pi^4 X_{00}^2}{64N_f^2 c_{4/3}^3} + \mathcal{O}\left((1-\gamma)^2\right)\right]\tilde{V}\log Q + \mathcal{O}\left(Q^0\right),
\end{aligned}
\tag{3.6.10}
$$

- $\mathbf{V_{\Delta_{\mathcal{O}}\to 4}}(\sigma)$

$$
\begin{aligned}
E^{\gamma\ll 1} =& \frac{c_{4/3}Q^{4/3}}{\tilde{V}^{1/3}}\left[1 + m_\sigma^2\frac{c_{2/3}}{256\pi^2\nu^2 N_f c_{4/3}^2}\left(4\log\left(\frac{3\sqrt{\frac{3}{2}}Q}{128\pi^3 c_{4/3}^{3/2}\nu^3\tilde{V}N_f^{3/2}}\right) - 3\right) + m_\sigma^4\right] \\
&+ c_{2/3}Q^{2/3}\tilde{R}\tilde{V}^{1/3}\left\{1 - \frac{X_{00}^2}{4\pi^2 N_f^3 c_{2/3}c_{4/3}^4\tilde{R}}\left(\frac{9m_\pi^2}{32\nu}\right)^2\left[1-\gamma\left(\frac{2}{3}\log Q - \frac{X_{10}}{X_{00}} - \log\left(\frac{32N_f\nu^2\pi^2 c_{4/3}\tilde{V}^{2/3}}{3}\right)\right)\right]\right. \\
&\left. - \frac{m_\sigma^2}{(8c_{4/3}\pi\nu)^2 N_f}c_{2/3}\log\left(\frac{3\sqrt{\frac{3}{2}}Q}{128\pi^3 c_{4/3}^{3/2}\nu^3\tilde{V}N_f^{3/2}}\right) + m_\sigma^4, m_\sigma^2\gamma, \gamma^2\right\} + \tilde{V}\log Q\left\{\frac{\gamma}{3\pi^2 N_f^4 c_{4/3}^5}\left(\frac{9m_\pi^2}{32\nu}\right)^2\right. \\
&\left.\times\left[\frac{5}{8\pi^2 c_{4/3}^4 N_f^2}\left(\frac{9m_\pi^2}{32\nu}\right)^2 X_{00}^4 - c_{2/3}\tilde{R}N_f X_{00}^2 + \frac{9X_{00}X_{01}}{32c_{4/3}}\right] + \frac{14c_{2/3}^3 m_\sigma^2\tilde{R}^2}{(32\pi\nu)^2 N_f c_{4/3}^3}\right\} + \mathcal{O}\left(Q^0\right) \\
E^{1-\gamma\ll 1} =& \frac{c_{4/3}Q^{4/3}}{\tilde{V}^{1/3}}\left[1 + \frac{m_\sigma^2 c_{2/3}}{256\pi^2 N_f c_{4/3}^2\nu^2}\left(4\log\left(\frac{3\sqrt{\frac{3}{2}}Q}{128\pi^3 c_{4/3}^{3/2}\nu^3\tilde{V}N_f^{3/2}}\right) - 3\right) + \mathcal{O}\left(m_\sigma^4\right)\right] \\
&+ c_{2/3}Q^{2/3}\tilde{R}\tilde{V}^{1/3}\left[1 - \frac{c_{2/3}m_\sigma^2}{(8c_{4/3}\pi\nu)^2 N_f}\log\left(\frac{3\sqrt{\frac{3}{2}}Q}{128\pi^3 c_{4/3}^{3/2}\nu^3\tilde{V}N_f^{3/2}}\right) + \mathcal{O}\left(m_\sigma^4\right)\right] \\
&+ \tilde{V}\log Q\left\{\frac{14c_{2/3}^2 m_\sigma^2\tilde{R}^2}{(32\pi\nu)^2 N_f c_{4/3}^3} - \frac{9(1-\gamma)m_\pi^4 X_{00}^2}{64N_f^2 c_{4/3}^3} + \mathcal{O}\left(m_\sigma^4, m_\sigma^2(1-\gamma), (1-\gamma)^2\right)\right\} + \mathcal{O}\left(Q^0\right),
\end{aligned}
\tag{3.6.11}
$$

where we introduced

$$c_{4/3}=\frac{3}{8}\left(\frac{\Lambda^2}{\pi N_f\nu^2}\right)^{2/3},\quad c_{2/3}=\frac{1}{4f^2}\left(\frac{\pi^2}{N_f\nu^2\Lambda^4}\right)^{1/3},\quad \tilde{R}=\frac{R}{6},\quad \tilde{V}=\frac{V}{2\pi^2},\quad \Lambda^4\equiv\begin{cases}\Lambda_0^4+\frac{m_\sigma^2}{16f^2} & \Delta_{\mathcal{O}}\to 0\\ \Lambda_0^4+\frac{m_\sigma^2}{8f^2} & \Delta_{\mathcal{O}}=2\\ \Lambda_0^4 & \Delta_{\mathcal{O}}\to 4\end{cases} \tag{3.6.12}$$

and we double-expanded X first in γ and then also in $1/Q$ as follows

$$\begin{aligned} &X=X_0+X_1\gamma+\mathcal{O}\left(\gamma^2\right), && X_k=X_{k0}+\frac{X_{k1}}{Q^{2/3}}+\mathcal{O}\left(Q^{-4/3}\right), && \text{for } \gamma\ll 1\\ &X=X_0+X_1(1-\gamma)+\mathcal{O}\left((1-\gamma)^2\right), && X_k=X_{k0}+\frac{X_{k1}}{Q^{4/3}}+\mathcal{O}\left(Q^{-2}\right), && \text{for } 1-\gamma\ll 1\,. \end{aligned} \tag{3.6.13}$$

Within the same double expansion we will solve for $\bar{\theta}$. In particular, we will solve the equation of motion, that at the leading order in this expansion, yields $\bar{\theta}_{00}(\alpha_i)=0$. Henceforth, the latter is interpreted as double-expanding the α_i. With a slight abuse of notation we use the same name for the coefficients of the expansions around $\gamma=0$ and $1-\gamma=0$. Interestingly, in the latter case there is no term of order $\mathcal{O}\left(Q^{-2/3}\right)$.

For $\theta=0$ eq.(3.6.9) reproduces the results in [19] [4]. When the theory is conformal (i.e. $m_\pi=m_\sigma=0$), the θ-dependence disappears and the scaling dimension depends only on dimensionless coefficients as

$$\Delta_Q=\tilde{V}^{1/3}E_Q=c_{4/3}Q^{4/3}+c_{2/3}Q^{2/3}+\mathcal{O}\left(Q^0\right), \tag{3.6.14}$$

in agreement with the general form of the large-charge expansion for generic non-supersymmetric CFTs [203]. As first pointed out in [18], the deviations from conformality lead to corrections depending on the background geometry and involve the appearance of logarithms of Q.

From eq.(3.6.9), we observe that θ does not affect the leading order in the large-charge expansion. Moreover, we have that the θ-vacuum is determined by X_{00} which can be obtained by solving $\bar{\theta}_{00}(\alpha_i)=0$ in terms of the α_i. In particular, $X_{00}=\sum_i^{N_f}\cos\alpha_{i00}$ (with the obvious notation) where the α_{i00}s are the solutions found in [2] for the α_i variables at the leading order in $\frac{m_\pi^2}{a}$ and we will refer to such results in the text. In particular, in the $1-\gamma\ll 1$ case, the minimum energy is achieved when X_{00}^2 is maximized due to the minus sign in front of the $\log Q$ term in the energy (3.6.9). It follows that the problem of maximizing X_{00} in terms of the α_{i00} is equivalent to the problem studied in [2] of maximizing X^2 in terms of the α_i which determines the vacuum structure of the superfluid phase of theory in absence of the dilaton. In other words, the results of [2] apply here by replacing $X\to X_{00}$ and $\alpha_i\to\alpha_{i00}$ and the θ-dependence of the vacuum in the presence of the dilaton is identical to the case without it.

Interestingly, when $\gamma\ll 1$ the situation is more subtle since the leading θ-dependent contribution is of the form $X_{00}^2\left(\frac{2}{3}\gamma\log Q-1\right)$. Therefore, at fixed γ there exists a critical charge below/above which the θ-vacuum has to maximize/minimize X_{00}^2. In other words, there is a phase transition in the large-charge regime as Q crosses

$$Q_c=e^{\frac{3}{2\gamma}}\,. \tag{3.6.15}$$

Therefore, for $Q<Q_c$ the θ-vacuum will be analogous to the $1-\gamma\ll 1$ case. We expect this to be the natural limit here as well given that for very charges larger than Q_c we should start exploring the UV asymptotically free fixed point rather than the IR interacting one.

[4] Our expression corrects a few misprints in eqs.(23) and (24) of [19]. We will give the corrected expression for $\theta=0$ in Sec.3.6.1

As we showed in [2], the α_{i00} assume the following expressions that solve eq.(3.6.6):

$$\alpha_{i00} = \begin{cases} \pi - \alpha, & i = 1, \dots, n \\ \alpha, & i = n+1, \dots, N_f \end{cases} \tag{3.6.16}$$

where α is given by

$$\alpha = \frac{\theta + (2k-n)\pi}{(N_f - 2n)}, \quad k = 0, \dots, N_f - 2n - 1\,, \quad n = 0, ..., \left[\frac{N_f - 1}{2}\right]. \tag{3.6.17}$$

As discussed in [2], X_{00}^2 is always maximized by solutions with $n = 0$. For even N_f the ground state solutions have $\alpha_{i00} = \frac{\theta}{N_f}$ in the interval $\theta \in [0, \pi]$ and $\alpha_{i00} = \frac{\theta - 2\pi}{N_f}$ for $\theta \in [\pi, 2\pi]$. The energies stemming from the two solutions cross at $\theta = \pi$ where for $N_f > 2$ we have spontaneous CP symmetry breaking. For odd N_f, the solutions that maximize X_{00}^2 are $\alpha_{i00} = \frac{\theta}{N_f}$ (for $\theta \in [0, \frac{\pi}{2}]$), $\alpha_{i00} = \frac{\theta - \pi}{N_f} + \pi$ (for $\theta \in [\frac{\pi}{2}, \frac{3\pi}{2}]$) , $\alpha_{i00} = \frac{\theta - 2\pi}{N_f}$ (for $\theta \in [\frac{3\pi}{2}, 2\pi]$). In particular, this entails that for odd N_f, CP is conserved at $\theta = \pi$, being the vacuum non-degenerate, while we have two first-order phase transitions at $\theta = \frac{\pi}{2}$ and $\theta = \frac{3\pi}{2}$.

We conclude this section by determining the θ-dependent parameters entering the ground state energy for $\gamma \ll 1$ case when $Q < Q_c$ where $X_{00} = N_f \cos\alpha$. We obtain

$$X_{00} = N_f \cos\left(\frac{\theta + 2k\pi}{N_f}\right) \tag{3.6.18}$$

$$X_{01} = \frac{9 m_\pi^4 \sin^2\left(\frac{\theta+2k\pi}{N_f}\right) \cos\left(\frac{\theta+2k\pi}{N_f}\right)}{8\ a\ c_{4/3}^2} \tag{3.6.19}$$

$$\bar{\theta}_{01} = \frac{m_\pi^2 X_{00} \sin(\frac{\theta+2\pi k}{N_f})}{a N_f} \tag{3.6.20}$$

$$\bar{\theta}_{11} = \frac{3 m_\pi^2 \sin\left(\frac{2(\theta+2\pi k)}{N_f}\right) \log\left(\frac{8192\pi^2 c_{4/3}^3 N_f^3 v^6}{27 Q^2}\right)}{32\ a\ c_{4/3}^2} \tag{3.6.21}$$

$$X_{10} = X_{11} = \bar{\theta}_{00} = \bar{\theta}_{10} = 0 \tag{3.6.22}$$

where the value of k relevant for a given value of θ has to be taken in accordance with the previous discussion.

3.6.1 Ground state energy with the axion

In this section, we focus on the theory in the presence of the axion field described by eq.(3.5.12) and consider the ansatz (3.6.2) for the ground state of Σ and [168]

$$\langle N \rangle = e^{-i\delta/a_{PQ}} \tag{3.6.23}$$

for the axion field. This leads us to study the following Lagrangian

$$\begin{aligned} \mathcal{L}\left[\Sigma_0, \sigma_0, \delta\right] = &-a\nu^2 e^{-4f\sigma_0}(\bar{\theta} - \delta)^2 - e^{-4f\sigma_0}\left(\Lambda^4 - \frac{m_\sigma^2}{16 f^2}\right) - V(\sigma_0) + \\ &+ 2\nu^2 m_\pi^2 X \cos\varphi\ e^{-f\sigma_0 y} + 2\mu^2\nu^2 N_f e^{-2f\sigma_0}\sin^2\varphi\ - \frac{R e^{-2f\sigma_0}}{12 f^2} \end{aligned} \tag{3.6.24}$$

and the corresponding EOMs:

$$\frac{\delta\mathcal{L}}{\delta\alpha}=\frac{\delta\mathcal{L}}{\delta\varphi}=\frac{\delta\mathcal{L}}{\delta\sigma_0}=\frac{\delta\mathcal{L}}{\delta\delta}=0,\quad \frac{\delta\mathcal{L}}{\delta\mu}=\frac{Q}{V}\ . \tag{3.6.25}$$

The main difference with the axion-less case is expressed in the equations for the α_i and δ:

$$ae^{-4f\sigma_0}(\bar\theta-\delta)-2m_\pi^2\sin\alpha_i\cos\varphi e^{-f\sigma_0 y}=0\,,\qquad i=1,..,N_f \tag{3.6.26}$$

$$\delta-\bar\theta=0\ . \tag{3.6.27}$$

These equations can be solved as $\delta=\theta$ and $\alpha_i=0$. Thus the θ-dependence disappears from the ground state energy and there is no CP violation since $(\bar\theta-\delta)=0$. In fact, by construction the axion realizes the Peccei-Quinn solution of the strong CP problem [204, 205] and, as a consequence, the classical solutions are equivalent to the ones at $\theta=0$ which are obtained by setting $X_{00}=N_f$ and $X_{01}=\bar\theta_{01}=0$ in eqs.(3.6.9), (3.6.10), (3.6.11). For instance, in the $V_{\Delta_{\mathcal{O}}=0}(\sigma)$ case, one obtains the results in [19]

$$\begin{aligned}E^{\gamma\ll1}=&\ \frac{c_{4/3}Q^{4/3}}{\tilde V^{1/3}}+Q^{2/3}\tilde V^{1/3}\left\{c_{2/3}\tilde R-\frac{1}{4\pi^2N_fc_{4/3}^4}\left(\frac{9m_\pi^2}{32\nu}\right)^2\left[1-\gamma\left(\frac{2}{3}\log Q-\log\left(\frac{32N_f\nu^2\pi^2c_{4/3}\tilde V^{2/3}}{3}\right)\right)\right]\right\}+\\&-\tilde V\log(Q)\left\{\frac{16\pi^2}{9}N_fc_{2/3}c_{4/3}\nu^2m_\sigma^2-\frac{\gamma}{3\pi^2N_f^2c_{4/3}^5}\left(\frac{9m_\pi^2}{32\nu}\right)^2\left[\frac{5}{8\pi^2c_{4/3}^4}\left(\frac{9m_\pi^2}{32\nu}\right)^2-c_{2/3}\tilde RN_f\right]\right\}\end{aligned} \tag{3.6.28}$$

for the case of $\gamma\ll1$, while for $1-\gamma\ll1$ we have

$$E^{1-\gamma\ll1}=\frac{c_{4/3}Q^{4/3}}{\tilde V^{1/3}}+c_{2/3}Q^{2/3}\tilde R\tilde V^{1/3}-\frac{9(1-\gamma)m_\pi^4\tilde V\log Q}{64c_{4/3}^3}-\frac{16}{9}\pi^2m_\sigma^2N_fc_{2/3}c_{4/3}\nu^2\tilde V\log Q\ . \tag{3.6.29}$$

What differs from [19] is the presence in the spectrum of a light axion which we must take into account when considering the second-order expansion.

3.7 Second-order expansion in the near-conformal regime

The spectrum of the theory in absence of the dilaton field has been detailed in [2]. There, we observed that the theory is characterized by the following symmetry-breaking pattern

$$SU(2N_f)\times U(1)_A\overset{2N_f^2-N_f}{\rightsquigarrow}Sp(2N_f)\longrightarrow SU(N_f)_V\times U(1)_B\overset{\frac{N_f^2-N_f}{2}}{\rightsquigarrow}Sp(N_f)_V \tag{3.7.1}$$

where $\rightsquigarrow$ and $\longrightarrow$ denote, respectively, spontaneous and explicit breaking. In fact, the axial symmetry is explicitly broken by the anomaly and therefore the would-be Goldstone boson is massive. The further explicit breaking is due to the introduction of a baryon charge while the last spontaneous breaking is the superfluid transition. In the absence of the dilaton, the spectrum of light modes is composed of $\frac{1}{2}N_f(N_f-1)$ massless Goldstones with speed $v_G=1$ that parameterizes the coset $\frac{SU(N_f)}{Sp(N_f)}$. They arrange themselves in the antisymmetric representation of the unbroken $Sp(N_f)$ plus a singlet which we denote as π_0. In addition, we find $\frac{1}{2}N_f(N_f-1)-1$ pseudo-Goldstone with mass $\frac{m_\pi^2X}{\mu N_f}$ plus a pseudo-Goldstone mode stemming from the would-be spontaneous breaking of $U(1)_A$ which we call the S (singlet) mode. As mentioned above, the $U(1)_A$ symmetry is quantum mechanically anomalous, and therefore the latter mode acquires a mass contribution proportional to the scale of the

anomaly, $\sqrt{a}$.
The rest of the spectrum is given by gapped modes with a mass of order μ which we will not consider here since they decouple from the large-charge dynamics. It is interesting to analyze how the spectrum changes when (near)conformal dynamics is realized through the dilaton dressing. In particular, conformal invariance dictates the existence of a massless mode with speed $v_G = \frac{1}{\sqrt{d-1}} = \frac{1}{\sqrt{3}}$ [18].
As we shall see, the latter arises from the mixing between the singlet mode π_0 with the dilaton that acts as its "radial mode" and changes its speed from $v_G = 1$ to $v_G = \frac{1}{\sqrt{3}}$. Having in mind the hierarchy of scales $m_\pi, m_\sigma \ll \sqrt{a} \leq \mu \ll 4\pi\nu$, we focus on the spectrum of light modes i.e. the modes whose mass is smaller than the chemical potential in the large-charge limit. To this end, we start by considering the modes with mass $\frac{m_\pi^2 X}{\mu N_f}$. These cannot mix with the dilaton and, therefore, their dispersion relation in the near-conformal phase can be obtained by generalizing the non-conformal expression of [2] to include the expectation value of the dilaton as

$$\omega_1^2 = k^2 - \frac{m_\pi^4 X^2 e^{-2f\sigma_0(y-2)}}{\mu^2 N_f^2} \ , \tag{3.7.2}$$

which matches Eq.(59) of [2] when $f = 0$. For $y = 2$ this mode has squared mass $\frac{m_\pi^4 X^2}{\mu^2 N_f^2}$, whereas in the limit $y = 3$ we have

$$\omega_1^2 = k^2 - \frac{27 m_\pi^4 X_{00}^2}{512\pi^2\nu^2 N_f^3 c_{4/3}^3} + \mathcal{O}\left(Q^{-2/3}\right) \ . \tag{3.7.3}$$

To study the remaining light modes, we expand around the vacuum solution as follows

$$\Sigma = e^{i\Omega}\Sigma_0 e^{i\Omega^t} \tag{3.7.4}$$

where Σ_0 is the classical solution (3.6.2) while the fluctuations are organized in the matrix Ω as

$$\Omega = \begin{pmatrix} \pi & 0 \\ 0 & -\pi^t \end{pmatrix} + \tilde{\beta} S \begin{pmatrix} \mathbb{1}_{N_f} & 0 \\ 0 & \mathbb{1}_{N_f} \end{pmatrix}, \quad \tilde{\beta} \equiv \frac{1}{\sqrt{2N_f}} \tag{3.7.5}$$

here $\pi = \sum_{a=0}^{\dim \frac{U(N_f)}{Sp(N_f)}} \pi^a T_a$ belongs to the algebra of the coset space $\frac{U(N_f)}{Sp(N_f)}$. The normalization condition on the generators is $\langle T_a T_b \rangle = \frac{\delta_{ab}}{2}$. Using the results contained in App..1, we find

$$\left\langle \partial_\mu \Sigma \partial^\mu \Sigma^\dagger \right\rangle = 4\sin^2\varphi \ \partial_\mu \pi^a \partial^\mu \pi^a + 8 N_f \tilde{\beta}^2 \partial_\mu S \partial^\mu S \tag{3.7.6}$$

$$\left\langle B \Sigma \partial_0 \Sigma^\dagger \right\rangle = -2i\sqrt{2N_f}\sin^2\varphi \partial_0 \pi^0 \tag{3.7.7}$$

$$\left\langle M\Sigma + M^\dagger \Sigma^\dagger \right\rangle = 2N_f \cos\varphi \left(X \cos\left(\sqrt{\frac{2}{N_f}} S\right) + Z \sin\left(\sqrt{\frac{2}{N_f}} S\right)\right) \tag{3.7.8}$$

$$\left\langle \log\Sigma - \log\Sigma^\dagger \right\rangle = 8 i N_f \tilde{\beta} S - \sum_i^{N_f} \alpha_i \ , \tag{3.7.9}$$

where we defined $Z \equiv \sum_{i=1}^{N_f} \sin\alpha_i$. Finally, by expanding the dilaton field around its background solution as $\sigma \to \sigma_0 + \hat{\sigma}(t,\mathbf{x})$, we obtain the following quadratic Lagrangian

$$\frac{\mathcal{L}}{4\nu^2 \sin^2\varphi\; e^{-2\sigma_0 f}} = \begin{pmatrix} \pi^0 & \hat{\sigma} & S \end{pmatrix} D^{-1} \begin{pmatrix} \pi^0 \\ \hat{\sigma} \\ S \end{pmatrix} + \sum_{a=1}^{\dim\left(\begin{smallmatrix}\square\\\square\end{smallmatrix}\right)} \partial^\mu \pi^a \partial_\mu \pi^a \tag{3.7.10}$$

with the inverse propagator D^{-1} defined as

$$D^{-1} = \begin{pmatrix} \omega^2 - k^2 & i\omega\mu f\sqrt{2N_f} & 0 \\ -i\omega\mu f\sqrt{2N_f} & \frac{\omega^2-k^2}{8\nu^2\sin^2\varphi} - M_\sigma^2 & \frac{1}{2}I_{\hat{\sigma}s} \\ 0 & \frac{1}{2}I_{\hat{\sigma}s} & \frac{\omega^2-k^2}{\sin^2\varphi} - M_s^2 \end{pmatrix}, \qquad I_{\hat{\sigma}S} = \frac{\sqrt{2} f \mu^2 m_\pi^4 \sqrt{N_f} X y Z}{m_\pi^4 X^2 - \mu^4 N_f^2 e^{2f\sigma_0(y-2)}} \tag{3.7.11}$$

where the Lagrangian masses for the dilaton field are given by

- $\mathbf{V_{\Delta_\mathcal{O}\to 0}}(\sigma)$

$$M_\sigma^2 = -\frac{f^2\mu^2 N_f e^{-6f\sigma_0}\left(\nu^2 m_\pi^4 X^2\left(y^2-2\right)e^{6f\sigma_0} + 2\mu^4\nu^2 N_f^2 e^{2f\sigma_0(y+1)} - 4\Lambda^4\mu^2 N_f e^{2f\sigma_0 y}\right)}{2\nu^2\left(\mu^4 N_f^2 e^{2f\sigma_0(y-2)} - m_\pi^4 X^2\right)} \tag{3.7.12}$$

- $\mathbf{V_{\Delta_\mathcal{O}=2}}(\sigma)$

$$M_\sigma^2 = -\frac{\mu^2 e^{-f\sigma_0 y}\left(-8f^2 e^{f\sigma_0 y}\left(2\mu^2\left(av^2\bar{\theta}^2+\Lambda^4\right)+m_\pi^4 N_f v^2 X^2\right)+4f^2 m_\pi^4 N_f v^2 X^2 y^2 e^{3f\sigma_0}+\mu^2 e^{f\sigma_0(y+2)}\left(8f^2\mu^2 N_f v^2+\right.\right.}{8v^2\left(\mu^4 e^{2f\sigma_0} - m_\pi^4 X^2\right)} \tag{3.7.13}$$

- $\mathbf{V_{\Delta_\mathcal{O}\to 4}}(\sigma)$

$$M_\sigma^2 = -\frac{\mu^2\left(4f^2\left(4\mu^2\left(av^2\bar{\theta}^2+\Lambda^4\right)+m_\pi^4 N_f v^2 X^2\left(2-y^2 e^{-f\sigma_0(y-3)}\right)-2\mu^4 N_f v^2 e^{2f\sigma_0}\right)-4f\mu^2 m_\sigma^2\sigma_0+\mu^2 m_\sigma^2\right)}{8v^2\left(m_\pi^4 X^2 - \mu^4 e^{2f\sigma_0}\right)} \tag{3.7.14}$$

while the mass of the S mode is the same for all three potentials and reads

$$M_S^2 = \frac{a\mu^4 N_f^3 e^{2f\sigma_0(y-1)} + 2\mu^2 m_\pi^4 X^2 e^{4f\sigma_0}}{2\mu^4 N_f^2 e^{2f\sigma_0 y} - 2m_\pi^4 X^2 e^{4f\sigma_0}}\ . \tag{3.7.15}$$

The π^a represents Goldstone modes with sound speed v_G=1 transforming in the antisymmetric representation of $Sp(N_f)$ analogous to the ones found in absence of the dilaton field in [2]. The π_0 field corresponds to the Goldstone mode of the coset $\frac{SU(N_f)}{Sp(N_f)}$ that transforms as a singlet of $Sp(N_f)$. For this reason, it mixes with the dilaton and the S according to eq.(3.7.11). At this point, one can investigate whether eq.(3.7.15) is in agreement with the Witten-Veneziano relation [206, 207]. The latter constrains the mass squared of the S-particle to be proportional to the number of flavours and the topological susceptibility in the limit $m_\pi \to 0$. Indeed, this agrees with the following limit of eq.(3.7.15) [5]

$$\lim_{\sigma_0\to 0,\ m_\pi\to 0} (3.7.15) \implies M_S^2 = \frac{aN_f}{2}\ . \tag{3.7.16}$$

[5] Our definition of M_S differs by a factor of 2 from the usual conventions.

Additionally, for $\sigma_0 \to 0$ we have

$$\lim_{\sigma_0\to 0}(3.7.15) \implies M_S^2 = \frac{a\mu^4 N_f^3 + 2\mu^2 m_\pi^4 X^2}{2\mu^4 N_f^2 - 2m_\pi^4 X^2}\ , \tag{3.7.17}$$

in agreement with eq.(64) of [2]. The remaining dispersion relations are obtained by solving the equation $\det(D^{-1}) = 0$. As a result, we have one massless degree of freedom and two gapped modes. In what follows we provide explicit expressions for the dispersion relations at the two extrema of the dimension of the fermion condensate $\gamma = 0$ and $\gamma = 1$ in the limit of small momenta and within the large-charge expansion. For the sake of simplicity, we consider only the case $\Delta_{\mathcal{O}} \to 0$. For the massless mode we obtain

$$\gamma = 0: \quad \omega_2 = \sqrt{\frac{9f^2 m_\pi^8 X_0^2 Z_0^2 e^{-4f\sigma_0} - 2\mu^4 M_\sigma^2 M_S^2 N_f^3 \sin^4\varphi}{9f^2 m_\pi^8 X_0^2 Z_0^2 e^{-4f\sigma_0} - 2\mu^4 M_S^2 N_f^3 \sin^4\varphi\ (2f^2\mu^2 N_f + M_\sigma^2)}}\ k + \mathcal{O}\left(k^2\right) \tag{3.7.18}$$

$$\gamma = 1: \quad \omega_2 = \sqrt{\frac{2f^2 m_\pi^8 N_f X_0^2 Z_0^2 - \mu^4 M_\sigma^2 M_S^2 \sin^4\varphi}{2f^2 N_f\left(m_\pi^8 X_0^2 Z_0^2 - \mu^6 M_S^2 \sin^4\varphi\ \right) - \mu^4 M_\sigma^2 M_S^2 \sin^4\varphi}}\ k + \mathcal{O}\left(k^2\right) \tag{3.7.19}$$

where we expanded Z in γ and $1-\gamma$ as for X in eq.(3.6.13) and kept only the leading term. In the large-charge limit, the above reduces to

$$\gamma = 0: \quad \omega_2 = k\left[\frac{1}{\sqrt{3}} + \frac{\sqrt{3}\ X_{00}^2}{(2\pi^2)^{2/3} c_{4/3}^5 N_f^3}\left(\frac{9m_\pi^2}{128\pi\nu}\right)^2 \left(\frac{V}{Q}\right)^{2/3} + \dots\right] + \mathcal{O}\left(k^2\right) \tag{3.7.20}$$

$$\gamma = 1: \quad \omega_2 = k\left[\frac{1}{\sqrt{3}} + 1\ \left(\frac{2^{5/3} c_{2/3}\nu^2 m_\sigma^2}{3\sqrt{3}\pi^{2/3}} + \frac{9\sqrt{3} m_\pi^4 X_{00}^2}{128\sqrt[3]{2}\pi^{8/3} c_{4/3}^4 N_f^2}\right)\left(\frac{V}{Q}\right)^{4/3} + \dots\right] + \mathcal{O}\left(k^2\right)\ . \tag{3.7.21}$$

These results agree with those in [19] for $\theta = 0$ i.e. $X_{00} = N_f$ (see Sec.3.7.1 for further details). At the conformal point $m_\sigma = m_\pi = 0$, eqs.(3.7.20) and (3.7.21) describe the expected conformal phonon whose speed approaches the value $v_G = \frac{1}{\sqrt{3}}$ as $Q \to \infty$ [18].

For the massive modes described by eq.(3.7.11), we write the dispersion relations as an expansion for small momenta

$$\omega_3 = M_3 + v_3 k^2 + \dots \tag{3.7.22}$$

$$\omega_4 = M_4 + v_4 k^2 + \dots \tag{3.7.23}$$

In the $\gamma = 0$ case, we have

$$M_{3,4} = \frac{1}{\sqrt{2}}\sqrt{8\nu^2\sin^2\varphi\left(2f^2\mu^2 N_f + M_\sigma^2\right) + M_S^2\sin^2\varphi \pm \frac{\sqrt{144 f^2\nu^2 m_\pi^8 X_0^2 Z_0^2 e^{-4f\sigma_0} + \mu^4 N_f^3 \sin^4\varphi\left(M_S^2 - 8\nu^2\left(2f^2\mu^2 N_f + M_\sigma^2\right)\right)^2}}{\mu^2 N_f^{3/2}}} \tag{3.7.24}$$

$$v_{3,4} = \frac{\mu^4 N_f^3 e^{4f\sigma_0}\left(-2M_{3,4}^2\sin^2\varphi\left(8\nu^2\left(f^2\mu^2 N_f + M_\sigma^2\right) + M_S^2\right) + 3M_{3,4}^4 + 8\nu^2 M_\sigma^2 M_S^2\sin^4\varphi\right) - 36 f^2\nu^2 m_\pi^8 X_0^2 Z_0^2}{2M_{3,4}\mu^4 N_f^3 e^{4f\sigma_0}\left(8\nu^2\sin^2\varphi\left(M_S^2\sin^2\varphi - 2M_{3,4}^2\right)\left(2f^2\mu^2 N_f + M_\sigma^2\right) - 2lM_{3,4}^2 M_S^2\sin^2\varphi + 3M_{3,4}^4\right) - 72 M_{3,4} f^2\nu^2 m_\pi^8 X_0^2 Z_0^2} \tag{3.7.25}$$

which in the large-charge limit yields

$$\omega_3 = \frac{8\ 2^{5/6}\pi^{2/3} f c_{4/3}\nu\sqrt{N_f}}{\sqrt{3}}\left(\frac{Q}{V}\right)^{1/3} + \frac{\left(640\pi^2 k^2 N_f^2 c_{4/3}^3 - 567 f^2 m_\pi^4 X_{00}^2\right)}{2048\ 2^{5/6}\sqrt{3}\pi^{8/3} f c_{4/3}^4 \nu N_f^{5/2}}\left(\frac{V}{Q}\right)^{1/3} + \dots \tag{3.7.26}$$

$$\omega_4 = \frac{\sqrt{3a}}{4\ 2^{2/3}\pi^{1/3}\sqrt{c_{4/3}}\nu}\left(\frac{Q}{V}\right)^{1/3} + \left[\frac{9\sqrt{3}m_\pi^4 X_{00}^2\left(9a + 256\pi^2 c_{4/3}^3\nu^2\right)}{4096\ 2^{10/3}\pi^{11/3}\sqrt{a}c_{4/3}^{11/2}\nu^3 N_f^3} + \frac{2^{5/3}\pi^{1/3}k^2\sqrt{c_{4/3}}\nu}{\sqrt{3}\sqrt{a}}\right]\left(\frac{V}{Q}\right)^{1/3} + \dots \tag{3.7.27}$$

For the case $\gamma = 1$, the mass and speed of the massive modes are given by

$$M_{3,4} = \frac{\sin\varphi}{\sqrt{2}}\sqrt{8\nu^2\left(2f^2\mu^2 N_f + M_\sigma^2\right) + M_S^2 \pm \sin^2\varphi\sqrt{\frac{64 f^2\nu^2 m_\pi^8 X_0^2 Z_0^2 + \mu^4 N_f^3\sin^4\varphi\left(M_S^2 - 8\nu^2\left(2f^2\mu^2 N_f + M_\sigma^2\right)\right)^2}{\mu^4 N_f^3\sin^8\varphi}}} \tag{3.7.28}$$

$$v_{3,4} = \frac{\mu^4\left(-2M_{3,4}^2\sin^2\varphi\left(8\nu^2\left(f^2\mu^2 N_f + M_\sigma^2\right) + M_S^2\right) + 3M_{3,4}^4 + 8\nu^2 M_\sigma^2 M_S^2\sin^4\varphi\right) - 16 f^2\nu^2 m_\pi^8 N_f X_0^2 Z_0^2}{\text{Den}} \tag{3.7.29}$$

$$\begin{aligned}\text{Den} = {} & 2M_{3,4}^3\mu^4\left(3M_{3,4}^2 - 2M_S^2\sin^2\varphi\right) - 16M_{3,4}\nu^2\big[2f^2 N_f\left(\mu^6\sin^2\varphi\left(2M_{3,4}^2 - M_S^2\sin^2\varphi\right)m_\pi^8 X_0^2 Z_0^2\right) \\ & + \mu^4 M_\sigma^2\sin^2\varphi\left(2M_{3,4}^2 - M_S^2\sin^2\varphi\right)\big]\end{aligned} \tag{3.7.30}$$

whose large-charge limit gives

$$\omega_3 = \frac{8\ 2^{5/6}\pi^{2/3} f\nu\sqrt{N_f}c_{4/3}}{\sqrt{3}}\left(\frac{Q}{V}\right)^{1/3} + \frac{5k^2}{16\ 2^{5/6}\sqrt{3}\pi^{2/3} f\nu\sqrt{N_f}c_{4/3}}\left(\frac{V}{Q}\right)^{1/3} + \dots \tag{3.7.31}$$

$$\omega_4 = \frac{\sqrt{3a}}{4\ 2^{2/3}\pi^{1/3}\sqrt{c_{4/3}}\nu}\left(\frac{Q}{V}\right)^{1/3} + \frac{2^{5/3}\pi^{1/3}k^2\sqrt{c_{4/3}}\nu}{\sqrt{3}\sqrt{a}}\left(\frac{V}{Q}\right)^{1/3} + \dots \tag{3.7.32}$$

Notice that the $\gamma = 1$ case leads to enhanced suppression of the θ-dependence in the large-charge limit compared to the $\gamma = 0$ case as already observed at the classical level.

3.7.1 Second-order expansion with the axion

Similarly to the previous section, we parametrize the fluctuations of the Σ field as in (3.7.4) and we take into account the fluctuations of the axion field that we write as [168]

$$N(x) = e^{i\hat{a}(x)/\nu_{PQ}}\ \langle N\rangle \tag{3.7.33}$$

with $\langle N\rangle$ given by eq.(3.6.23). Therefore, (3.5.12) gives another term to consider with respect to the previous section which is

$$-\frac{i}{2}a_{PQ}(\log N - \log N^\dagger) = \frac{a_{PQ}}{\nu_{PQ}}\hat{a} - \delta\ . \tag{3.7.34}$$

As a consequence, we again have modes with dispersion relation (3.7.2) with $X_{00} = N_f$, while the remaining light fluctuations are described by the Lagrangian below

$$\begin{aligned}\mathcal{L} = {} & 4\nu^2\sin^2\varphi\partial_\mu\pi^a\partial^\mu\pi^a e^{-2\sigma f} + 4\nu^2\partial_\mu S\partial^\mu S e^{-2\sigma f} + 8\sqrt{2N}\mu\nu^2\sin^2\varphi\ \partial_0\pi^0 e^{-2\sigma f} + 2\nu^2\mu^2 N_f\sin^2\varphi e^{-2\sigma f} + \\ & + 2N_f^2\nu^2 m_\pi^2\cos\varphi\cos\left(\sqrt{\frac{2}{N_f}}S\right)e^{-y\sigma f} - a\nu^2\left(\bar{\theta} + \sqrt{2N_f}S + \frac{a_{PQ}}{2\nu_{PQ}}\hat{a} - \delta\right)^2 e^{-2\sigma f} \\ & - \Lambda_0^4 e^{-4\sigma f} - \frac{R}{12f^2}e^{-2\sigma f} + \left(\partial_\mu\hat{a}\ \partial^\mu\hat{a}\right)e^{-2\sigma f} + \frac{1}{2}\left(\partial_\mu\sigma\partial^\mu\sigma\right)e^{-2\sigma f} - V(\sigma)\ ,\end{aligned} \tag{3.7.35}$$

from which we obtain the normalised quadratic Lagrangian as

$$\frac{\mathcal{L}}{4\nu^2\sin^2\varphi\; e^{-2\sigma_0 f}} = \begin{pmatrix} \pi^0 & \hat{\sigma} & S & \hat{a} \end{pmatrix} D^{-1} \begin{pmatrix} \pi^0 \\ \hat{\sigma} \\ S \\ \hat{a} \end{pmatrix} + \sum_{a=1}^{\dim\left(\begin{smallmatrix}\square\\\square\end{smallmatrix}\right)} \partial^\mu \pi^a \partial_\mu \pi^a \tag{3.7.36}$$

where the inverse propagator D^{-1} is given by

$$D^{-1} = \begin{pmatrix} \omega^2 - k^2 & i\omega\mu f\sqrt{2N_f} & 0 & 0 \\ -i\omega\mu f\sqrt{2N_f} & \frac{\omega^2-k^2}{8\nu^2\sin^2\varphi} - M_\sigma^2 & 0 & 0 \\ 0 & 0 & \frac{\omega^2-k^2}{\sin^2\varphi} - M_S^2 & \frac{I_{S\hat{a}}}{2} \\ 0 & 0 & \frac{I_{S\hat{a}}}{2} & \frac{\omega^2-k^2}{4\nu^2\sin^2\varphi} - M_{\hat{a}}^2 \end{pmatrix}. \tag{3.7.37}$$

The Lagrangian masses appearing in D^{-1} are

- $\mathbf{V}_{\boldsymbol{\Delta}_\mathcal{O}\to\mathbf{0}}(\sigma)$

$$M_\sigma^2 = -\frac{f^2\mu^2 e^{-2f\sigma_0(y-2)}\left(\nu^2 m_\pi^4 N_f\left(y^2-2\right)e^{2f\sigma_0(y-2)} + 2\mu^4\nu^2 N_f e^{4f\sigma_0(y-2)} - 4\Lambda^4\mu^2 e^{2f\sigma_0(2y-5)}\right)}{2\nu^2\left(\mu^4 e^{2f\sigma_0(y-2)} - m_\pi^4\right)}, \tag{3.7.38}$$

- $\mathbf{V}_{\boldsymbol{\Delta}_\mathcal{O}=\mathbf{2}}(\sigma)$

$$M_\sigma^2 = -\frac{4f^2\mu^2\nu^2 m_\pi^4 N_f\left(y^2-2\right) + \mu^4 e^{2f\sigma_0(y-2)}\left(8f^2\mu^2\nu^2 N_f + m_\sigma^2\right) - 16f^2\Lambda^4\mu^4 e^{2f\sigma_0(y-3)}}{8\nu^2\left(\mu^4 e^{2f\sigma_0(y-2)} - m_\pi^4\right)}, \tag{3.7.39}$$

- $\mathbf{V}_{\boldsymbol{\Delta}_\mathcal{O}\to\mathbf{4}}(\sigma)$

$$M_\sigma^2 = -\frac{2f^2\mu^2\nu^2 m_\pi^4 N_f\left(y^2-2\right) + \mu^4 e^{2f\sigma_0(y-3)}\left(m_\sigma^2(2f\sigma_0-1) - 8f^2\Lambda^4\right) + 4f^2\mu^6\nu^2 N_f e^{2f\sigma_0(y-2)}}{4\nu^2\left(\mu^4 e^{2f\sigma_0(y-2)} - m_\pi^4\right)} \tag{3.7.40}$$

for the dilaton and

$$M_S^2 = \frac{a\mu^4 N_f e^{2f\sigma_0(y-1)} + 2\mu^2 m_\pi^4 e^{4f\sigma_0}}{2\mu^4 e^{2f\sigma_0 y} - 2m_\pi^4 e^{4f\sigma_0}}, \tag{3.7.41}$$

$$M_{\hat{a}}^2 = \frac{a\; a_{PQ}^2 e^{-2f\sigma_0}}{16\nu_{PQ}^2\left(1 - \frac{m_\pi^4 e^{-2f\sigma_0(y-2)}}{\mu^4}\right)} \tag{3.7.42}$$

for the remaining modes. The interaction term between the S-particle and the fluctuation of the axion $\hat{a}$ is

$$I_{S\hat{a}} = -\frac{\sqrt{N_f}\; a\mu^4 a_{PQ} e^{2f\sigma_0(y-3)}}{2\sqrt{2}\nu_{PQ}\left(\mu^4 e^{2f\sigma_0(y-2)} - m_\pi^4\right)}\,. \tag{3.7.43}$$

The inverse propagator (3.7.37) takes the form of a block matrix. The upper left 2×2 block represents the mixing between π_0 and the $\hat{\sigma}$ in the absence of the θ-angle. Diagonalizing it, we find both a massless and a gapped mode with dispersion relations given by

$$\omega_{5.6} = \sqrt{k^2 + 4\nu^2\sin^2\phi\left(2f^2\mu^2 N_f + M_\sigma^2 \pm \sqrt{\frac{f^2k^2\mu^2 N_f\csc^2\phi}{\nu^2} + \left(2f^2\mu^2 N_f + M_\sigma^2\right)^2}\right)} \tag{3.7.44}$$

The spectrum in the $\Delta_{\mathcal{O}} \to 0$ case has been previously studied in [19]. In that case, the explicit expression of the dispersion relation of the massless mode in the two extreme cases $\gamma = 0$ and $\gamma = 1$ reads

$$\gamma = 0: \quad \omega_5 = \frac{k}{\sqrt{3}} + k\, \frac{\sqrt{3}}{(2\pi^2)^{2/3} c_{4/3}^5 N_f} \left(\frac{9m_\pi^2}{128\pi\nu}\right)^2 \left(\frac{V}{Q}\right)^{2/3} + \dots \tag{3.7.45}$$

$$\gamma = 1: \quad \omega_5 = \frac{k}{\sqrt{3}} + k \left[\frac{2\ 2^{2/3} c_{2/3} \nu^2 m_\sigma^2 N_f}{3\sqrt{3}\pi^{2/3}} + \frac{9\sqrt{3} m_\pi^4}{256\sqrt[3]{2}\pi^{8/3} c_{4/3}^4}\right] \left(\frac{V}{Q}\right)^{4/3} + \dots \tag{3.7.46}$$

The above results correct a typo in eqs.(53) and (54) of [19]. The gapped mode arising from the mixing between π_0 and the dilaton has a mass of order $\mathcal{O}(\mu)$. The lower right 2×2 block describes the mixing between the S mode and the axion $\hat{a}$ and by diagonalizing it we obtain the dispersion relations of the propagating modes which read

$$\omega_{7,8} = \frac{1}{2}\sqrt{4k^2 + 2\sin^2\varphi \left(4\nu^2 M_{\hat{a}}^2 + M_S^2\right) \pm \frac{e^{-2f\sigma_0}}{\nu_{PQ}} \sqrt{2a^2\nu^2 N_f a_{PQ}^2 + 4\nu_{PQ}^2 \sin^4\varphi\, e^{4f\sigma_0} \left(M_S^2 - 4\nu^2 M_{\hat{a}}^2\right)^2}} \tag{3.7.47}$$

For $f = 0$ the above reproduces the dispersion relations in absence of the dilaton, which were computed in [2]. Finally, we provide explicit results for these dispersion relations in the $\Delta_{\mathcal{O}} \to 0$ case. For $\gamma = 0$ and in the large-charge expansion, we have

$$\begin{aligned}\omega_7 = {} & \frac{\sqrt{\frac{3a\tilde{\nu}}{c_{4/3}N_f}}}{82^{1/6}\pi^{1/3}\nu_{PQ}\nu} \left(\frac{Q}{V}\right)^{1/3} + \frac{3^5}{16^4} \frac{\sqrt{a} m_\pi^4 \sqrt{\tilde{\nu}_{PQ}}}{2^{2/3}\sqrt{3}\pi^{11/3}\nu_{PQ} c_{4/3}^{11/2} \nu^3 N_f^{3/2}} \left(\frac{V}{Q}\right)^{1/3} + \\ & + \frac{\sqrt{N_f}\nu_{PQ}\left[\nu_{PQ}^2\left(512\pi^2 k^2 c_{4/3}^3 \nu^2 N_f + 27 m_\pi^4\right) + 256\pi^2 k^2 c_{4/3}^3 \nu^4 a_{PQ}^2\right]}{\sqrt{3a}\pi^{5/3} c_{4/3}^{5/2} \nu \tilde{\nu}_{PQ}^{3/2}} \left(\frac{V}{Q}\right)^{1/3} + \dots\end{aligned} \tag{3.7.48}$$

$$\begin{aligned}\omega_8 = {} & \frac{\sqrt{512\pi^2 k^2 c_{4/3}^3 N_f \tilde{\nu} + 27 m_\pi^4 a_{PQ}^2}}{16\pi c_{4/3}^{3/2}\sqrt{2\tilde{\nu}N_f}} + \\ & + \frac{3^3 m_\pi^8 a_{PQ}^2 N_f^{5/2}\left(27a\tilde{\nu}^2 - 2048\pi^2 \nu_{PQ}^4 c_{4/3}^3 \nu^2 N_f^2\right)}{16^3 \cdot 8^2 \cdot 2^{1/6}\pi^{13/3} a c_{4/3}^{13/2} \nu^2 \tilde{\nu}^{5/2} \sqrt{512\pi^2 k^2 c_{4/3}^3 N_f \tilde{\nu} + 27 m_\pi^4 a_{PQ}^2}} \left(\frac{V}{Q}\right)^{2/3} + \dots\end{aligned} \tag{3.7.49}$$

while for $\gamma = 1$ we obtain

$$\omega_7 = \frac{\sqrt{3\tilde{\nu}}}{8 \cdot 2^{1/6}\nu_{PQ}\pi^{1/3}\nu\sqrt{N_f c_{4/3}}} \left(\frac{Q}{V}\right)^{1/3} + \frac{4 \cdot 2^{1/6}\pi^{1/3}\nu_{PQ} k^2 \sqrt{c_{4/3}}\nu\sqrt{N_f}}{\sqrt{3a\tilde{\nu}}} \left(\frac{V}{Q}\right)^{1/3} + \dots \tag{3.7.50}$$

$$\omega_8 = k + \frac{9\nu^2 m_\pi^4 a_{PQ}^2}{32\ 2^{2/3}\pi^{4/3} k c_{4/3}^2 \tilde{\nu}} \left(\frac{V}{Q}\right)^{2/3} + \dots \tag{3.7.51}$$

with $\tilde{\nu} \equiv 2\nu_{PQ}^2 N_f + a_{PQ}^2 \nu^2$.

The upshot of this subsection is that the effect of eliminating the θ-angle via the axion, in the large charge regime, is the introduction of a new light state affecting the spectrum and dynamics of the theory expressed in the new dispersion relations ω_7 and ω_8.

3.7.2 Conformal dimension and vacuum energy of type I Goldstones

Using the state-operator correspondence we generalised the corrections determined in [18, 19] to the large-charge quasi-anomalous dimension Δ as a function of the dilaton, fermion mass, and background geometry to include the impact of the θ angle, axion physics, and dilaton potential yielding:

$\mathbf{V_{\Delta_{\mathcal{O}}\to 0}}(\sigma)$, $\gamma \ll 1$

$$\begin{aligned}\frac{\Delta}{\Delta^*} = 1 &- \left(\frac{9m_\pi^2}{32\pi\nu}\right)^2 \frac{1-\gamma\log\left(\frac{3\rho^{2/3}}{16(2\pi^2)^{1/3}c_{4/3}\nu^2 N_f}\right)}{4c_{4/3}^5 N_f}\cos^2\left(\frac{\theta+2\pi k}{N_f}\right)\left(\frac{1}{2\pi^2\rho}\right)^{2/3} \\ &+ \frac{\gamma}{c_{4/3}^6 N_f}\cos^2\left(\frac{\theta+2\pi k}{N_f}\right)\left(\frac{27m_\pi^4\,\sin^2\left(\frac{\theta+2\pi k}{N_f}\right)}{256\,a\,c_{4/3}^3 N_f^2} + \frac{5\left(\frac{9m_\pi^2}{64\pi\nu}\right)^2\cos^2\left(\frac{\theta+2\pi k}{N_f}\right)}{6c_{4/3}^4 N_f} - \frac{c_{2/3}}{2}\left(\frac{2\pi^2\rho}{Q}\right)^{2/3}\right) \\ &\times\left(\frac{9m_\pi^2}{32\pi\nu}\right)^2\left(\frac{1}{2\pi^2\rho}\right)^{4/3}\log Q - \frac{16}{9}\pi^2 c_{2/3}\nu^2 N_f m_\sigma^2\left(\frac{1}{2\pi^2\rho}\right)^{4/3}\log Q \end{aligned} \tag{3.7.52}$$

$\mathbf{V_{\Delta_{\mathcal{O}}\to 0}}(\sigma)$, $(1-\gamma) \ll 1$

$$\frac{\Delta}{\Delta^*} = 1 - \frac{9m_\pi^4}{64c_{4/3}^4}(1-\gamma)\cos^2\left(\frac{\theta+2\pi k}{N_f}\right)\left(\frac{1}{2\pi^2\rho}\right)^{4/3}\log Q - \frac{16}{9}\pi^2 c_{2/3}\nu^2 N_f m_\sigma^2\left(\frac{1}{2\pi^2\rho}\right)^{4/3}\log Q\,. \tag{3.7.53}$$

$\mathbf{V_{\Delta_{\mathcal{O}}=2}}(\sigma)$, $\gamma \ll 1$

$$\begin{aligned}\frac{\Delta}{\Delta^*} = 1 &- \left(\frac{9m_\pi^2}{32\pi\nu}\right)^2 \frac{1-\gamma\log\left(\frac{3\rho^{2/3}}{16(2\pi^2)^{1/3}c_{4/3}\nu^2 N_f}\right)}{4c_{4/3}^5 N_f}\cos^2\left(\frac{\theta+2\pi k}{N_f}\right)\left(\frac{1}{2\pi^2\rho}\right)^{2/3} - \frac{c_{2/3}m_\sigma^2}{2c_{4/3}}\left(\frac{1}{2\pi^2\rho}\right)^{2/3} \\ &+ \frac{\gamma}{c_{4/3}^6 N_f}\cos^2\left(\frac{\theta+2\pi k}{N_f}\right)\left(\frac{27m_\pi^4\,\sin^2\left(\frac{\theta+2\pi k}{N_f}\right)}{256\,a\,c_{4/3}^3 N_f^2} + \frac{5\left(\frac{9m_\pi^2}{64\pi\nu}\right)^2\cos^2\left(\frac{\theta+2\pi k}{N_f}\right)}{6c_{4/3}^4 N_f} - \frac{c_{2/3}}{2}\left(\frac{2\pi^2\rho}{Q}\right)^{2/3}\right) \\ &\times\left(\frac{9m_\pi^2}{32\pi\nu}\right)^2\left(\frac{1}{2\pi^2\rho}\right)^{4/3}\log Q \end{aligned} \tag{3.7.54}$$

$\mathbf{V_{\Delta_{\mathcal{O}}=2}}(\sigma)$, $(1-\gamma) \ll 1$

$$\frac{\Delta}{\Delta^*} = 1 - \frac{c_{2/3}m_\sigma^2}{2c_{4/3}}\left(\frac{1}{2\pi^2\rho}\right)^{2/3} - \frac{9m_\pi^4}{64c_{4/3}^4}(1-\gamma)\cos^2\left(\frac{\theta+2\pi k}{N_f}\right)\left(\frac{1}{2\pi^2\rho}\right)^{4/3}\log Q\,. \tag{3.7.55}$$

$\mathbf{V_{\Delta_{\mathcal{O}}\to 4}}(\sigma)$, $\gamma \ll 1$

$$\begin{aligned}\frac{\Delta}{\Delta^*} = 1 &- \frac{c_{2/3}m_\sigma^2}{256\pi^2 c_{4/3}^2\nu^2 N_f}\left(3 - 4\log\left(\frac{3\sqrt{\frac{3}{2}}\rho}{64\pi c_{4/3}^{3/2}\nu^3 N_f^{3/2}}\right)\right) + \frac{c_{2/3}^2 m_\sigma^2}{256\pi^2 c_{4/3}^3\nu^2 N_f}\left(3 - 8\log\left(\frac{3\sqrt{\frac{3}{2}}\rho}{64\pi c_{4/3}^{3/2}\nu^3 N_f^{3/2}}\right)\right)\frac{1}{Q^{2/3}} \\ &- \left(\frac{9m_\pi^2}{32\pi\nu}\right)^2 \frac{1-\gamma\log\left(\frac{3\rho^{2/3}}{16(2\pi^2)^{1/3}c_{4/3}\nu^2 N_f}\right)}{4c_{4/3}^5 N_f}\cos^2\left(\frac{\theta+2\pi k}{N_f}\right)\left(\frac{1}{2\pi^2\rho}\right)^{2/3} \end{aligned} \tag{3.7.56}$$

$\mathbf{V_{\Delta_{\mathcal{O}}\to 4}(\sigma)}$**,** $(1-\gamma)\ll 1$

$$\frac{\Delta}{\Delta^*}=1-\frac{c_{2/3}m_\sigma^2}{256\pi^2 c_{4/3}^2\nu^2 N_f}\left(3-4\log\left(\frac{3\sqrt{\frac{3}{2}}\rho}{64\pi c_{4/3}^{3/2}\nu^3 N_f^{3/2}}\right)\right)+\frac{c_{2/3}^2 m_\sigma^2}{256\pi^2 c_{4/3}^3\nu^2 N_f}\left(3-8\log\left(\frac{3\sqrt{\frac{3}{2}}\rho}{64\pi c_{4/3}^{3/2}\nu^3 N_f^{3/2}}\right)\right)\frac{1}{Q^{2/3}} \tag{3.7.57}$$

Here Δ^* is the conformal dimension at the fixed point at leading order in the semiclassical expansion and $\rho\equiv Q/V$ is the charge density. As eq.(3.6.14) illustrates, in the conformal limit $m_\pi=m_\sigma=0$, the scaling dimension of the lowest-lying operator with baryon charge Q takes the form predicted by the large-charge EFT [11, 35]

$$\Delta_Q=k_{4/3}Q^{4/3}+k_{2/3}Q^{2/3}+k_0\log Q+\mathcal{O}\left(Q^0\right)\,, \tag{3.7.58}$$

where the coefficients that appear should not be confused with $c_{4/3}$ and $c_{2/3}$ introduced in eq.(3.6.12). Instead the latter should be viewed as the leading order of a semiclassical expansion of the former, generated by integrating out the heavy degrees of freedom when building the large charge EFT. By inspection, we found out that the parameter controlling the leading quantum correction to the classical result (3.6.9) is

$$\frac{c_{4/3}}{c_{2/3}^2}=\frac{6}{\pi^2}f^4\Lambda^4\,. \tag{3.7.59}$$

This can be traced back to the observations made in [18], where the authors mapped a dilaton-dressed 2-derivatives action with $U(1)$ symmetry (analogous to the π_0, $\hat{\sigma}$ sub-sector of the present theory) to the familiar $\lambda\phi^4$ model with quartic coupling $\lambda=f^4\Lambda^4$. In fact, it is known that within this model the Wilson coefficient of the large charge EFT can be computed as a semiclassical expansion in λ by considering the double-scaling limit $Q\to\infty$, $\lambda\to 0$ with 't Hooft-like coupling λQ fixed [13, 26]. However, as observed in [38], the knowledge of the spectrum of gapless modes is enough to compute exactly the k_0 coefficient in eq.(3.7.58), which is related to the renormalization of their vacuum energy. In our case, the massless spectrum described by the large charge EFT is composed of the $\frac{1}{2}N_f(N_f-1)-1$ modes with dispersion relation $\omega_1$and the $\frac{1}{2}N_f(N_f-1)$ π^a modes. In the conformal limit, these are $N_f^2-N_f-1$ type I Goldstone bosons of the spontaneous symmetry breaking (see [2] for details and transformation properties)

$$SU(N_f)_L\times SU(N_f)_R\times U(1)_B\times U(1)_A\rightsquigarrow Sp(N_f)_L\times Sp(N_f)_R \tag{3.7.60}$$

and all have sound speed $v_G=1$ with the exception of the conformal mode π_0 with $v_G=\frac{1}{\sqrt{3}}$. We do not include the singlet mode S since it decouples due to the axial anomaly. Consider the action describing a type I Goldstone field χ at low energy

$$S_G=\int_{\mathcal{M}}dtdx\left(\frac{1}{2}(\partial_t\chi)^2+\frac{v_G^2}{2}\left(\nabla\chi\right)^2\right)\,, \tag{3.7.61}$$

its one-loop vacuum energy reads

$$E_{\text{Casimir}}=\frac{1}{2}Tr\{\log\left(-\partial_t^2-v_G^2\nabla^2\right)\}=\frac{1}{4\pi}\int_{-\infty}^{\infty}d\omega\sum_{\mathbf{p}}\log\left(\omega^2+v_G^2E^2(\mathbf{p})\right)=\frac{v_G}{2}\sum_{\mathbf{p}}E(\mathbf{p}) \tag{3.7.62}$$

where $E(\mathbf{p})^2$ are the eigenvalues of the Laplacian on the sphere, i.e. $\nabla^2 f_{\mathbf{p}}(\mathbf{r}) + E^2(\mathbf{p}) f_{\mathbf{p}}(\mathbf{r}) = 0$. Being this contribution of order Q^0, in odd dimension is not renormalized by the classical vacuum energy and is, therefore, universal to all the CFT whose large-charge dynamics realize the same conformal superfluid phase [203, 11]. Conversely, in the case of an even number of spacetime dimensions, there is a universal $Q^0 \log Q$ term arising from the renormalization of the energy. In fact, as shown in [38], in dimensional regularization E_G has a pole for $d \to 4$ which is linked to a calculable logarithm of the charge with coefficient $-\frac{v_G}{48}$. Hence, we obtain

$$k_0 = -\frac{1}{48}\left(\frac{1}{\sqrt{3}} + (N_f + 1)(N_f - 2)\right). \tag{3.7.63}$$

This is a robust non-perturbative prediction of the large-charge approach which would be interesting to test via lattice simulations

Chapter 4

Conclusions and Outlooks

In this thesis, we have employed different techniques to study the CFT data of different strongly coupled CFT. In particular, we have combined the large charge expansion with resurgence and near-conformal field dynamics to gain insight of the non-perturbative properties of field theories.

In Chap. 2, we studied the analytic structure of the fixed charge expansion for $O(N)$-invariant models in different space-time dimensions as well as QED_3. We have seen that in $d = 3 - \epsilon$ dimensions the contribution to the $O(N)$ fixed charge conformal dimensions, obtained in the double scaling limit of large charge and vanishing ϵ, is non-Borel summable. Additionally, we have shown that the series is doubly factorial divergent and displays $\sqrt{Q}$ optimal truncation order. Resurgence technologies helped us show that the singularities in the Borel plane are connected to worldline instantons that were found in the alternative double scaling limit of large Q and N of Ref. [50]. We have also explored the case of $d = 4 - \epsilon$ and shown that in the same large Q and small ϵ regime the next order corrections to the scaling dimensions amount to a convergent series. The resummed series exhibits a new branch cut singularity which we found to be relevant for the stability of the large charge sector of the $O(N)$ model for negative ϵ. In the future, it would be interesting to include the contribution of radial and conformal modes to learn how they affect the analytic structure of the fixed charge expansion. For the QED_3 model we discovered that at leading order in the large number of matter field expansion, the large charge scaling dimensions are Borel summable, single factorial divergent and with order Q optimal truncation order. It would be also interesting to investigate whether a non-Borel summable expansion emerges at subleading $1/N_f$ orders (Δ_0 has been computed in [85] for QED_3 and in [88] for $QED_3 - GN$).

In Chap. 3, we investigated the spectrum, the pattern of chiral symmetry breaking and the dispersion relations at low energy of two-color QCD as a function of the baryon chemical potential, the topological term responsible for strong CP breaking as well as the quark masses. The analysis is applicable to $Sp(2N)$ gauge groups with fermions in the fundamental representation. We explicitly considered the dynamics stemming from two, three, six, seven and eight light matter flavors and determined the normal and superfluid ground state. We showed that the vacuum acquires a rich structure stemming from the presence of the CP violating topological operator and unveiled novel phases. We analysed these phases, studied the dependence of the critical chemical potential on the θ angle, delineating the boundary between the normal phase and the superfluid phase. By investigating the behaviour of the CP order parameter we characterised the order of the phase transitions which are shown to be first order. The results are readily applicable, in the normal phase, to the θ and axion physics of composite Goldstone Higgs models. In

particular, a new composite strong source of CP violation can be relevant to investigating composite electroweak baryogenesis [208, 209, 210] while the nonzero chemical potential analysis is useful for studying asymmetric dark matter [209, 211, 212] and the interplay with CP violation. Our predictions can guide and be tested by first principle lattice simulations at nonzero baryon chemical potential but including also the effects of the topological susceptibility [213, 214]. In the future, higher derivative terms can be consistently included in the framework such as the Wess-Zumino-Witten term and its possible gauging [215] following [216].

.1 Details of the second-order expansion

In this Appendix, we provide details on the derivation of the dispersion relations of the fluctuations that we parametrize as

$$\Sigma = e^{i\Omega}\Sigma_0 e^{i\Omega^t} \tag{.1.1}$$

where Σ_0 corresponds to homogeneous ground state (3.6.2) while Ω has the form

$$\Omega = \begin{pmatrix} \pi & 0 \\ 0 & -\pi^t \end{pmatrix} + \tilde{\beta} S \begin{pmatrix} \mathbb{1}_{N_f} & 0 \\ 0 & \mathbb{1}_{N_f} \end{pmatrix} = \nu + \tilde{\beta} S \; \mathbb{1}_{2N_f}, \quad \tilde{\beta} = \frac{1}{\sqrt{2N_f}} \tag{.1.2}$$

here $\pi = \sum_{a=0}^{\dim\left(\begin{smallmatrix}\square\\\square\end{smallmatrix}+1\right)} \pi^a T_a$ belongs to the algebra of the coset space $\frac{U(N_f)}{Sp(N_f)}$. The normalization condition on the generators is $\langle T_a T_b \rangle = \frac{\delta_{ab}}{2}$. Writing $\Sigma = e^{2i\tilde{\beta}S} U(\alpha_i)\overline{\Sigma}$, we have that $\overline{\Sigma}$ can be written as

$$\begin{aligned}
\overline{\Sigma} = e^{i\nu}\Sigma_c e^{i\nu^t} &= \begin{pmatrix} e^{i\pi} & 0 \\ 0 & e^{-i\pi^t} \end{pmatrix} \left(\begin{pmatrix} 0 & \mathbb{1}_{N_f} \\ -\mathbb{1}_{N_f} & 0 \end{pmatrix} \cos\varphi + \begin{pmatrix} \sigma_2 \otimes \mathbb{1}_{N_f/2} & 0 \\ 0 & \sigma_2 \otimes \mathbb{1}_{N_f/2} \end{pmatrix} \sin\varphi \right) \begin{pmatrix} e^{i\pi} & 0 \\ 0 & e^{-i\pi^t} \end{pmatrix} \\
&= \begin{pmatrix} e^{i\pi} & 0 \\ 0 & e^{-i\pi^t} \end{pmatrix} \begin{pmatrix} 0 & \mathbb{1}_{N_f} \\ -\mathbb{1}_{N_f} & 0 \end{pmatrix} \begin{pmatrix} e^{i\pi^t} & 0 \\ 0 & e^{-i\pi} \end{pmatrix} \cos\varphi \\
&+ \begin{pmatrix} e^{i\pi} & 0 \\ 0 & e^{-i\pi^t} \end{pmatrix} \begin{pmatrix} \sigma_2 \otimes \mathbb{1}_{N_f/2} & 0 \\ 0 & \sigma_2 \otimes \mathbb{1}_{N_f/2} \end{pmatrix} \begin{pmatrix} e^{i\pi^t} & 0 \\ 0 & e^{-i\pi} \end{pmatrix} \sin\varphi \\
&= \begin{pmatrix} 0 & \mathbb{1}_{N_f} \\ -\mathbb{1}_{N_f} & 0 \end{pmatrix} \cos\varphi + e^{2i\nu}\, \mathbb{1}_2 \otimes \sigma_2 \otimes \mathbb{1}_{N_f/2} \sin\varphi.
\end{aligned} \tag{.1.3}$$

Using this expression is easy to show that (for simplicity of notation, henceforth we indicate the trace operation with the brackets)

$$\partial_\mu \overline{\Sigma} = 2ie^{2i\nu}\partial_\mu \nu\, \mathbb{1}_2 \otimes \sigma_2 \otimes \mathbb{1}_{N_f/2} \sin\varphi, \tag{.1.4}$$

$$\partial_\mu \overline{\Sigma}^\dagger = -2i\mathbb{1}_2 \otimes \sigma_2 \otimes \mathbb{1}_{N_f/2} \partial_\mu \nu e^{-2i\nu} \sin\varphi, \tag{.1.5}$$

$$\overline{\Sigma}\partial_0 \overline{\Sigma}^\dagger = \begin{pmatrix} 0 & -\sigma_2 \otimes \mathbb{1}_{N_f} \partial_0 \pi^t e^{-2i\pi^t} \\ -\sigma_2 \otimes \mathbb{1}_{N_f} \partial_0 \pi e^{-2i\pi} & 0 \end{pmatrix} \sin\varphi\cos\varphi - 2i\partial_0\nu \sin^2\varphi \tag{.1.6}$$

which implies $\left\langle \partial_\mu \overline{\Sigma} \partial^\mu \overline{\Sigma}^\dagger \right\rangle = 8\sin^2(\varphi)\langle \partial_\mu \pi \partial^\mu \pi \rangle$ and $\left\langle B\overline{\Sigma}\partial_0\overline{\Sigma}^\dagger \right\rangle = -2i\sin^2(\varphi)\langle \partial_0 \pi \rangle$ where $B = \frac{1}{2}\sigma_3 \otimes \mathbb{1}_{N_f}$. Additionally we have

$$\left\langle M\overline{\Sigma} + M^\dagger \overline{\Sigma}^\dagger \right\rangle = 4N_f \cos\varphi \tag{.1.7}$$

$$\begin{aligned}
\left\langle B\overline{\Sigma}B^t\overline{\Sigma}^\dagger \right\rangle &= \left\langle Be^{i\nu}\Sigma_0 e^{i\nu^t} B^t e^{-i\nu^t}\Sigma_0^\dagger e^{-i\nu} \right\rangle \\
&= \left\langle B\Sigma_0 B^t \Sigma_0^\dagger \right\rangle
\end{aligned} \tag{.1.8}$$

since $[B, \nu] = 0$.
Making use of the above results, we obtain that the matrix Σ satisfies

$$\partial_\mu \Sigma = e^{2i\tilde{\beta}S} U(\alpha_i) \left(2i\tilde{\beta}\partial_\mu S \overline{\Sigma} + \partial_\mu \overline{\Sigma} \right), \tag{.1.9}$$

$$\partial_\mu \Sigma^\dagger = e^{-2i\tilde{\beta}S} U(\alpha_i) \left(-2i\tilde{\beta}\partial_\mu S \overline{\Sigma}^\dagger + \partial_\mu \overline{\Sigma}^\dagger \right) \tag{.1.10}$$

$$\Sigma\partial_\mu\Sigma^\dagger = -2i\tilde{\beta}\partial_\mu S + \overline{\Sigma}\partial_\mu\overline{\Sigma}^\dagger \; . \tag{.1.11}$$

From which we can obtain the relevant traces as

$$\begin{aligned}
\left\langle \partial_\mu \Sigma \partial^\mu \Sigma^\dagger \right\rangle &= \left\langle \partial_\mu \overline{\Sigma} \partial^\mu \overline{\Sigma}^\dagger \right\rangle + 4\tilde{\beta}^2 \left\langle \partial_\mu S \partial^\mu S \right\rangle + 2i\tilde{\beta} \partial^\mu S \left\langle \overline{\Sigma} \partial_\mu \overline{\Sigma}^\dagger \right\rangle \\
&= 8 \sin^2 \varphi \left\langle \partial_\mu \pi \partial^\mu \pi \right\rangle + 8 N_f \tilde{\beta}^2 \partial_\mu S \partial^\mu S \\
&= 4 \sin^2 \varphi \ \partial_\mu \pi^a \partial^\mu \pi^a + 8 N_f \tilde{\beta}^2 \partial_\mu S \partial^\mu S \qquad (.1.12) \\
\left\langle B \Sigma \partial_0 \Sigma^\dagger \right\rangle &= \left\langle B \overline{\Sigma} \partial_0 \overline{\Sigma}^\dagger \right\rangle \\
&= -2i \sin^2 \varphi \left\langle \partial_0 \pi \right\rangle \\
&= -2i \sqrt{2N_f} \sin^2 \varphi \ \partial_0 \pi^0 \qquad (.1.13) \\
\left\langle M\Sigma + M^\dagger \Sigma^\dagger \right\rangle &= \left\langle e^{2i\tilde{\beta}S} M U(\alpha_i) \overline{\Sigma} + e^{-2i\tilde{\beta}S} M^\dagger U(\alpha_i)^\dagger \overline{\Sigma}^\dagger \right\rangle \\
&= 2N_f \cos\varphi \left(X \cos\left(\sqrt{\frac{2}{N_f}} S \right) + Z \sin\left(\sqrt{\frac{2}{N_f}} S \right) \right) \qquad (.1.14) \\
\left\langle \log \Sigma - \log \Sigma^\dagger \right\rangle &= 8 i N_f \tilde{\beta} S - \sum_i^{N_f} \alpha_i \ . \qquad (.1.15)
\end{aligned}$$

Finally, by plugging these results into the Lagrangian (3.5.11), we arrive at

$$\begin{aligned}
\mathcal{L} = {} & 4\nu^2 \sin^2 \varphi \partial_\mu \pi^a \partial^\mu \pi^a e^{-2\sigma f} + 4\nu^2 \partial_\mu S \partial^\mu S e^{-2\sigma f} + 8\sqrt{2N} \mu \nu^2 \sin^2 \varphi \partial_0 \pi^0 e^{-2\sigma f} \\
& + 2\nu^2 \mu^2 N_f \sin^2 \varphi e^{-2\sigma f} + 4 N_f \nu^2 m_\pi^2 \cos\varphi \left[X \cos\left(\sqrt{2} \sqrt{\frac{1}{N_f}} S \right) + Z \sin\left(\sqrt{2} \sqrt{\frac{1}{N_f}} S \right) \right] e^{-y\sigma f} \\
& - a v^2 (\bar{\theta} + \sqrt{2N_f} S)^2 e^{-2\sigma f} - \Lambda_0^4 e^{-4\sigma f} - \frac{R}{12 f^2} e^{-2\sigma f} + \frac{1}{2} \big(\partial_\mu \sigma \partial^\mu \sigma \big) e^{-2\sigma f} \\
& - \frac{m_\sigma^2}{16 f^2} \left(e^{-4\sigma f} + 4\sigma f - 1 \right) \ . \qquad (.1.16)
\end{aligned}$$

By expanding the above to the quadratic order in the fluctuations of the dilaton field, we obtain the quadratic Lagrangian (3.7.10).

Bibliography

[1] Oleg Antipin, Jahmall Bersini, Francesco Sannino, and Matías Torres. The analytic structure of the fixed charge expansion. *JHEP*, 06:041, 2022.

[2] Jahmall Bersini, Alessandra D'Alise, Francesco Sannino, and Matías Torres. The θ-angle and axion physics of two-color QCD at fixed baryon charge. *JHEP*, 11:080, 2022.

[3] Jahmall Bersini, Alessandra D'Alise, Francesco Sannino, and Matías Torres. Charging the conformal window at nonzero θ angle. *Phys. Rev. D*, 107(12):125024, 2023.

[4] Gonzalo Barriga, Fabrizio Canfora, Marcela Lagos, Matías Torres, and Aldo Vera. On the robustness of solitons crystals in the Skyrme model. *Nucl. Phys. B*, 983:115913, 2022.

[5] Jahmall Bersini, Alessandra D'Alise, Matias Torres, and Francesco Sannino. The Dilatonic Dynamics of Baryonic Crystals, Branes and Spheres. 10 2023.

[6] Gonzalo Barriga, Matías Torres, and Aldo Vera. Exact modulated hadronic tubes and layers at finite volume in a cloud of π and ω mesons. *Nucl. Phys. B*, 1001:116501, 2024.

[7] Brian C. Odom, D. Hanneke, B. D'Urso, and G. Gabrielse. New Measurement of the Electron Magnetic Moment Using a One-Electron Quantum Cyclotron. *Phys. Rev. Lett.*, 97:030801, 2006.

[8] Celine Degrande, Valentin V. Khoze, and Olivier Mattelaer. Multi-Higgs production in gluon fusion at 100 TeV. *Phys. Rev. D*, 94:085031, 2016.

[9] N. Brambilla et al. QCD and Strongly Coupled Gauge Theories: Challenges and Perspectives. *Eur. Phys. J. C*, 74(10):2981, 2014.

[10] Philippe de Forcrand. Simulating QCD at finite density. *PoS*, LAT2009:010, 2009.

[11] Simeon Hellerman, Domenico Orlando, Susanne Reffert, and Masataka Watanabe. On the CFT Operator Spectrum at Large Global Charge. *JHEP*, 12:071, 2015.

[12] Gil Badel, Gabriel Cuomo, Alexander Monin, and Riccardo Rattazzi. Feynman diagrams and the large charge expansion in $3-\varepsilon$ dimensions. *Phys. Lett. B*, 802:135202, 2020.

[13] Gil Badel, Gabriel Cuomo, Alexander Monin, and Riccardo Rattazzi. The Epsilon Expansion Meets Semiclassics. *JHEP*, 11:110, 2019.

[14] Orestis Loukas, Domenico Orlando, and Susanne Reffert. Matrix models at large charge. *JHEP*, 10:085, 2017.

[15] Domenico Orlando, Susanne Reffert, and Francesco Sannino. A safe CFT at large charge. *JHEP*, 08:164, 2019.

[16] Anton De La Fuente. The large charge expansion at large N. *JHEP*, 08:041, 2018.

[17] Luis Alvarez-Gaume, Orestis Loukas, Domenico Orlando, and Susanne Reffert. Compensating strong coupling with large charge. *JHEP*, 04:059, 2017.

[18] Domenico Orlando, Susanne Reffert, and Francesco Sannino. Near-Conformal Dynamics at Large Charge. *Phys. Rev. D*, 101(6):065018, 2020.

[19] Domenico Orlando, Susanne Reffert, and Francesco Sannino. Charging the Conformal Window. *Phys. Rev. D*, 103(10):105026, 2021.

[20] Gabriel Cuomo, Luca V. Delacretaz, and Umang Mehta. Large Charge Sector of 3d Parity-Violating CFTs. *JHEP*, 05:115, 2021.

[21] Masataka Watanabe. Chern-Simons-matter theories at large baryon number. *JHEP*, 10:245, 2021.

[22] Samuel Favrod, Domenico Orlando, and Susanne Reffert. The large-charge expansion for Schrödinger systems. *JHEP*, 12:052, 2018.

[23] Vito Pellizzani. Operator spectrum of nonrelativistic CFTs at large charge. *Phys. Rev. D*, 105(12):125018, 2022.

[24] Nicola Dondi, Simeon Hellerman, Ioannis Kalogerakis, Rafael Moser, Domenico Orlando, and Susanne Reffert. Fermionic CFTs at large charge and large N. *JHEP*, 08:180, 2023.

[25] Simeon Hellerman, Daniil Krichevskiy, Domenico Orlando, Vito Pellizzani, Susanne Reffert, and Ian Swanson. The unitary Fermi gas at large charge and large N. *JHEP*, 05:323, 2024.

[26] Oleg Antipin, Jahmall Bersini, Francesco Sannino, Zhi-Wei Wang, and Chen Zhang. Charging the $O(N)$ model. *Phys. Rev. D*, 102(4):045011, 2020.

[27] Oleg Antipin, Jahmall Bersini, and Pantelis Panopoulos. Yukawa interactions at Large Charge. 8 2022.

[28] Oleg Antipin, Jahmall Bersini, Pantelis Panopoulos, Francesco Sannino, and Zhi-Wei Wang. Infinite order results for charged sectors of the Standard Model. *JHEP*, 02:168, 2024.

[29] Daniele Dorigoni. An Introduction to Resurgence, Trans-Series and Alien Calculus. *Annals Phys.*, 409:167914, 2019.

[30] Inês Aniceto, Gokce Basar, and Ricardo Schiappa. A Primer on Resurgent Transseries and Their Asymptotics. *Phys. Rept.*, 809:1–135, 2019.

[31] Philippe Di Francesco, Pierre Mathieu, and David Sénéchal. *Conformal Field Theory*. Springer New York, NY, 12 1996.

[32] Slava Rychkov. *EPFL Lectures on Conformal Field Theory in D>= 3 Dimensions*. SpringerBriefs in Physics. 1 2016.

[33] G. Mack. Convergence of Operator Product Expansions on the Vacuum in Conformal Invariant Quantum Field Theory. *Commun. Math. Phys.*, 53:155, 1977.

[34] J. L. Cardy. Conformal invariance and universality in finite-size scaling. *J. Phys. A*, 17(7):L385, 1984.

[35] Alexander Monin, David Pirtskhalava, Riccardo Rattazzi, and Fiona K. Seibold. Semiclassics, Goldstone Bosons and CFT data. *JHEP*, 06:011, 2017.

[36] Alberto Nicolis, Riccardo Penco, Federico Piazza, and Riccardo Rattazzi. Zoology of condensed matter: Framids, ordinary stuff, extra-ordinary stuff. *JHEP*, 06:155, 2015.

[37] Alberto Nicolis. Low-energy effective field theory for finite-temperature relativistic superfluids. 8 2011.

[38] Gabriel Cuomo. A note on the large charge expansion in 4d CFT. *Phys. Lett. B*, 812:136014, 2021.

[39] Michael E. Peskin and Daniel V. Schroeder. *An Introduction to quantum field theory*. Addison-Wesley, Reading, USA, 1995.

[40] Sidney Coleman. *Aspects of Symmetry: Selected Erice Lectures*. Cambridge University Press, 1985.

[41] Walter D. Goldberger, Benjamin Grinstein, and Witold Skiba. Distinguishing the Higgs boson from the dilaton at the Large Hadron Collider. *Phys. Rev. Lett.*, 100:111802, 2008.

[42] Riccardo Rattazzi and Alberto Zaffaroni. Comments on the holographic picture of the randall-sundrum model. *Journal of High Energy Physics*, 2001(04):021, 2001.

[43] Zackaria Chacko and Rashmish K Mishra. Effective theory of a light dilaton. *Physical Review D*, 87(11):115006, 2013.

[44] Thomas Appelquist, James Ingoldby, and Maurizio Piai. Dilaton Effective Field Theory. *Universe*, 9(1):10, 2023.

[45] Oscar Cata, Vicent Mateu, Dean J. Mitchell, and Santiago Peris. Chiral Perturbation Theory, the $1/N_c$ Expansion and Regge Theory. *JHEP*, 06:137, 2019.

[46] Thomas Appelquist, James Ingoldby, and Maurizio Piai. Dilaton potential and lattice data. *Phys. Rev. D*, 101(7):075025, 2020.

[47] Oscar Catà and Christoph Müller. Chiral effective theories with a light scalar at one loop. *Nucl. Phys. B*, 952:114938, 2020.

[48] Sidney Coleman. *Aspects of symmetry: selected Erice lectures*. Cambridge University Press, 1988.

[49] Moshe Moshe and Jean Zinn-Justin. Quantum field theory in the large N limit: A Review. *Phys. Rept.*, 385:69–228, 2003.

[50] Nicola Dondi, Ioannis Kalogerakis, Domenico Orlando, and Susanne Reffert. Resurgence of the large-charge expansion. *JHEP*, 05:035, 2021.

[51] Luis Alvarez-Gaume, Domenico Orlando, and Susanne Reffert. Large charge at large N. *JHEP*, 12:142, 2019.

[52] Lorenzo Di Pietro, Marcos Mariño, Giacomo Sberveglieri, and Marco Serone. Resurgence and 1/N Expansion in Integrable Field Theories. *JHEP*, 10:166, 2021.

[53] Christian Schubert. Perturbative quantum field theory in the string inspired formalism. *Phys. Rept.*, 355:73–234, 2001.

[54] MICHAEL E. FISHER. Critical point phenomena — the role of series expansions. *The Rocky Mountain Journal of Mathematics*, 4(2):181–201, 1974.

[55] Anthony J Guttmann. Series extension: predicting approximate series coefficients from a finite number of exact coefficients. *Journal of Physics A: Mathematical and Theoretical*, 49(41):415002, September 2016.

[56] William R. Frazer. Applications of Conformal Mapping to the Phenomenological Representation of Scattering Amplitudes. *Phys. Rev.*, 123:2180–2182, 1961.

[57] D. L. Hunter and George A. Baker. Methods of Series Analysis. 1. Comparison of Current Methods Used in the Theory of Critical Phenomena. *Phys. Rev. B*, 7:3346–3376, 1973.

[58] D. I. Kazakov, D. V. Shirkov, and O. V. Tarasov. Analytical Continuation of Perturbative Results of the $g\phi^4$ Model Into the Region g Is Greater Than or Equal to 1. *Theor. Math. Phys.*, 38:9–16, 1979.

[59] Jan Fischer. On the role of power expansions in quantum field theory. *Int. J. Mod. Phys. A*, 12:3625–3663, 1997.

[60] M. A. Stephanov. QCD critical point and complex chemical potential singularities. *Phys. Rev. D*, 73:094508, 2006.

[61] Irinel Caprini, Jan Fischer, Gauhar Abbas, and B. Ananthanarayan. Perturbative Expansions in QCD Improved by Conformal Mappings of the Borel Plane. 11 2017.

[62] Nicola Andrea Dondi, Gerald V. Dunne, Manuel Reichert, and Francesco Sannino. Analytic Coupling Structure of Large N_f (Super) QED and QCD. *Phys. Rev. D*, 100(1):015013, 2019.

[63] Ovidiu Costin and Gerald V. Dunne. Physical Resurgent Extrapolation. *Phys. Lett. B*, 808:135627, 2020.

[64] Nicola Andrea Dondi, Gerald V. Dunne, Manuel Reichert, and Francesco Sannino. Towards the QED beta function and renormalons at $1/N_f^2$ and $1/N_f^3$. *Phys. Rev. D*, 102(3):035005, 2020.

[65] I. Jack and D. R. T. Jones. Anomalous dimensions for ϕ^n in scale invariant $d = 3$ theory. *Phys. Rev. D*, 102(8):085012, 2020.

[66] Marcos Mariño. *Instantons and Large N: An Introduction to Non-Perturbative Methods in Quantum Field Theory*. Cambridge University Press, 9 2015.

[67] F. J. Dyson. Divergence of perturbation theory in quantum electrodynamics. *Phys. Rev.*, 85:631–632, 1952.

[68] R. D. Pisarski. FIXED POINT STRUCTURE OF (PHI**6) in three-dimensions AT LARGE N. *Phys. Rev. Lett.*, 48:574–576, 1982.

[69] J. D. Brock, A. Aharony, R. J. Birgeneau, K. W. Evans-Lutterodt, J. D. Litster, P. M. Horn, G. B. Stephenson, and A. R. Tajbakhsh. Orientational and positional order in a tilted hexatic liquid-crystal phase. *Phys. Rev. Lett.*, 57:98–101, Jul 1986.

[70] Amnon Aharony. Critical phenomena in disordered systems. *Journal of Magnetism and Magnetic Materials*, 7(1):198–206, 1978.

[71] Eugene Demler, Werner Hanke, and Shou-Cheng Zhang. SO (5) theory of antiferromagnetism and superconductivity. *Rev. Mod. Phys.*, 76:909–974, 2004.

[72] Daniele Dorigoni and Yasuyuki Hatsuda. Resurgence of the Cusp Anomalous Dimension. *JHEP*, 09:138, 2015.

[73] Carl Bender and Steven Orszag. *Advanced Mathematical Methods for Scientists and Engineers: Asymptotic Methods and Perturbation Theory*, volume 1. 01 1999.

[74] Daniel Shanks. Non-linear transformations of divergent and slowly convergent sequences. *Journal of Mathematics and Physics*, 34(1-4):1–42, 1955.

[75] R. Camporesi. Harmonic analysis and propagators on homogeneous spaces. *Phys. Rept.*, 196:1–134, 1990.

[76] Oleg Antipin, Jahmall Bersini, Francesco Sannino, Zhi-Wei Wang, and Chen Zhang. More on the cubic versus quartic interaction equivalence in the $O(N)$ model. *Phys. Rev. D*, 104:085002, 2021.

[77] Simone Giombi and Jonah Hyman. On the large charge sector in the critical O(N) model at large N. *JHEP*, 09:184, 2021.

[78] Oleg Antipin, Jahmall Bersini, Francesco Sannino, Zhi-Wei Wang, and Chen Zhang. Charging non-Abelian Higgs theories. *Phys. Rev. D*, 102(12):125033, 2020.

[79] Oleg Antipin, Jahmall Bersini, Francesco Sannino, Zhi-Wei Wang, and Chen Zhang. Untangling scaling dimensions of fixed charge operators in Higgs theories. *Phys. Rev. D*, 103(12):125024, 2021.

[80] I. Jack and D. R. T. Jones. Anomalous dimensions at large charge in d=4 O(N) theory. *Phys. Rev. D*, 103(8):085013, 2021.

[81] Rafael Moser, Domenico Orlando, and Susanne Reffert. Convexity, large charge and the large-N phase diagram of the φ^4 theory. *JHEP*, 02:152, 2022.

[82] Thomas Appelquist, Daniel Nash, and L. C. R. Wijewardhana. Critical Behavior in (2+1)-Dimensional QED. *Phys. Rev. Lett.*, 60:2575, 1988.

[83] Daniel Nash. Higher Order Corrections in (2+1)-Dimensional QED. *Phys. Rev. Lett.*, 62:3024, 1989.

[84] Vadim Borokhov, Anton Kapustin, and Xin-kai Wu. Topological disorder operators in three-dimensional conformal field theory. *JHEP*, 11:049, 2002.

[85] Silviu S. Pufu. Anomalous dimensions of monopole operators in three-dimensional quantum electrodynamics. *Phys. Rev. D*, 89(6):065016, 2014.

[86] Tai Tsun Wu and Chen Ning Yang. Dirac Monopole Without Strings: Monopole Harmonics. *Nucl. Phys. B*, 107:365, 1976.

[87] Tai Tsun Wu and Chen Ning Yang. Some Properties of Monopole Harmonics. *Phys. Rev. D*, 16:1018–1021, 1977.

[88] Éric Dupuis, Rufus Boyack, and William Witczak-Krempa. Anomalous Dimensions of Monopole Operators at the Transitions between Dirac and Topological Spin Liquids. *Phys. Rev. X*, 12(3):031012, 2022.

[89] C. A. Baker et al. An Improved experimental limit on the electric dipole moment of the neutron. *Phys. Rev. Lett.*, 97:131801, 2006.

[90] C. Abel et al. Measurement of the Permanent Electric Dipole Moment of the Neutron. *Phys. Rev. Lett.*, 124(8):081803, 2020.

[91] R. D. Peccei and Helen R. Quinn. Constraints Imposed by CP Conservation in the Presence of Instantons. *Phys. Rev. D*, 16:1791–1797, 1977.

[92] R. D. Peccei and Helen R. Quinn. CP Conservation in the Presence of Instantons. *Phys. Rev. Lett.*, 38:1440–1443, 1977.

[93] Steven Weinberg. A New Light Boson? *Phys. Rev. Lett.*, 40:223–226, 1978.

[94] Frank Wilczek. Problem of Strong P and T Invariance in the Presence of Instantons. *Phys. Rev. Lett.*, 40:279–282, 1978.

[95] Jihn E. Kim. Weak Interaction Singlet and Strong CP Invariance. *Phys. Rev. Lett.*, 43:103, 1979.

[96] Mikhail A. Shifman, A. I. Vainshtein, and Valentin I. Zakharov. Can Confinement Ensure Natural CP Invariance of Strong Interactions? *Nucl. Phys. B*, 166:493–506, 1980.

[97] Michael Dine, Willy Fischler, and Mark Srednicki. A Simple Solution to the Strong CP Problem with a Harmless Axion. *Phys. Lett. B*, 104:199–202, 1981.

[98] Rabindra N. Mohapatra and G. Senjanovic. Natural Suppression of Strong p and t Noninvariance. *Phys. Lett. B*, 79:283–286, 1978.

[99] Ann E. Nelson. Naturally Weak CP Violation. *Phys. Lett. B*, 136:387–391, 1984.

[100] Stephen M. Barr. A Natural Class of Nonpeccei-quinn Models. *Phys. Rev. D*, 30:1805, 1984.

[101] Ann E. Nelson. Calculation of θ Barr. *Phys. Lett. B*, 143:165–170, 1984.

[102] Francesco Sannino. Conformal Dynamics for TeV Physics and Cosmology. *Acta Phys. Polon. B*, 40:3533–3743, 2009.

[103] Giacomo Cacciapaglia, Claudio Pica, and Francesco Sannino. Fundamental Composite Dynamics: A Review. *Phys. Rept.*, 877:1–70, 2020.

[104] Francesco Sannino and Kimmo Tuominen. Orientifold theory dynamics and symmetry breaking. *Phys. Rev. D*, 71:051901, 2005.

[105] Dennis D. Dietrich, Francesco Sannino, and Kimmo Tuominen. Light composite Higgs from higher representations versus electroweak precision measurements: Predictions for CERN LHC. *Phys. Rev. D*, 72:055001, 2005.

[106] Dennis D. Dietrich and Francesco Sannino. Conformal window of SU(N) gauge theories with fermions in higher dimensional representations. *Phys. Rev. D*, 75:085018, 2007.

[107] Francesco Sannino. Conformal Windows of SP(2N) and SO(N) Gauge Theories. *Phys. Rev. D*, 79:096007, 2009.

[108] Tuomas Karavirta, Jarno Rantaharju, Kari Rummukainen, and Kimmo Tuominen. Determining the conformal window: SU(2) gauge theory with $N_f = 4$, 6 and 10 fermion flavours. *JHEP*, 05:003, 2012.

[109] Hiroshi Ohki, Tatsumi Aoyama, Etsuko Itou, Masafumi Kurachi, C. J. David Lin, Hideo Matsufuru, Tetsuya Onogi, Eigo Shintani, and Takeshi Yamazaki. Study of the scaling properties in SU(2) gauge theory with eight flavors. *PoS*, LATTICE2010:066, 2010.

[110] Jarno Rantaharju, Tuomas Karavirta, Viljami Leino, Teemu Rantalaiho, Kari Rummukainen, and Kimmo Tuominen. The gradient flow running coupling in SU2 with 8 flavors. *PoS*, LATTICE2014:258, 2014.

[111] Randy Lewis, Claudio Pica, and Francesco Sannino. Light Asymmetric Dark Matter on the Lattice: SU(2) Technicolor with Two Fundamental Flavors. *Phys. Rev. D*, 85:014504, 2012.

[112] Ari Hietanen, Randy Lewis, Claudio Pica, and Francesco Sannino. Composite Goldstone Dark Matter: Experimental Predictions from the Lattice. *JHEP*, 12:130, 2014.

[113] Ari Hietanen, Randy Lewis, Claudio Pica, and Francesco Sannino. Fundamental Composite Higgs Dynamics on the Lattice: SU(2) with Two Flavors. *JHEP*, 07:116, 2014.

[114] Rudy Arthur, Vincent Drach, Martin Hansen, Ari Hietanen, Claudio Pica, and Francesco Sannino. SU(2) gauge theory with two fundamental flavors: A minimal template for model building. *Phys. Rev. D*, 94(9):094507, 2016.

[115] Viljami Leino, Kari Rummukainen, Joni M. Suorsa, Kimmo Tuominen, and Sara Tähtinen. Infrared Behaviour of SU(2) Gauge Theory with N_f fundamental flavours. *PoS*, Confinement2018:225, 2019.

[116] Francis Bursa, Luigi Del Debbio, Liam Keegan, Claudio Pica, and Thomas Pickup. Mass anomalous dimension in SU(2) with six fundamental fermions. *Phys. Lett. B*, 696:374–379, 2011.

[117] M. Hayakawa, K. I. Ishikawa, S. Takeda, and N. Yamada. Running coupling constant and mass anomalous dimension of six-flavor SU(2) gauge theory. *Phys. Rev. D*, 88(9):094504, 2013.

[118] T. Appelquist et al. Two-Color Gauge Theory with Novel Infrared Behavior. *Phys. Rev. Lett.*, 112(11):111601, 2014.

[119] Viljami Leino, Teemu Rantalaiho, Kari Rummukainen, Joni M. Suorsa, Kimmo Tuominen, and Sara Tähtinen. Gradient flow running coupling in SU(2) Nf=6 flavors. *PoS*, LATTICE2016:218, 2016.

[120] Joni M. Suorsa, Viljami Leino, Jarno Rantaharju, Teemu Rantalaiho, Kari Rummukainen, Kimmo Tuominen, and Sara Tähtinen. Mass anomalous dimension of SU(2) using the spectral density method. *PoS*, LATTICE2016:389, 2016.

[121] Atsushi Nakamura. Quarks and Gluons at Finite Temperature and Density. *Phys. Lett. B*, 149:391, 1984.

[122] Simon Hands, John B. Kogut, Maria-Paola Lombardo, and Susan E. Morrison. Symmetries and spectrum of SU(2) lattice gauge theory at finite chemical potential. *Nucl. Phys. B*, 558:327–346, 1999.

[123] John B. Kogut, Dominique Toublan, and D. K. Sinclair. Diquark condensation at nonzero chemical potential and temperature. *Phys. Lett. B*, 514:77–87, 2001.

[124] John B. Kogut, Dominique Toublan, and D. K. Sinclair. The Phase diagram of four flavor SU(2) lattice gauge theory at nonzero chemical potential and temperature. *Nucl. Phys. B*, 642:181–209, 2002.

[125] Shin Muroya, Atsushi Nakamura, and Chiho Nonaka. Behavior of hadrons at finite density: Lattice study of color SU(2) QCD. *Phys. Lett. B*, 551:305–310, 2003.

[126] Simon Hands, Seyong Kim, and Jon-Ivar Skullerud. Deconfinement in dense 2-color QCD. *Eur. Phys. J. C*, 48:193, 2006.

[127] Seamus Cotter, Pietro Giudice, Simon Hands, and Jon-Ivar Skullerud. Towards the phase diagram of dense two-color matter. *Phys. Rev. D*, 87(3):034507, 2013.

[128] Tamer Boz, Seamus Cotter, Leonard Fister, Dhagash Mehta, and Jon-Ivar Skullerud. Phase transitions and gluodynamics in 2-colour matter at high density. *Eur. Phys. J. A*, 49:87, 2013.

[129] V. V. Braguta, E. M. Ilgenfritz, A. Yu. Kotov, A. V. Molochkov, and A. A. Nikolaev. Study of the phase diagram of dense two-color QCD within lattice simulation. *Phys. Rev. D*, 94(11):114510, 2016.

[130] Lukas Holicki, Jonas Wilhelm, Dominik Smith, Björn Wellegehausen, and Lorenz von Smekal. Two-colour QCD at finite density with two flavours of staggered quarks. *PoS*, LATTICE2016:052, 2017.

[131] V. G. Bornyakov, V. V. Braguta, E. M. Ilgenfritz, A. Yu. Kotov, A. V. Molochkov, and A. A. Nikolaev. Observation of deconfinement in a cold dense quark medium. *JHEP*, 03:161, 2018.

[132] Tamer Boz, Ouraman Hajizadeh, Axel Maas, and Jon-Ivar Skullerud. Finite-density gauge correlation functions in QC2D. *Phys. Rev. D*, 99(7):074514, 2019.

[133] N. Yu. Astrakhantsev, V. G. Bornyakov, V. V. Braguta, E. M. Ilgenfritz, A. Yu. Kotov, A. A. Nikolaev, and A. Rothkopf. Lattice study of static quark-antiquark interactions in dense quark matter. *JHEP*, 05:171, 2019.

[134] Tamer Boz, Pietro Giudice, Simon Hands, and Jon-Ivar Skullerud. Dense two-color QCD towards continuum and chiral limits. *Phys. Rev. D*, 101(7):074506, 2020.

[135] Kei Iida, Etsuko Itou, and Tong-Gyu Lee. Two-colour QCD phases and the topology at low temperature and high density. *JHEP*, 01:181, 2020.

[136] Jonas Wilhelm, Lukas Holicki, Dominik Smith, Björn Wellegehausen, and Lorenz von Smekal. Continuum Goldstone spectrum of two-color QCD at finite density with staggered quarks. *Phys. Rev. D*, 100(11):114507, 2019.

[137] V. G. Bornyakov, V. V. Braguta, A. A. Nikolaev, and R. N. Rogalyov. Effects of Dense Quark Matter on Gluon Propagators in Lattice QC_2D. *Phys. Rev. D*, 102:114511, 2020.

[138] Kei Iida, Etsuko Itou, and Tong-Gyu Lee. Relative scale setting for two-color QCD with N_f=2 Wilson fermions. *PTEP*, 2021(1):013B05, 2021.

[139] N. Astrakhantsev, V. V. Braguta, E. M. Ilgenfritz, A. Yu. Kotov, and A. A. Nikolaev. Lattice study of thermodynamic properties of dense QC_2D. *Phys. Rev. D*, 102(7):074507, 2020.

[140] T. G. Khunjua, K. G. Klimenko, and R. N. Zhokhov. The dual properties of chiral and isospin asymmetric dense quark matter formed of two-color quarks. *JHEP*, 06:148, 2020.

[141] Toru Kojo and Daiki Suenaga. Thermal quarks and gluon propagators in two-color dense QCD. *Phys. Rev. D*, 103(9):094008, 2021.

[142] William E. Caswell. Asymptotic Behavior of Nonabelian Gauge Theories to Two Loop Order. *Phys. Rev. Lett.*, 33:244, 1974.

[143] B. Holdom. The Renormalization Group Equation for the $U(1)$ Coupling. *Phys. Lett. B*, 213:365–369, 1988.

[144] B. Holdom. Two U(1)'s and Epsilon Charge Shifts. *Phys. Lett. B*, 166:196–198, 1986.

[145] Andrew G. Cohen and Howard Georgi. Walking Beyond the Rainbow. *Nucl. Phys. B*, 314:7–24, 1989.

[146] Zackaria Chacko and Rashmish K. Mishra. Effective Theory of a Light Dilaton. *Phys. Rev. D*, 87(11):115006, 2013.

[147] Shinya Matsuzaki and Koichi Yamawaki. Dilaton Chiral Perturbation Theory: Determining the Mass and Decay Constant of the Technidilaton on the Lattice. *Phys. Rev. Lett.*, 113(8):082002, 2014.

[148] Aya Kasai, Ken-ichi Okumura, and Hiroshi Suzuki. A dilaton-pion mass relation. 9 2016.

[149] Martin Hansen, Kasper Langæble, and Francesco Sannino. Extending Chiral Perturbation Theory with an Isosinglet Scalar. *Phys. Rev. D*, 95(3):036005, 2017.

[150] Maarten Golterman and Yigal Shamir. Low-energy effective action for pions and a dilatonic meson. *Phys. Rev. D*, 94(5):054502, 2016.

[151] Maarten Golterman and Yigal Shamir. Effective pion mass term and the trace anomaly. *Phys. Rev. D*, 95(1):016003, 2017.

[152] Thomas Appelquist, James Ingoldby, and Maurizio Piai. Dilaton EFT Framework For Lattice Data. *JHEP*, 07:035, 2017.

[153] Maarten Golterman and Yigal Shamir. Large-mass regime of the dilaton-pion low-energy effective theory. *Phys. Rev. D*, 98(5):056025, 2018.

[154] Maarten Golterman, Ethan T. Neil, and Yigal Shamir. Application of dilaton chiral perturbation theory to $N_f = 8$, SU(3) spectral data. *Phys. Rev. D*, 102(3):034515, 2020.

[155] Thomas Appelquist, James Ingoldby, and Maurizio Piai. Nearly Conformal Composite Higgs Model. *Phys. Rev. Lett.*, 126(19):191804, 2021.

[156] Maarten Golterman and Yigal Shamir. Dilaton chiral perturbation theory and applications. *PoS*, LATTICE2021:372, 2022.

[157] R. J. Crewther and Lewis C. Tunstall. Origin of $\Delta I = 1/2$ Rule for Kaon Decays: QCD Infrared Fixed Point. *Phys. Rev. D*, 91:034016, 2015.

[158] Roman Zwicky and Kerstin Engel. Recent Developments in Flavor Physics and CP Violation. *Symmetry*, 15(5):1034, 2023.

[159] Alessandro Amato, Viljami Leino, Kari Rummukainen, Kimmo Tuominen, and Sara Tähtinen. From chiral symmetry breaking to conformality in SU(2) gauge theory. 6 2018.

[160] Viljami Leino, Tobias Rindlisbacher, Kari Rummukainen, Francesco Sannino, and Kimmo Tuominen. Safety versus triviality on the lattice. *Phys. Rev. D*, 101(7):074508, 2020.

[161] Oleg Antipin and Francesco Sannino. Conformal Window 2.0: The large N_f safe story. *Phys. Rev. D*, 97(11):116007, 2018.

[162] Daniel F. Litim and Francesco Sannino. Asymptotic safety guaranteed. *JHEP*, 12:178, 2014.

[163] Daniel F. Litim, Matin Mojaza, and Francesco Sannino. Vacuum stability of asymptotically safe gauge-Yukawa theories. *JHEP*, 01:081, 2016.

[164] Thomas Appelquist, P. S. Rodrigues da Silva, and Francesco Sannino. Enhanced global symmetries and the chiral phase transition. *Phys. Rev. D*, 60:116007, 1999.

[165] Edward Witten. Current Algebra Theorems for the U(1) Goldstone Boson. *Nucl. Phys. B*, 156:269–283, 1979.

[166] G. Veneziano. U(1) Without Instantons. *Nucl. Phys. B*, 159:213–224, 1979.

[167] R. J. Crewther, P. Di Vecchia, G. Veneziano, and Edward Witten. Chiral Estimate of the Electric Dipole Moment of the Neutron in Quantum Chromodynamics. *Phys. Lett. B*, 88:123, 1979. [Erratum: Phys.Lett.B 91, 487 (1980)].

[168] Paolo Di Vecchia and Francesco Sannino. The Physics of the θ-angle for Composite Extensions of the Standard Model. *Eur. Phys. J. Plus*, 129:262, 2014.

[169] Ken Kawarabayashi and Nobuyoshi Ohta. The Problem of η in the Large N Limit: Effective Lagrangian Approach. *Nucl. Phys. B*, 175:477–492, 1980.

[170] Maxim Pospelov and Adam Ritz. Theta vacua, QCD sum rules, and the neutron electric dipole moment. *Nucl. Phys. B*, 573:177–200, 2000.

[171] Rouven Essig et al. Working Group Report: New Light Weakly Coupled Particles. In *Snowmass 2013: Snowmass on the Mississippi*, 10 2013.

[172] S. D. H. Hsu and F. Sannino. New solutions to the strong CP problem. *Phys. Lett. B*, 605:369–375, 2005.

[173] Frank Wilczek and Guy Moore. Superheavy Light Quarks and the Strong P, T Problem. 1 2016.

[174] M. K. Gaillard, M. B. Gavela, R. Houtz, P. Quilez, and R. Del Rey. Color unified dynamical axion. *Eur. Phys. J. C*, 78(11):972, 2018.

[175] M. B. Gavela, M. Ibe, P. Quilez, and T. T. Yanagida. Automatic Peccei–Quinn symmetry. *Eur. Phys. J. C*, 79(6):542, 2019.

[176] Luca Di Luzio, Belen Gavela, Pablo Quilez, and Andreas Ringwald. An even lighter QCD axion. *JHEP*, 05:184, 2021.

[177] J. B. Kogut, Misha A. Stephanov, D. Toublan, J. J. M. Verbaarschot, and A. Zhitnitsky. QCD - like theories at finite baryon density. *Nucl. Phys. B*, 582:477–513, 2000.

[178] Edward Witten. Large N Chiral Dynamics. *Annals Phys.*, 128:363, 1980.

[179] Edward Witten. An SU(2) Anomaly. *Phys. Lett. B*, 117:324–328, 1982.

[180] Roger F. Dashen. Some features of chiral symmetry breaking. *Phys. Rev. D*, 3:1879–1889, 1971.

[181] Davide Gaiotto, Zohar Komargodski, and Nathan Seiberg. Time-reversal breaking in QCD_4, walls, and dualities in 2 + 1 dimensions. *JHEP*, 01:110, 2018.

[182] Paolo Di Vecchia, Giancarlo Rossi, Gabriele Veneziano, and Shimon Yankielowicz. Spontaneous CP breaking in QCD and the axion potential: an effective Lagrangian approach. *JHEP*, 12:104, 2017.

[183] Andrei V. Smilga. QCD at theta similar to pi. *Phys. Rev. D*, 59:114021, 1999.

[184] Michel H. G. Tytgat. QCD at theta similar to pi reexamined: Domain walls and spontaneous CP violation. *Phys. Rev. D*, 61:114009, 2000.

[185] Michael Creutz. Quark masses and chiral symmetry. *Phys. Rev. D*, 52:2951–2959, 1995.

[186] Ryuichiro Kitano, Ryutaro Matsudo, Norikazu Yamada, and Masahito Yamazaki. Peeking into the θ vacuum. *Phys. Lett. B*, 822:136657, 2021.

[187] Max A. Metlitski and Ariel R. Zhitnitsky. Theta-parameter in 2 color QCD at finite baryon and isospin density. *Nucl. Phys. B*, 731:309–334, 2005.

[188] S. Gandolfi, J. Lippuner, A. W. Steiner, I. Tews, X. Du, and M. Al-Mamun. From the microscopic to the macroscopic world: from nucleons to neutron stars. *J. Phys. G*, 46(10):103001, 2019.

[189] Holger Bech Nielsen and S. Chadha. On How to Count Goldstone Bosons. *Nucl. Phys. B*, 105:445–453, 1976.

[190] Andrei V. Smilga and J. J. M. Verbaarschot. Spectral sum rules and finite volume partition function in gauge theories with real and pseudoreal fermions. *Phys. Rev. D*, 51:829–837, 1995.

[191] Sidney Coleman. *Aspects of Symmetry: Selected Erice Lectures*. Cambridge University Press, Cambridge, U.K., 1985.

[192] John L. Cardy. Conformal invariance and universality in finite-size scaling. *J. Phys. A*, 17:L385–L387, 1984.

[193] J. L. Cardy. Universal amplitudes in finite-size scaling: generalisation to arbitrary dimensionality. *J. Phys. A*, 18(13):L757–L760, 1985.

[194] V. A. Miransky and Koichi Yamawaki. Conformal phase transition in gauge theories. *Phys. Rev. D*, 55:5051–5066, 1997. [Erratum: Phys.Rev.D 56, 3768 (1997)].

[195] Holger Gies and Joerg Jaeckel. Chiral phase structure of QCD with many flavors. *Eur. Phys. J. C*, 46:433–438, 2006.

[196] David B. Kaplan, Jong-Wan Lee, Dam T. Son, and Mikhail A. Stephanov. Conformality Lost. *Phys. Rev. D*, 80:125005, 2009.

[197] Hidenori S. Fukano and Francesco Sannino. Conformal Window of Gauge Theories with Four-Fermion Interactions and Ideal Walking. *Phys. Rev. D*, 82:035021, 2010.

[198] Thomas Appelquist, James Ingoldby, and Maurizio Piai. Dilaton effective field theory. *Universe*, 9(1):10, 2023.

[199] Thomas Appelquist, James Ingoldby, and Maurizio Piai. Dilaton potential and lattice data. *Physical Review D*, 101(7):075025, 2020.

[200] Taro V. Brown, Maarten Golterman, Svend Krøjer, Yigal Shamir, and K. Splittorff. The ϵ-regime of dilaton chiral perturbation theory. *Phys. Rev. D*, 100(11):114515, 2019.

[201] Maarten Golterman and Yigal Shamir. Explorations beyond dilaton chiral perturbation theory in the eight-flavor SU(3) gauge theory. *Phys. Rev. D*, 102:114507, 2020.

[202] D. T. Son. Low-energy quantum effective action for relativistic superfluids. 4 2002.

[203] Luis Álvarez Gaumé, Domenico Orlando, and Susanne Reffert. Selected topics in the large quantum number expansion. *Phys. Rept.*, 933:1–66, 2021.

[204] Roberto D Peccei and Helen R Quinn. Cp conservation in the presence of pseudoparticles. *Physical Review Letters*, 38(25):1440, 1977.

[205] Roberto D Peccei and Helen R Quinn. Constraints imposed by cp conservation in the presence of pseudoparticles. *Physical Review D*, 16(6):1791, 1977.

[206] Edward Witten. Current algebra theorems for the u (1)"goldstone boson". *Nuclear Physics B*, 156(2):269–283, 1979.

[207] Gabriele Veneziano. U (1) without instantons. *Nuclear Physics B*, 159(1-2):213–224, 1979.

[208] James M. Cline, Matti Jarvinen, and Francesco Sannino. The Electroweak Phase Transition in Nearly Conformal Technicolor. *Phys. Rev. D*, 78:075027, 2008.

[209] Thomas A. Ryttov and Francesco Sannino. Ultra Minimal Technicolor and its Dark Matter TIMP. *Phys. Rev. D*, 78:115010, 2008.

[210] Sebastian Bruggisser, Benedict Von Harling, Oleksii Matsedonskyi, and Géraldine Servant. Electroweak Phase Transition and Baryogenesis in Composite Higgs Models. *JHEP*, 12:099, 2018.

[211] Yonit Hochberg, Eric Kuflik, Hitoshi Murayama, Tomer Volansky, and Jay G. Wacker. Model for Thermal Relic Dark Matter of Strongly Interacting Massive Particles. *Phys. Rev. Lett.*, 115(2):021301, 2015.

[212] Martin Hansen, Kasper Langæble, and Francesco Sannino. SIMP model at NNLO in chiral perturbation theory. *Phys. Rev. D*, 92(7):075036, 2015.

[213] Luigi Del Debbio, Leonardo Giusti, and Claudio Pica. Topological susceptibility in the SU(3) gauge theory. *Phys. Rev. Lett.*, 94:032003, 2005.

[214] B. Alles, Massimo D'Elia, A. Di Giacomo, and C. Pica. Analysis of systematic errors in the calculation of renormalization constants of the topological susceptibility on the lattice. *Phys. Rev. D*, 74:094503, 2006.

[215] Zhi-yong Duan, P. S. Rodrigues da Silva, and Francesco Sannino. Enhanced global symmetry constraints on epsilon terms. *Nucl. Phys. B*, 592:371–390, 2001.

[216] J. T. Lenaghan, F. Sannino, and K. Splittorff. The Superfluid and conformal phase transitions of two color QCD. *Phys. Rev. D*, 65:054002, 2002.